

**MEASUREMENT AND ACCURACY ASSESMENT
OF COORDINATES USING
TOTAL STATION AND AERIAL PHOTOGRAMMETRY**

By

SADEQ ABU-ZA'NOUNEH

HANI AL-DARAWEESH MAJDI ABU-GHAYYADAH



CIVIL & ARCHITECTURAL ENGINEERING DEPARTMENT
COLLEGE OF ENGINEERING AND TECHNOLOGY
PALESTINE POLYTECHNIC UNIVERSITY

HEBRON- WEST BANK
PALESTINE

MAY-2007

بِسْمِ اللَّهِ الرَّحْمَنِ الرَّحِيمِ

Palestine Polytechnic University



College of Engineering & Technology

Civil & Architecture Engineering Department

Graduation Project

**MEASUREMENT AND ACCURACY ASSESMENT
OF COORDINATES USING
TOTAL STATION AND AERIAL PHOTOGRAMMETRY**

By

SADEQ ABU-ZA'NOUNEH

HANI AL-DARAWEESH

MAJDI ABU-GHAYYADAH

Project Supervisor

ENG.MAHER OWAIWI

HEBRON-PALESTINE

MAY-200

Certification

Palestine Polytechnic University



HEBRON-PALESTINE

**MEASUREMENT AND ACCURACY ASSESMENT
OF COORDINATES USING
TOTAL STATION AND AERIAL PHOTOGRAMMETRY**

By

SADEQ ABUZA'NOUNEH

HANI AL DARAWEESH

MAJDI ABU-GHAYYADAH

In accordance with the recommendation of project supervisor and acceptance of all examining committee members, this project has been submitted to the Department of Civil and Architectural Engineering in the college of Engineering and Technology in partial fulfillment of requirements of the Department for Degree of Bachelor of Surveying and Geomatics Engineering.

Signature of Project Supervisor

Signature of Department Chairman

Name.....

Name.....

MAY-2007

إلى الذين ساروا مع الفجر ليخطوا لنا طريق العودة.....الشهداء

إلى الأسود الرابضة خلف القضبان.....الأسرى

إلى نبع الحنان والمحبة.....أمي الغالية

إلى رمز البذل والعطاء.....أ. الحبيب

إلى من هم عنوان سعادتي.....إخوتي

إلى روح المرحوم المهندس.....كمال غطاشه

إلى الشموع التي تحترق لتنير لنا الطريق.....أساتذتي

إلى كل من نحبهم ويحبوننا

إلى كل هؤلاء نهدي هذا العمل البسيط

فريق العمل:

صادق أبو زعنونه

مجدي أبو غياضه

هاني الدراويش

تقدير

Acknowledgments

بداية نشكر المولى عز وجل الذي أعاننا على إنجاز هذا العمل المتواضع .
بوليتكنك فلسطين التي احتضنت مسيرتنا التعليمية ونشكر دائرة الهندسة المدنية والمعماري
الممثلة برئيسها الدكتور نبيل الجولاني للحصول على درجة البكالوريوس في تخصص هندسة
المساحة والجيوماتكس.

و نتوجه بالشكر العميق إلى أمهاتنا الذين كدوا وبذلوا بوسعهم لنواكب هذه الطريق.

كما نتوجه بالشكر العميق إلى مشرفنا الأستاذ ماهر العويوي على ما قدمه لنا من نصيح و
إرشاد ومساعدة قيمة خلال إنجاز هذا المشروع.

ونتوجه ببالغ الشكر والتقدير إلى جميع مدرسي قسم هندسة المساحة والجيوماتكس ونخص
بالذكر المهندس فيضي شبانه والدكتور نافذ ناصر الدين والمهندس خليل كرامه والمهندس
غادي زكارنه مد الشريف والمهندس نضال أبو رجب.

Abstract

MEASUREMENT AND ACCURACY ASSESMENT OF COORDINATES USING EDM AND AERIAL PHOTOGRAMMETRY

Project Team

SADEQ ABUZA'NOUNEH

HANI AL DARAWEESH

MAJDI ABU-GHAYYADAH

Supervisor By:

ENG.MAHER OWAIWI

Nowadays several methods are used to determine object coordinates. This research discuss the accuracy quality, time consuming and economic efficiency of two main survey methods, EDM and aerial photogrammetry.

Accuracy is defined that how closely the measured quantity nearest to the true value or the most probable value.

The project including collection of 31 control and check points which are distributed on four quarters on the model, and are collected (surveyed) using electronic distance measurements instrument.

ZI-imaging photogrammetric software was used to build three photogrammetric models using three, six and nine EDM surveyed points. An accuracy assessment of

the surveyed check points and the corresponding photogrammetry points of the three models was tested and reported.

The important of this project is realized by comparing the result of the EDM, and photogrammetry technique in terms of time consuming, accuracy and economical efficiency.

It found that the photogrammetric works have less time than the land survey method, when the number of control points increase to accomplish the model, the RMSE decreases and the accuracy increase, photogrammetric maps can be printed at large scale such as 1:1000 with accuracy reaches to sub meters, and 2m contour interval.

تقييم الدقة في الإحداثيات المقاسه بواسطة الدستومات والصور الجوية

مجدي ابوغيضة

هاني الدراويش

:

المهندس ماهر العويوي

- رق المساحية في جمع الاحداثيات قد تنوعت وامتدت من المساحة الارضية
- الحصول على الموقع لتشمل استخدام الصور الجوية الملتقطة
- أو الصور الفضائية
- طريق الاقمار الصناعية .

لكن يبقى السؤال الذي يطرح نفسه بنفسه هي جودة ودقة والجدوى الاقتصادية في استخدام اياً من

!

لذا فان هذا المشروع يبحث في هذا السؤال البسيط ذو المعنى الكبير.

تم في هذا المشروع جمع نقطة إحداثيات كنقاط مرجعيه . . لفحص دقة نتائج الصور الجوية مرصوده بجهاز الدستومات .
(models) من زوج الصور الجوية

(RMSE) يقل كلما زاد عدد نقاط التحكم (control points) وهذا يعني زيادة . .
أن عملية المسح الجوي تأخذ وقتا أقل مقارنة بالمسح . .
التصوير الجوي و أجزاء من السنتيمتر في المسح .

كما يمكن طباعة الخرائط الجوية الناتجة من صور هذا المشروع بمقياس رسم . . :
كنتورية تصل .

CHAPTER

1

INTRODUCTION

The following contents are going to be covered in this chapter:

1.1 Overview

1.2 Project importance

1.3 Study area

1.4 Project methodology

1.5 Project outline

1.6 Project time table "Schedule"

CHAPTER ONE

Introduction

1.1 Overview

Due to errors, repeated measurement of the same quantity will often yield different value. A discrepancy is defined the algebraic difference between two measurements of the same quantity. When small discrepancies exist between repeated measurements, it is generally believed that only small errors exist.

Accuracy is defined that how closely the measured quantity nearest to the true value or the most probable value.

Accuracy assessment of a geodetic network depends largely on the technique used, such as land survey or aerial photo.

Other parameters that affect the accuracy are the scale of the output planometric map or orthophoto.

The project will have the following activities:

- 1- Surveying and collecting of control and check points using land survey method.
- 2- Generation of photogrammetric model using softcopy stereoplotter.
- 3- Calculation and collection coordinate points from photogrammetric model.
- 4- GIS analysis, and accuracy assessment.

1.2 Project importance

The important of this project is realized by comparing the result of the land survey and Photogrammetry methods in terms of time consuming accuracy and economical efficiency.

When using deferent surveying methods the result may be passes or fail. If the result is pass within the required accuracy the method that gives the required accuracy choice is the choose the less times and will economical efficiency, but if the result is fail then the generated model must not use for accurate works, so the project must limited with the specification and repeat your work or guess the most effective factor that enter the errors.

1.3 Studying area

The study area is part of Wadi Al Harrieh, southern part of Hebron city, as illustrated in fig. (1.1).

The study area is covered by pairs of aerial images that are captured in 2004. The model covers about (1300) Donum of Wadi Al Harrieh including the Palestine Polytechnic University.

1.4 Project methodology

The study area is covered with an overlap photographs, fig. (1.2). These overlap photos were exposed by photogrammetric RMK 30/29 camera with 305.004mm focal length and from elevation of 3000m above mean sea level. Accurate topographic features, such as building, roads..., are easily distinguished from these aerial photos.

1.4.1 Control and check points collection using land survey method

1. The study area is divided to 4 quarters.
2. Well define 9 control points and 31 check points were identified. These points distribute evenly to the 4 quarters. The 9 control points were chosen on the ground and are well define.
3. The EDM instrument is used to determine the coordinates of control and check points.
4. All coordinates of the control and check points are taken within the allowable errors.
5. x, y and z coordinates of these controls or check points are considered to be free of errors and are used to check the accuracy of the photogrammetry measurements.
- 6- The total time required to complete the survey is measured.

1.4.2 Photogrammetry method

1. Using control points of land survey method
 - 3 control points are used to build the photogrammetric model.
 - Measure the coordinate of 31 check points from the generated model.
 - Compute the RMSE for the total model.
 - Repeat the model using 6 control points.
 - Measure the coordinate of 31 check points from the generated model.
 - Compute the RMSE for the total model.
 - Repeat the model using 9 control points.
 - Compare resultant RMSE with the three models with map standards.
 - Correlate the result of three models to determine the effects of control points on the model accuracy.
 - Measure the total time required to complete the model.

2. Relation between photogrammetry model and control points collection method.
 - Compare the results of the three generated photogrammetry models when using land survey method.

1.5 Project outline

Chapter 1: Introduction.

Chapter 2: land survey Techniques

This chapter talks about EDM and basic principle for measurements and errors in Total Station.

Chapter 3: Aerial Photogrammetry

This chapter gives introduction to photogrammetry, image processing, workstation and photogrammetric.

Chapter 4: Accuracy Standards.

This chapter discuss different types of errors and available Accuracy Standards.

Chapter 5: Measurements and Calculations.

This chapter illustrates the use field surveying (traverse correction using least square method).

Point coordinates calculation, also, is shows how technique.

ZI-imaging software is used to build the models (oriented the photos) and it discuss the RMSE for each generated models and comparing with the different standards.

Chapter 6: Data Analysis.

GIS analysis showing results as maps.

Chapter 7: Conclusions and Recommendations.

1.6 Project time table "Schedule"

Table (1.1): Project Schedule for first course in year 2006 - 2007

NO	Activity	weeks	Time frame in weeks														
			1	2	3	4	5	6	7	8	9	10	11	12	13	14	
1	Choosing the project	2															
2	Reconnaissance	2															
3	Preparing the first chapter	3															
4	Initial land survey	5															
5	First office calculations	3															
6	Writing the second chapter	2															
7	Writing the third and forth chapter	3															
8	Project introduction report revision	2															
9	Final project introduction report printing and handing	4															

Table (1.2): Project Schedule for second course in year 2006 - 2007

NO	Activity	weeks	Time frame in weeks													
			1	2	3	4	5	6	7	8	9	10	11	12	13	14
1	Complete field survey	3														
2	Complete calculations of coordinates	2														
3	Photo scanning	1														
4	Building the models	2														
5	Collecting coordinates from the models	3														
6	Writing the sixth chapter	4														
7	Preparing the maps	2														
8	Writing conclusion and recommendation	3														
9	Final project report printing and handing	2														

CHAPTER

2

LAND SURVEY TECHNIQUE

The following contents are going to be covered in this chapter:

2.1 Overview

2.2 Electronic distance measurement

2.3 Basic principles of electromagnetic waves in EDM instruments

2.4 Errors in Total Station

2.5 Applications of the Total Station

CHAPTER TWO

Land survey Technique

2.1 Overview

We currently live in what is often termed the information age. Aided by new and emerging technologies, data are being collected at unprecedented rates in all walks of life. In the field of surveying, for example, total station instruments, global positioning system (GPS) equipment. Digital metric cameras and satellite imaging systems are only some of the new instruments that are now available for rapid generation of vast quantities of measured data.

Geographic information systems (GIS) have evolved concurrently with the development of these new data acquisition instruments. GIS are now used extensively for management, planning, and design. They are being applied worldwide at all levels of government, in business and industry by public utilities, and in private engineering and surveying offices. Implementation of a GIS depends upon large quantities of data from a variety of sources; many of them consisting of measurements made with new instruments such as those noted above.

Before measured data can be utilized, however, whether for surveying and mapping projects, for engineering design, or for use in a geographic information system. They must be processed. One of the most important aspects of this is to account for the fact that no measurements are exact. That is, they always contain errors.

2.2 Electronic distance measurement

Electronic distance measuring (EDM) equipment includes electro-optical (light waves) and electromagnetic (microwaves) instruments. The first generation of electro-optical instruments, typified by the Geodimeter, was originally developed in Sweden in the early 1950s. The basic principle of electro-optical devices is the indirect determination of the time required for a light beam to travel between two stations. The instrument, set up on one station, emits a modulated light beam to a passive reflector set up on the other end of the line to be measured. The reflector, acting as a mirror, returns the light pulse to the instrument, where a phase comparison is made between the projected and reflected pulses, [ref.3].

2.3 Basic principles of electromagnetic waves in EDM instruments

Electromagnetic waves can be represented by a sinusoidal wave motion. The number of times in 1 second that a wave completes a cycle is called the frequency (f), and is measured in Hz.

The length of one cycle is called the wavelength (λ), which can be determined as a function of the frequency from

$$\lambda = \frac{v}{f} \quad \dots\dots\dots (2.1)$$

Where: v is the speed of propagation of the wave.

The speed of electromagnetic waves in a vacuum is called the speed of light, c, and is taken to be 299,792,458 m s⁻¹. The accuracy of an EDM instrument depends ultimately on the accuracy of the estimated velocity of the electromagnetic wave through the atmosphere.

In an EDM system, distance is measured by the difference in phase angle between the transmitted and received versions of a sinusoidal wave. The double path length (2D) between instrument and reflector is the distance covered by the radiation from an EDM measurement. It can be represented in terms of the wavelength of the measuring unit:

$$2D = n\lambda_m + \Delta\lambda_m \quad \dots\dots\dots (2.2)$$

The distance from instrument to reflector is D, λ_m is the wavelength of the measuring unit, n is the integer number of wavelengths traveled by the wave, and $\Delta\lambda_m$ is the fraction of the wavelength traveled by the wave. Therefore, the distance D is made of two separate elements. An EDM instrument using continuous electromagnetic waves can only determine $\Delta\lambda_m$ by phase comparison, fig. (2.1).

If the phase angle of the transmitted wave measured at the instrument is ω_1 , and the phase angle measured on receipt is ω_2 , then

$$\Delta\lambda_m = \frac{|\omega_2 - \omega_1|}{2\pi} \lambda_m \quad \dots\dots\dots (2.3)$$

The phase angle ω_2 can apply to any incoming wavelength, so phase comparison will only provide a determination of the fraction of a wavelength traveled by the wave, leaving the total number, n, ambiguous.

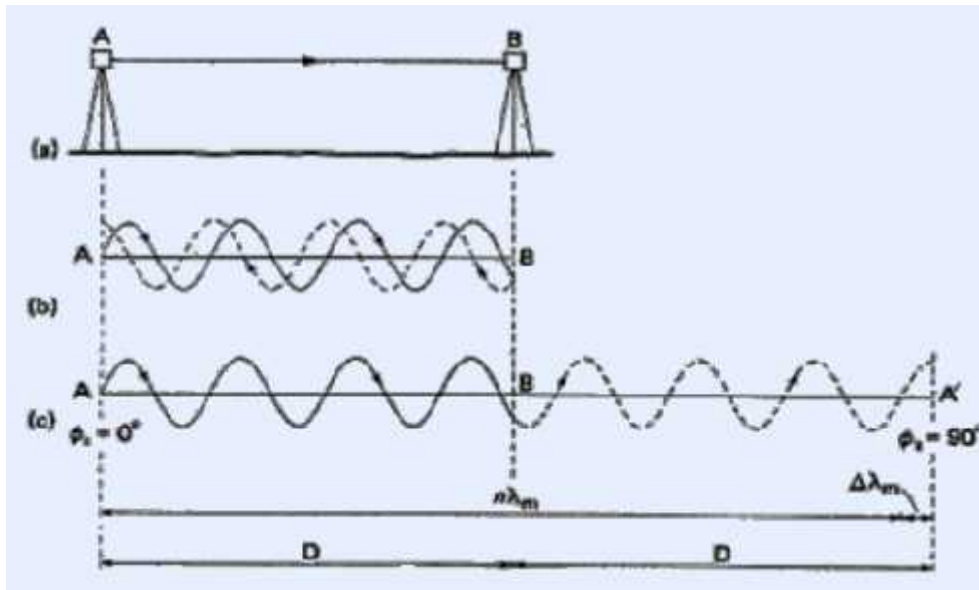


Fig. (2.1): Phase comparison, [ref.14].

From fig. (2.1):

- a. An EDM is set up at (A) and a reflector at (B) for determination of the slope length (D). During measurement, an electromagnetic wave is continuously transmitted from (A) towards (B) where it is reflected back to (A).
- b. The electromagnetic wave path from (A) to (B) has been shown, and for clarity, the same sequence is shown in (c), but the return wave has been opened out.
- c. Points (A) and (A') are effectively the same, since the transmitter and receiver would be side by side in the same unit at (A). The lowermost portion also illustrates the ideal of modulation of the carrier wave by the measuring wave, [ref.14].

2.4 Errors in Total Station

The total station is an instrument which comprise from EDM and theodolite.

The errors in distances measured by Total Station are caused by:

- a. The effects of atmospheric conditions on propagated wave velocities of light waves and electromagnetic waves in air.
- b. The differences between the effective centers of the transmitter and reflector and their respective plump lines.
- c. Transmitter nonlinearity.

2.4.1 Errors in distance measurement in Total Station

The path of electromagnetic energy is the true distance that is measured by the EDM, and will be determined by the variability in the refractive index through the atmosphere.

$$\text{Refractive index (k)} = \frac{\text{velocity in vacuum}}{\text{velocity in medium}} = \frac{c}{v} \quad \dots\dots\dots (2.4)$$

Since the medium is air, the velocity is nearly the same as that of a vacuum, and so the refractive index is nearly one, and for standard conditions may be taken to be 1.000320. The exact value of the refractive index is dependent on the atmospheric conditions of temperature, pressure, water vapor pressure, frequency of the radiated signal, and composition. Therefore, for measurements of the highest accuracy, adequate atmospheric observations must be made. Other potential error sources are from path curvature (similar to the curvature of the earth).

2.4.2 Scale error

One source of error that is adjusted for in our instrument is a scale correction in units of Part Per Million (ppm) that adjusts for slight errors in the reference frequency and in the accuracy of the average group refractive index along the line of measurement. The ppm value is set to 0 on the total station.

Atmospheric correction is one scale error adjustment that takes into account both atmospheric pressure and temperature. It is an absolute correction for the true velocity of propagation, and not a relative scale correction like reduction to sea level. To determine the atmospheric correction to an accuracy of 1ppm, measure the ambient temperature to an accuracy of 1°C and atmospheric pressure to 3 Millie Bar (mb).

For most applications, and approximate value for the atmospheric correction within about 10 ppm is adequate. This can be obtained by taking the average temperature for the day and the height above mean sea level of the survey site. A temperature change of about 10°C or a change in height above sea level of about 350 m = 35 mb varies the scale correction by only 10 ppm. The atmospheric correction is computed in accordance with the following formula:

$$\Delta D = 281.8 - 0.29065P + 0.00366T \quad \dots\dots\dots (2.5)$$

Where:

ΔD = atmospheric correction (ppm),

P = atmospheric pressure (mb),

T = ambient temperature (°C).

Temperature is measured in either degrees Fahrenheit or degrees Celsius, and the two are related by:

$$^{\circ}C = \frac{5}{9} * (^{\circ}F - 32) \quad \dots\dots\dots (2.6)$$

For extreme conditions of 30°C temperature change and 100 mb pressure change, one can expect variations in scale error of 50 ppm in a day. This maximum value is ten times greater than the stated initial accuracy of the instrument, and therefore should be accounted for by adjusting the scale error on the theodolite occasionally during the day's surveying effort.

The correction in ppm for the reduction to mean sea level is based upon the formula:

$$\Delta D^2 = -10^3 \frac{H}{R} \quad \dots\dots\dots (2.7)$$

Where:

ΔD^2 = reduction to Mean Sea Level (MSL) in ppm, H = height of EDM above MSL, and R = 6378 km (Earth Radius), [ref.3].

2.5 Applications of the Total Station

- Layout of control points on or offset to construction lines.
- Checking or tying in to property boundaries.
- Layout of excavation lines.
- As-built checks.
- Layout of construction control lines on concrete pad for subcontractor use
- Light topographical measurements for cut/fill balance

CHAPTER

3

AERIAL PHOTOGRAMMETRY

The following contents are going to be covered in this chapter:

3.1 Overview

3.2 Type of photographs

3.3 Taking vertical aerial photographs

3.4 Acquisitions of aerial photos

3.5 Stereoviewing

3.6 Parallax angle

3.7 X- Parallax

3.8 Two images - not one!

3.9 Specifications for ground control

3.10 Types of control points

3.11 Space resection

3.12 Stereoplotters

3.13 Types of Stereoplotters

3.14 Stereoplotter operations

3.15 Image matching

3.16 Aerotriangulation

3.17 Digital Elevation Model (DEM)

CHAPTER THREE

Aerial Photogrammetry

3.1 Overview

Photogrammetry was being defined by American society for Photogrammetry and remote sensing as art, science, and technology of extract according to process of recording, measuring, also interpretation of signature analysis.

Photogrammetry divided into geometrical and interpretation, geometrical information implies planning cities (master plane) also measurement coordinates and other recorded information but interpretation is to interpret the photos according to pattern, tone, shape, size, texture and shadow, so visual interpretation is the most information obtained from interpretation, exceed that some time to make easy measurement such as areas, distance but not the accuracy such as geometry Photogrammetry, [ref.6].

3.2 Type of photographs

Photographs used in photogrammetry are classified into two types according to camera altitude:

Terrestrial photographs: this type is taken by cameras that have altitude nearest to ground (the positional orientation of which are measured directly at the time exposure. There are variety examples of which type such as phototheodolite ballistic camera.

The second type of photos are aerial photographs taken by plane or by satellite, this means the exposure of photos may be recorded directly by GPS or with suitable evaluation after exposed photo according to suitable known coordinates (control point).

The quality of the photo that was exposed depends on the condition of exposure so these photos may be vertical or oblique, fig. (3.1).

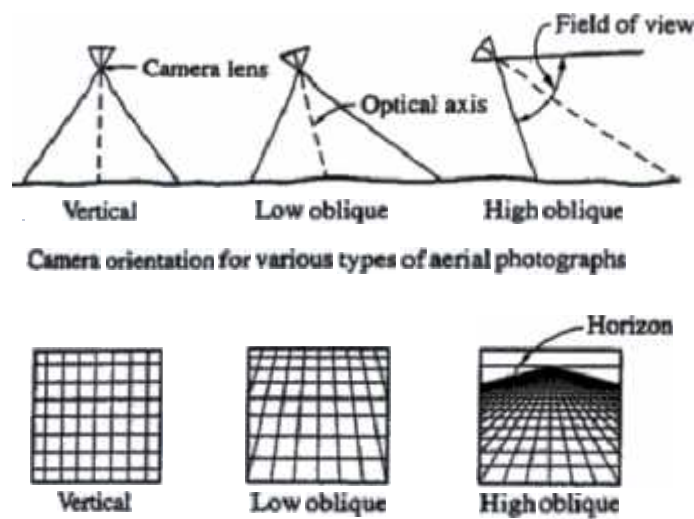


Fig. (3.1): Camera orientation, [ref.6].

Vertical photos: defined as the optical axis of the camera is perpendicular to the ground and this is the best condition to extract the geometrical information.

Oblique photos : the optical axis is tilt to the ground from (3° - 90°) so an oblique may be high or low according to the tilt angle, if the horizon appear then the photo is high oblique.

Unfortunately vertical photo are seldom obtained in practical condition so in metric calculation, photo accepted if the tilt less than 1° and seldom exceed 3° , [ref.6].

3.3 Taking vertical aerial photographs

Photographs are usually taken along a series of parallel passes take in consideration the good coverage, the overlap coverage must be include, such as forward coverage (end lap) with and between the flight line, to ensure that three 3D vision had been obtained overlap must be 55-65%, and side lap coverage between parallel flight line normally approximately 30% to ensure a good coverage and no areas left without photographed.

The adjacent photos called a pairs of photos and their overlap is stereo overlap, fig.(3.2).

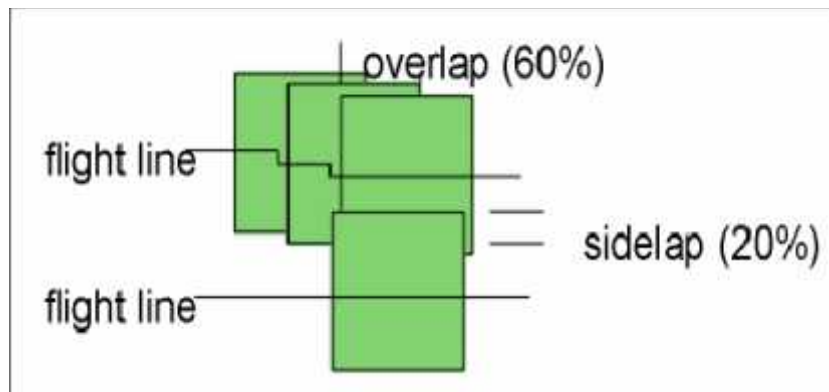


Fig. (3.2): End lap & Side lap, [ref.11].

Block is the adjacent side lap photo, the flight line is the direction or bath of the plane traveling, that taken as an X-axis in the calculations.

3.4 Acquisitions of aerial photos

3.4.1 Scanners

Photogrammetric scanners are devices used to convert the content of photographs from analog form (a continuous-tone image) to digital form (an array of pixels with their gray levels quantified by numerical values).

Once the image is in digital form, coordinate measurement can take place in a computer environment, either through a manual process involving a human operator who points at features displayed on a computer screen, or through automated image-processing algorithms.

A number of photogrammetric quality scanners are commercially available. They vary in approaches taken in the digital conversion (or quantization); however their fundamental concepts are the same. It is essential that a photogrammetric scanner have:

- **Sufficient geometric**

Geometric or spatial resolution of a scanner is an indication of the pixel size of the resultant image. The smaller the pixel size, the greater the detail that can be detected in the image.

- **Radiometric resolution**

Radiometric resolution of a scanner is an indication of the number of quantization levels (corresponding to image density differences) associated with a single pixel. Minimum radiometric resolution should be 256 levels (8-bit) with scanners being capable of 1024 levels (10-bit) or higher.

The geometric quality of a scanner can be expressed by the positional accuracy of the pixels in the resultant image. If a digital image is to produce the same level of accuracy as is attainable by using film images and a comparator, the positions of the pixel in the digital image need to be at the same spatial accuracy. Hence, the

geometric positional accuracy of a high-quality photogrammetric scanner should be at the 2- to 3- μm level.

High-quality photogrammetric scanners should be capable of producing digital images with minimum pixel sizes on the order of 5 to 15 μm . This roughly corresponds to the resolution threshold of typical aerial photographs under actual flight conditions, [ref.6].

3.4.2 Digital cameras

3.4.2.1 Flying spot scanners

They are structured basically by a rotating mirror and a detector, while the aircraft moves the reflect the image to the detector (sensor), the mirror rotates perpendicular to the flight direction so second direction of the image is achieved by the aircraft movement, fig. (3.3).

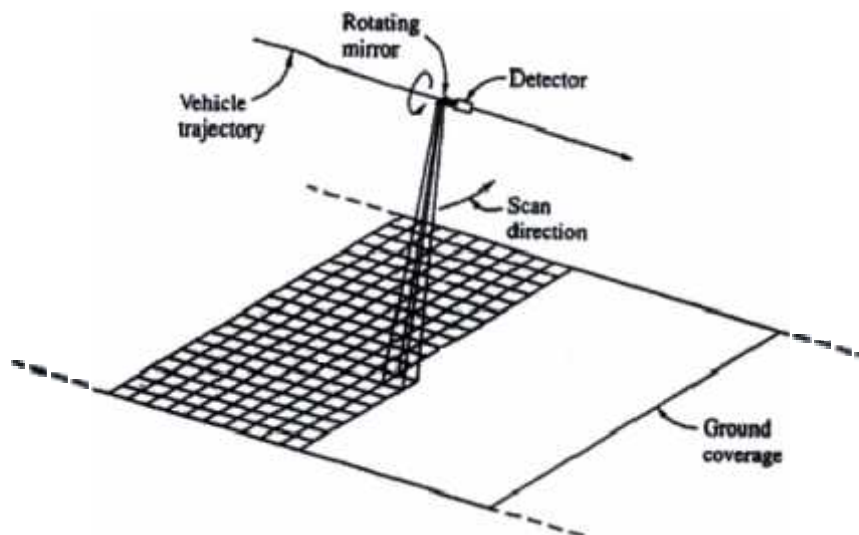


Fig. (3.3): Geometry of flying spot scanner, [ref.6].

3.4.2.2 Linear array sensor

Charged Coupled Devices (CCD's) are fixed to get the image vertical or by fixed and forward or backward, so that stereoscopic vision can be achieved. CCD's can produce panchromatic or true color or multispectral color. Panchromatic can be interpolated to sub pixel. Linear CCD cameras have a good geometric quality with less distortion, fig. (3.4).

Because the trajectory of the aircraft is uncertain, it is important to have a high precision position of sensors, so to solve the problem inertial navigation system is attached, using accelerometer to measure the acceleration, and gyroscopes to measure the rotation angles (ω ϕ K), in addition to precise GPS receivers, otherwise sensed image is unusable, The residual in CCD camera are around 0.1 pixel.

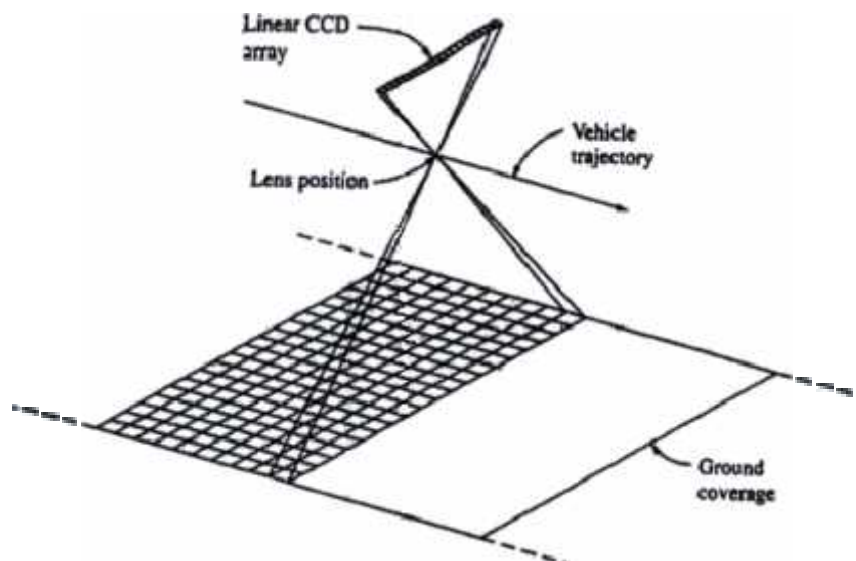


Fig (3.4): Geometry of a linear array sensor, [ref.6].

3.4.2.3 Digital frame camera

The effect of large forward movement of aircraft is eliminated, so allows longer exposure duration, and good results in weak lighting, Typical matrix CCD camera has image size of 7000*9000, and its principle as traditional camera, using conical image geometry, CCD matrix have different colors filter, can be in one camera with different filter, or different equipments one for each other, the geometry in the camera is excellent compared to traditionally camera because of film processing, printing, film movement, and dust on the film are neglected, Camera still need calibration as traditional cameras, fig. (3.5).

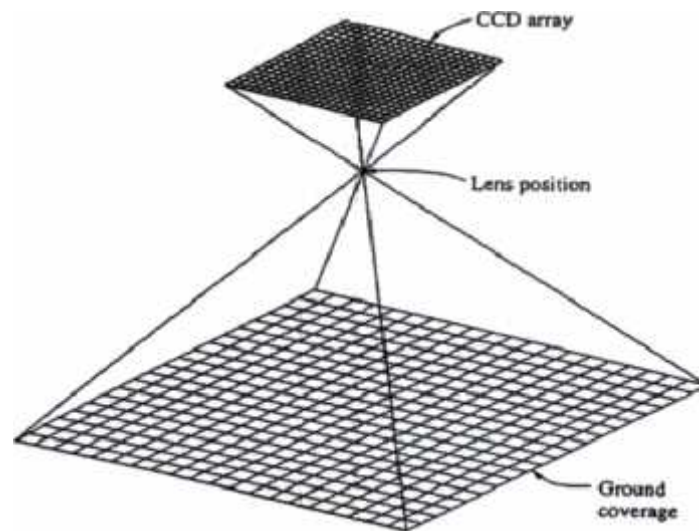


Fig. (3.5): Geometry of a digital frame camera, [ref.6].

3.5 Stereoviewing

Stereo viewing is to visualize to the overlap photos using suitable stereo, such as pocket stereo, mirror stereoscope, the stereo viewing is dependent on the X-parallax and parallax angle, fig. (3.6).

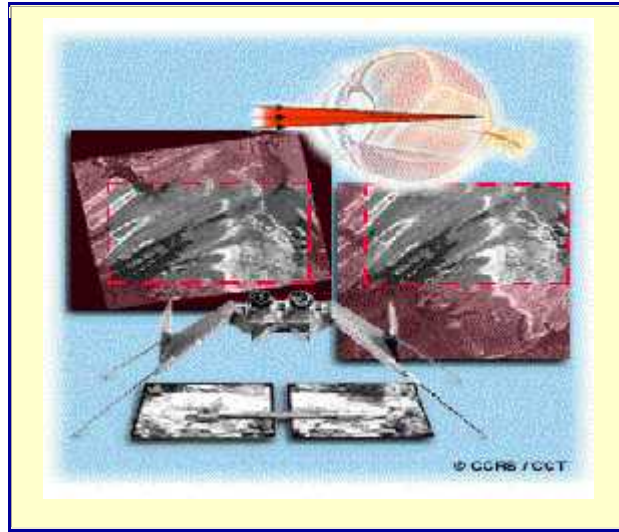


Fig. (3.6): Stereoviewing, [ref.9].

Pocket stereo has limitation of required spacing between corresponding images is slightly more than 5 cm.

The conjoined points is the point on photo and the repeat on the other are very important to have simple calculated assumed photos are truly vertical.

3.6 Parallax angle

The parallax angle, also known as the convergence angle, is formed by the intersection of the left eye's line of sight with that of the right eye. The closer this point of intersection is to the eyes, the larger the convergence angle. The brain perceives the height of an object by associating depth at its top and its base with the convergence angles formed by viewing the top and base, fig. (3.7).

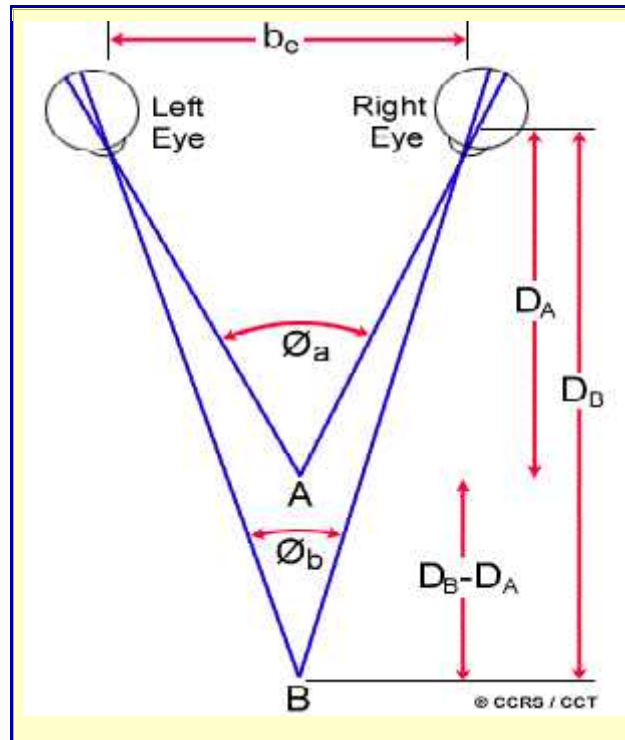


Fig. (3.7): Parallaxic angle, [ref.9].

The X parallax and the parallaxic angle are related. As X parallax increases, so too does the parallaxic angle, as the eyes scan overlapping areas between a stereo image pair, the brain receives a continuous 3-D impression of the ground. This is caused by the brain constantly perceiving the changing parallaxic angles of an infinite number of image points making up the terrain. The perceived 'virtual' 3-D model is known as a stereomodel, [ref.9].

3.7 X- Parallax

Parallax is defined as the stereoscopic parallax, caused by shift in the position of observation, so to ensure parallax the aircraft take the first photo at certain time, then the other is taken at different time, then conjected point have been established, X-Parallax is very important to stereovision also to mathematical calculation to

determine the elevation, position according to float mark make dislanding at same elevation.

$$h = H - \frac{Bf}{Pa} \dots\dots\dots(3.1)$$

Where:

h: elevation at point .

H: elevation at aircraft.

B: air base.

f: camera focal length.

The Position is:

$$X = \frac{BXa}{Pa} \dots\dots\dots(3.2)$$

$$Y = \frac{BYa}{Pa} \dots\dots\dots(3.3)$$

Where:

(Xa, Ya):photo coordinate

Parallax may be measured with bar parallax or by calculation of photo coordinates fig. (3.8).

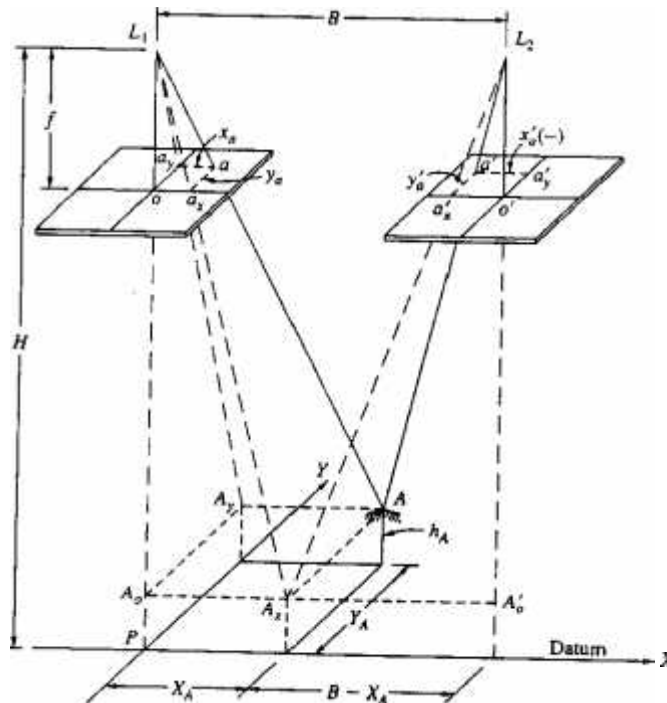


Fig. (3.8): Geometry of an overlapping pair of vertical photographs, [ref.6].

To ensure the parallax on imagery photo, satellite collects data with two different look angles or two different beam positions, [ref.6].

3.8 Two images - not one!

Generally monoscopic and stereoscopic each of them has a certain application according to the case, but viewing earth surface in stereo provide the interpreters with more qualitative and quantitative information than the single photo, multi users had been used stereo viewing in their work such as, geological, hydrologists, scientists, engineers.

Stereo give the information about slopes, shapes more clearly than 2D representation, also can clear the relationships between features and minerals and drainage systems that are not obvious from single images.

Stereoscopic you can extract metric information with full component X,Y,Z and generate the digital elevation model, but on single photo 2D (X,Y) may be obtained and rectified photo to generate the orthophoto that haven't Z component, fig. (3.9).

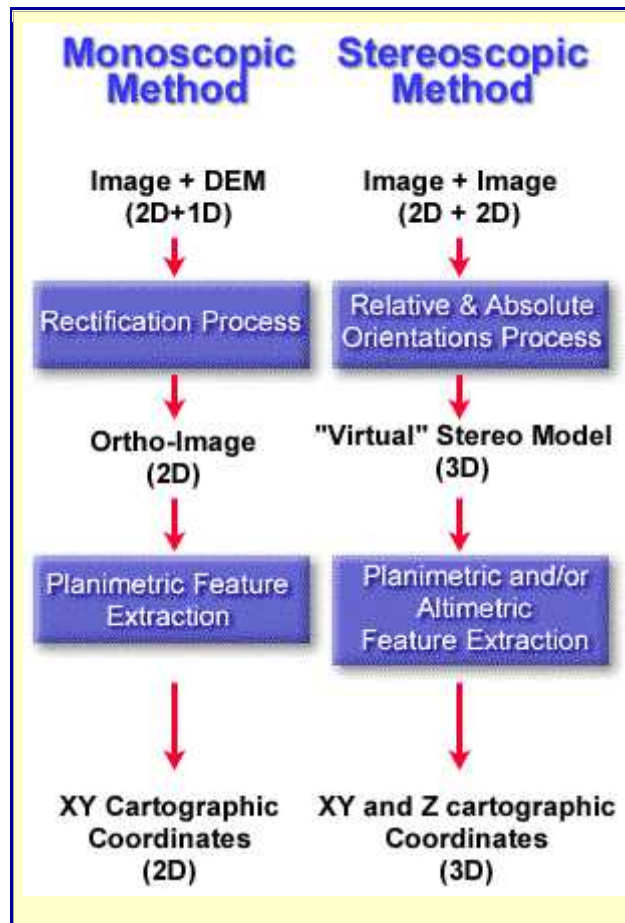


Fig. (3.9): 2D versus 3D viewing methods, [ref.9].

Stereopair directly provide X,Y,Z according to mathematical solution specially collinearity equations (APPENDIX B) this condition states that the exposure center, the location of ground point and its image point that all lie on the same line.

Orthophoto, accuracy depend on the accuracy of the DEM, errors in DEM will propagate through orthophoto generation and feature extraction process, as a result planimetric feature extracted from the stereo model is less accuracy than the orthophoto or is a rectification, so in digital each pixel must be relocate to its correct location, so resampling add anew error to these product but stereo viewing extract data done directly on the raw images (without resampling). It has been proven that

the ability to identify certain features in mono images is more difficult than in stereo. In thematic applications, stereo display gives a clear perception of terrain to better locate features such as control points, forest cover, clear cuts, and river and stream beds, [ref.9].

3.9 Specifications for ground control

The aim of ground control is to provide identified locations within the stereo overlap which have known coordinates, in order to allow an exterior or absolute orientation of the stereomodel.

The definition of a ground control point is an artificial or natural point on a photograph which has one to three coordinates which have been determined by an independent ground survey or by photogrammetric triangulation, [ref.15].

3.10 Types of control points

Generally ground control is categorized into one of three types, table (3.1).

Table (3.1): Types of ground control points, [ref.15].

Point Type	Known Coordinates	Typical Symbol
Full or 3D	XYZ	▲
Position or planimetric	XY	△
Height	Z	○

3.11 Space resection

Exposure station may be recorded at exposure time by GPS or may be calculated later. If exposure not recorded at exposure time, calculation done using space resection to determine exterior orientation three angles ($\check{S}, w, |$) and (X, Y, Z) as on the photo.

To solve the equation a minimum number of control point is three full control point.

The linearized forms of the space resection collinearity equations for apoint A is:

$$b_{11}d\check{S} + b_{12}dw + b_{13}d| - b_{14}dX_L - b_{15}dY_L - b_{16}dZ_L = J + \hat{\ }_{xa} \dots\dots\dots(3.4)$$

$$b_{21}d\check{S} + b_{22}dw + b_{23}d| - b_{24}dX_L - b_{25}dY_L - b_{26}dZ_L = J + \hat{\ }_{ya} \dots\dots\dots(3.5)$$

Where $(b_{11}, b_{12}, \dots, b_{26}, d\check{S}, dw, dk)$ is defined in appendix B.

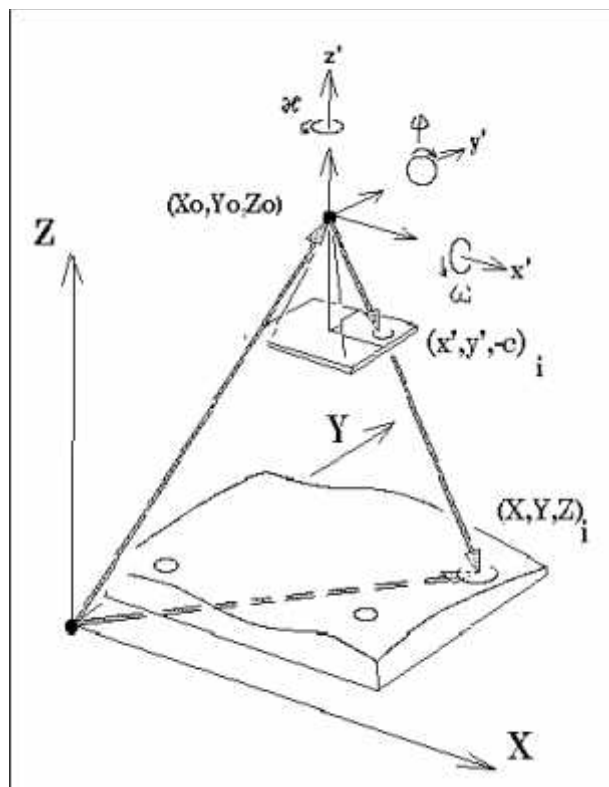


Fig. (3.10): \check{S}, w, k and X, Y, Z in space resection, [ref.13].

Collinearity is nonlinear, then linearized from according to Taylor's thermo, so initial approximation must be noted for unknown orientation parameter. Assume the photo is vertical so $\tilde{S}, w = 0$, $H=Zl$ can be computed as initial according to, [ref.6].

$$(AB)^2 = \left[\frac{xb}{f}(H - h_B) - \frac{xa}{f}(H - h_A) \right]^2 + \left[\frac{y_a}{f}(H - h_B) - \frac{y_a}{f}(H - h_A) \right]^2 \dots\dots\dots(3.6)$$

Because this equation needed two control point:

AB: ground distance between A, B.

x_a, y_a, x_b, y_b : Photo coordinates.

f: camera focal length.

Kappa may be determine according tow dimensional conformal coordinates transformation

$$X = ax' - by' + Tx \dots\dots\dots(3.7)$$

$$Y = ay' - bx' + Ty \dots\dots\dots(3.8)$$

Where:

x', y' : photo coordinate

X, Y : ground coordinate

T_x, T_y : Translation

a, b :factors

$$| = \tan^{-1}\left(\frac{a}{b}\right) \dots\dots\dots(3.9)$$

$$XL = T_x$$

$$YL = T_y$$

3.12 Stereoplotters

A general overview of existing stereoplotter designs and general operating procedures is presented in next section, for the purposes of this study, only instruments that perform a complete restitution of the interior and exterior orientation

of the photography taken will be considered. Since the inception of commercially viable photogrammetry in the 1930s, several generations of Stereomapping systems have become obsolete, only those which are capable of generating digital geospatial data will be discussed in next section.

3.13 Types of stereoplotters

The three main component systems in all stereoplotters are the projection, viewing, measuring, and tracing systems. Stereoplotters are most often grouped according to the type of projection system used in the instrument.

3.13.1 Analytical stereoplotters

Analytical stereoplotters use a mathematical image ray projection based on the collinearity equation model. The mechanical component of the instrument consists of a precise computer controlled stereo comparator. Since the photo stages must move only in the x and y image directions, the measurement system can be built to produce a highly accurate and precise image measurement. The x and y photo coordinates are encoded, and all interior and exterior orientation parameters are included in the mathematical projection model. Except for the positive format size that will fit on the photo stage, the analytical stereoplotter has no physical constraints on the camera focal length or model scale that can be accommodated, fig. (3.11), [ref.15].



Fig. (3.11): Typical analytical stereoplotter, [ref.15].

The viewing system is an optical train system typically equipped with zoom optics. The measuring mark included in the viewing system may be changeable in style, size, and color. The illumination system should have an adjustable intensity for each eye.

The measuring system consists of an input device for the operator to move the model point in three dimensions. The input device is encoded, and the digital measure of the model point movement is sent to the computer. The software then drives the stages to the proper location accounting for interior and exterior orientation parameters, fig. (3.12), these operations occur in real time so that the operator, looking in the eyepieces, sees the fused image of the floating mark moving in three dimensions relative to the stereomodel surface.

The operator's input device for model position may be a hand-driven free-moving digitizer cursor on instruments designed primarily for compilation, or it may be a hand wheel/foot disk control or similar device on instruments supporting fine pointing for aerotriangulation.

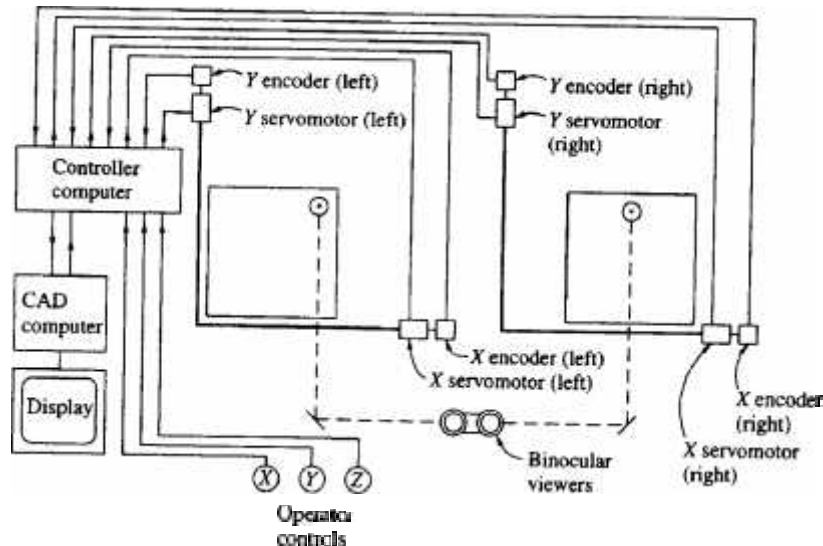


Fig. (3.12): Schematic diagram of components and operation of analytical plotter, [ref.6].

Analytical stereoplotters are accurate because the interior orientation parameters of the camera are included in the projection software. Therefore, any systematic error in the photography can be corrected in the photo coordinates before the photogrammetric projection is performed. Correcting for differential film deformations, lens distortions, and atmospheric refraction justifies measuring the photo coordinates to accuracies of 0.003 mm and smaller in analytical stereoplotters. To achieve this accuracy, the analytical stereoplotter must have the capability to perform a stage calibration using measurements of reference grid lines etched on the photo stage.

3.13.2 Digital stereoplotters

The latest generation of stereoplotters is the digital (or softcopy) stereoplotter, these instruments will display a digital image on a workstation screen in place of a film or glass diapositive. The instrument operates as an analytical stereoplotter except that

the digital image will be viewed and measured. The accuracy of digital stereoplotters is governed by the pixel size of the digital image. The pixel size directly influences the resolution of the photo coordinate measurement. A digital stereoplotter can be classified according to the photo coordinate observation error at image scale. Then it should be comparable to an analytical stereoplotter having the same observation error, and the standards and guidelines in this manual should be equally as applicable. At the time of writing this document, the generally accepted guidance is that softcopy and analytical stereoplotters can achieve the same resulting map accuracies for most projects. Some projects may require that the aerial photography be captured at a lower altitude to achieve required accuracies. The Contractor's opinion regarding softcopy data (flight heights, image scanning specifications) requirements should be considered. Softcopy stereoplotters, fig. (3.13), shows a typical softcopy workstation.



Fig. (3.13): Typical softcopy workstation, [ref.15].

3.14 Stereoplotter operations

Models in stereoplotters must be georeferenced to the ground for measuring or mapping in three consecutive steps: interior, relative, and absolute orientation.

3.14.1 Interior orientation

Interior orientation involves placing the photographs in proper relation to the perspective center of the stereoplotter by matching the fiducial marks to corresponding marks on the photography holders and by setting the principal distances of the stereoplotter to correspond to the focal length of the camera (adjusted for overall film shrinkage). This requires camera calibration information as well as quantification of the effects of atmospheric refraction. These procedures, commonly called photo coordinate refinement.

3.14.2 Relative orientation

Relative orientation involves reproducing in the stereoplotter the relative angular relationship that existed between the camera orientations in space when the photographs were taken. This is an iterative process and should result in a stereoscopic model easily viewed, in every part, without "Y-parallax" the separation of the two images so they do not fuse into a stereoscopic model. When this step is complete, there exists in the stereoplotter a stereoscopic model for which 3-D coordinates may be measured at any point; but it may not be exactly the desired scale, it may not be level, and water surfaces may be tipped. According this model the process involves, fig. (3.14).

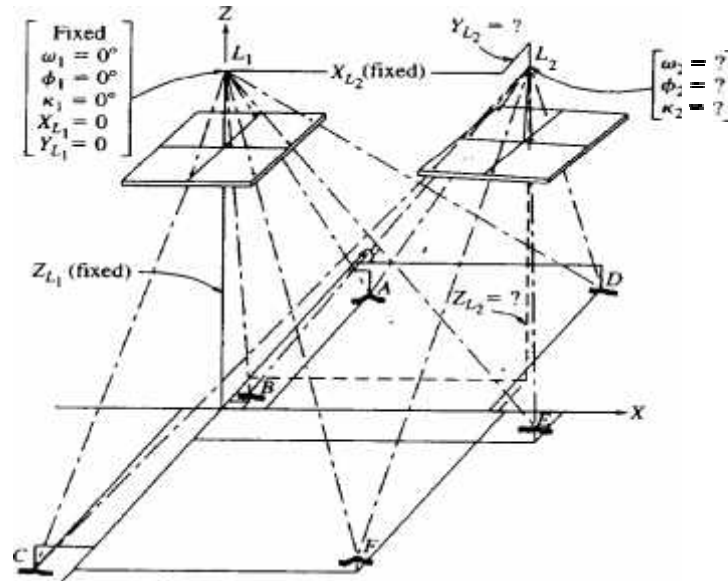


Fig. (3.14): Analytical relative orientation of a stereopair, [ref.6].

- Fix the exterior orientation elements \dot{S}, w, K, X_L and Y_L of the left photo of the stereopair to zero values.
- Also for convenience, Z_L of the left photo Z_{L1} is set equal to f ,
- And X_L of the right photo X_{L2} is set equal to the photo base b .

(With these choices for Z_{L1} and X_{L2} , initial approximations for the unknowns are more easily calculated, as will be explained later.)

- This leaves five elements of the right photo that must be determined, fig. (3.14) illustrates a stereomodel formed by analytical relative orientation.

Although the coplanarity condition equation can be used for analytical relative orientation, the collinearity condition is more commonly applied.

In applying collinearity, each object point in the stereomodel contributes four equations: a pair of equations for the x and y photo coordinates of its image in the

left photo, and a pair of equations for the x and y photo coordinates of its image in the right photo. In addition to the five unknown orientation elements, each object point adds three more unknowns which are their X, Y, and Z coordinates in the stereomodel.

Thus each point used in relative orientation results in a net gain of one equation for the overall solution, and therefore at least 5 object points are required for a solution. If 6 or more points are available, an improved solution is possible through least squares. If 6 points were used for relative orientation, a system of 24 equations with 23 unknowns would result: and if 12 points were used, the system would consist of 48 equations and 41 unknowns.

Prior to solving the linearized collinearity equations, initial approximations for all unknown values must be determined. For photography that was intended to be vertical, values of zero are commonly used for initial estimates of \check{S}_2, w_2, K_2 , and Y_{L2} . An initial value for Z_{L2} may be selected equal to the value used for Z_{L1} . If the constraints that were noted earlier are used for the parameters, that is, $\check{S}_1 = w_1 = K_1 = X_{L1} = Y_{L1} = 0$, $Z_{L1} = f$, and $X_{L2} = b$, then the scale of the stereomodel is approximately equal to photo scale. Thus the x and y photo coordinates of the left photo are good approximations for X and Y object space coordinates, and zeros are good approximations for Z object space coordinates, respectively.

3.14.3 Absolute orientation

Absolute orientation uses the known ground coordinates of points identifiable in the stereoscopic model to scale and to level the model. When this step is completed, the X, Y, and Z ground coordinates of any point on the stereoscopic model may be measured and/or mapped.

For a small stereomodel such as that computed from one stereopair, analytical absolute orientation can be performed using a three-dimensional conformal coordinate transformation.

This requires a minimum of two horizontal and three vertical control points, but additional control points provide redundancy, which enables a least squares solution.

In the process of performing absolute orientation, stereomodel coordinates of control points are related to their three-dimensional coordinates in a ground-based system. It is important for the ground system to be a true Cartesian coordinate system, such as local vertical, since the three dimensional conformal coordinate transformation is based on straight, orthogonal axes.

Once the transformation parameters have been computed, they can be applied to the remaining stereomodel points, including the X_L , Y_L and Z_L coordinates of the left and right photographs. This gives the coordinates of all stereomodel points in the ground system, [ref.6].

3.15 Image matching

Digital image is a finite two dimensional image a set of digital values which known pixel or picture element, digital image represented by binary values (bits) according to electromagnetic intensity.

Softcopy use the digital image, so some orientation of photos may be done without display the photos, according to generate pass point or tie point this done by image matching to locate specific point and search to their conjugate according to image matching and suitable best of correlation.

Image matching is a technique to determine identical points in two or more images according to area based matching or feature based matching, area based matching dealing with gray value (colors) according to suitable window, such as linear,

- Cross correlation.
- Least square differences.
- Centered least square.
- Scalar product.

3.16 Photogrammetry

Providing control by ground survey for every stereopair in a large block is very costly and inefficient, but photogrammetry is a control densification technique which avoids the cost of a full ground survey, photogrammetric observations and a least squares estimation solution are used to coordinate additional points visible on the photographs, based on a much reduced control point array from survey, the new points are known as "pass" points and can be points of natural detail or be physically marked on the photographic emulsion, physical marking may be done by stick-on markers, by mechanically drilling a hole in the emulsion or by burning a hole with a very fine laser. In each case an annulus or marker points are also made in order to easily and unambiguously locate the point.

The point marking must be done in stereo (special instruments are available to do this) to ensure the surface detail is appropriate, however the point is only marked on one photograph in a forward or side overlap, both as an efficiency and to avoid any appearance of the marker floating or sinking relative to the surface, these points are difficult to observe because they only appear on one photograph, as the observer must fuse the stereomodel and "see" the marked point on the surface, the most

efficient pattern of pass points is the classic von Gruber layout of six points in a "H" pattern.

The photographs/overlaps are usually staggered between runs to optimize the coverage or simply because the navigation is not absolutely perfect, however it is also convenient for physically marked points so that the pass points are only ever marked on one photograph in a side overlap, side overlap points are often called "tie" points because they tie the strips together, control points must still be provided to establish the orientation of the strip or block relative to the datum, fig. (3.15).

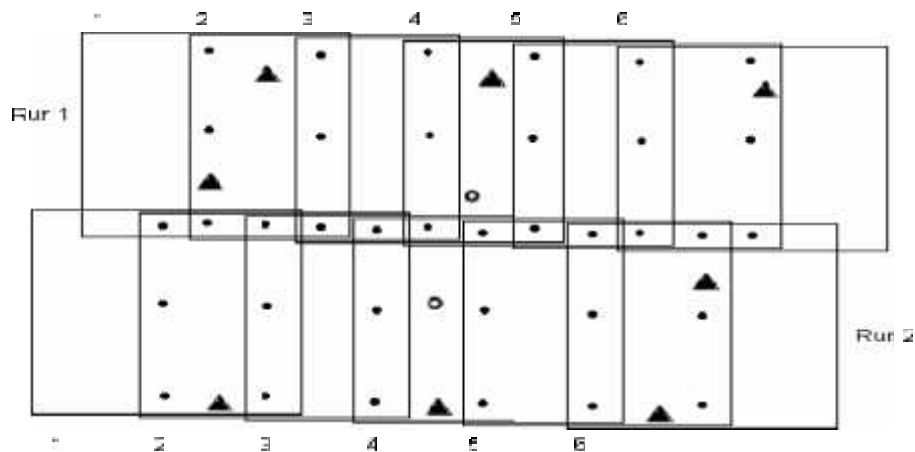


Fig. (3.15): Block of photos in overlapped position, [ref.6].

The requirement for ground control will continue to diminish because of GPS receivers, if the position of the camera station is known with precision estimates, this data can be used to constrain the aerotriangulation solution, some ground control will always be necessary as a check, but it may be reduced to a few points in even very large blocks of photographs, [ref.6].

3.17 Digital Elevation Model (DEM)

Digital elevation model is statistical representation of continuous surface of the ground by large number of related point with known X, Y, Z coordinates in arbitrary distribution in field.

DEM: is representation of elevation that used to generate contour or the built orthophoto map and other application.

DEM: represented either by mathematically defined surface or by point, line (contour), the methods that are used in GIS to represent the DEM.

1. Regular grids (altitude matrices)
2. Triangular Irregular Network (TIN)

DEM is simply called Digital Terrain Model (DTM) that related to Digital Surface Model (DSM).

Digital Surface Models (DSMs) are topographic elevation models of the earth's surface that provide you with a geometrically correct reference frame over which other data layers can be draped. The (DSM) data includes buildings, vegetation, and roads, as well as natural terrain features.

Digital Terrain Model (DTM), or "bald earth" in which it is often referred, is created by digitally removing all of the cultural features inherent to a DSM by exposing the underlying terrain, DTM generated using workstation stereoploter, in digital form each of grid has elevation that calculated by the principle of image matching described previous,[ref.6].

DEM accuracy: Vertical accuracy of DEM is simply the average vertical error of potentially all points interpolated within DEM grid accuracy of the data profiles, also the data scale and resolution.

There are no generally accepted specifications about the accuracy of DEM in relation to the type of terrain or in relation to grid size of the DEM.

There are only vague values of thumb concerning the relation with grid size.

A 5m grid expects to be very accurate to perhaps 10 to 25 cm RMSE in case of smooth terrain and perhaps at least two time for rough terrain excluding rocky areas, for 10 to 50 grid spacing RMSE exposed to be about 0.5m perhaps 2.5m in smooth cause, as general thumb of rule vertical accuracy of DEM may be determine:

1. (1/20) th of the grid size in smooth case.
2. (1/10) th of the grid size in rough case.

CHAPTER

4

ACCURACY STANDARDS

The following contents are going to be covered in this chapter:

4.1 Overview

4.2 Error sources

4.3 Survey accuracy standards

4.4 Map accuracy standards

4.5 Map testing

4.6 Photogrammetry accuracy standards

4.7 Relation ship between NSSDA and other accuracies

4.8 Relationship between NSSDA and NMAS

4.9 ASPRS classes

CHAPTER FOUR

Accuracy Standards

4.1 Overview

The term accuracy refers to the closeness between measurements and their expectations (or, in conventional terms, to their true values). The farther a measurement is from its expected value, the less accurate it is. Precision, on the other hand, pertains to the closeness to one another of a set of repeated observations of a random variable. Thus, if such observations are closely clustered together, then the observations are said to have been obtained with high precision. It should be apparent, then, that observations may be precise but not accurate if they are closely grouped together but about a value that is different from the expectation (or true value) by a significant amount. Also, observations may be accurate but not precise if they are well distributed about the expected value but are significantly dispersed from one another. Finally, observations will be both precise and accurate if they are closely grouped around the expected value (or the distribution mean).

4.2 Error sources

4.2.1 Instrumental errors.

These errors are caused by imperfections in instrument construction or adjustment. For example, the divisions on a Theodolite or total station instrument may not be spaced uniformly. These error sources are present whether the equipment is read manually or digitally.

4.2.2 Natural errors.

These errors are caused by changing conditions in the surrounding environment. These include variations in atmospheric pressure, temperature, wind, gravitational fields, and magnetic fields.

4.2.3 Personal errors

These errors arise due to limitations in human senses, such as the ability to read a micrometer or to center a level bubble. The sizes of these errors are affected by personal ability to see and by manual dexterity. These factors may be influenced further by temperature, insects, and other physical conditions that cause humans to behave in a less precise manner than they would under ideal conditions.

Some of these errors result from physical conditions that cause them to occur in a systematic way, whereas others occur with apparent randomness. Accordingly, errors are classified as either systematic or random. But before defining systematic and random errors, it is helpful to define mistakes. These three terms are defined as follows:

1) Mistakes.

These are caused by confusion or by an observer's carelessness. They are not classified as errors and must be removed from any set of observations. Such as (a) mistakes in reading graduated scales, and (b) blunders in recording.

2) Systematic Errors.

These errors follow some physical law and thus can be predicted. Some systematic errors are removed by following correct measurement procedures (e.g., balancing

back sight and foresight distances in differential leveling to compensate for earth curvature and refraction). Others are removed, by deriving corrections based on the physical conditions that were responsible for their creation (e.g., applying a computed correction for earth curvature and refraction on a trigonometric leveling observation. Additional examples of systematic errors are (a) temperature not being standard while taping, (b) an index error of the vertical circle of a Theodolite or total station instrument, and (c) use of a level rod that is not standard length. Corrections for systematic errors can be computed and applied to measurements to eliminate their effects.

3) Random Errors.

These are the errors that remain after all mistakes and systematic errors have been removed from the measured values. In general, they are the result of human and instrument imperfections. They are generally small and are as likely to be negative as positive. They usually do not follow any physical law and therefore must be dealt with according to the mathematical laws of probability. Examples of random errors are:

- (a) Imperfect centering over a point during distance measurement with an EDM instrument.
- (b) Bubble not centered at the instant a level rod is read.
- (c) Small errors in reading graduated scales. It is impossible to avoid random errors in measurements entirely. Although they are often called accidental errors, their occurrence should not be considered an accident, [ref.5].

4.3 Survey accuracy standards

All maps warranting accuracy classification must be referenced to, or controlled by, conventional field surveys. The surveying standards are independent of these map accuracy standards. Survey accuracies based on relative closure estimates cannot necessarily be correlated with map accuracy positional error estimates. Survey accuracy is a function of the specifications and a procedure used, the resultant internal or external closures, and is independent of the map scale or map contour interval. The accuracy of the conventional field survey used to test the map accuracy must exceed that of the map.

4.3.1 Palestine traverse standards

The Palestinian department of surveying at the Palestinian ministry of housing allows the following errors in traverse, table (4.1).

Table (4.1): Allowable error in closed traverse in Palestinian standards, [ref.4].

Measurement type	Allowable error	
	Important areas (Urban)	Less important areas (Rural)
Measured distances (m)	$\Delta L = 0.0005L + 0.03$	$\Delta L = 0.0007L + 0.03$
Angle closure error (sec)	$\Delta = 60''\sqrt{n}$	$\Delta = 90''\sqrt{n}$
Linear closure error (m)	$v = 0.0006\sum L + 0.20$	$v = 0.0009\sum L + 0.20$

Where:

L= Measured length (m).

Δ = Angle closure error (sec).

ΔL = Difference between two measurements of one line (m).

n= Number of measured angles.

4.3.2 FGDC Relative Accuracy Standards for Horizontal and Vertical Control

When a horizontal control point classified with a particular order and class, the National Geodetic Standards (NGS), which is also known as Federal Geographic Data Committee (FGDC), certifies that the geodetic latitude and longitude of that control point bear a relation of specific accuracy to the coordinates of all other points in the horizontal control network.

This relation expressed as distance accuracy (1: a), distance accuracy is the ratio of the relative positional error of a pair of control points to the horizontal separation of those points, table (4.2).

Table (4.2): FGDC horizontal distance accuracy standards, [ref.3].

Survey classification	Minimum distance accuracy (ratio)
First order	1:100000
Second order, class 1	1:50000
Second order, class 2	1:20000
Third order, class 1	1:10000
Third order, class 2	1:5000

The distance accuracy (1: a) is defined in Equation

$$a=d/s \dots\dots\dots (4.1)$$

In which:

a = distance accuracy denominator

d = distances between survey points

s= propagated standard deviation of distance between survey points obtained from a weighted and minimally constrained least squares adjustment.

The vertical FGDC accuracy standards can be summarized in the following table.

Table (4.3): FGDC vertical distance accuracy standards, [ref.3].

Survey classification	Maximum elevation difference accuracy, mm/km
First order, class 1	0.5
First order, class 2	0.7
Second order, class 1	1.0
Second order, class 2	1.3

4.3.3 Horizontal control accuracy standards for traverses (FGCS, 1994)

The FGCS horizontal control accuracy standards for traverse of year 1994 can be summarized in the following table.

Table (4.4): Horizontal control accuracy standards for traverses (FGCS), [ref.3].

Order class	First	Second		Third	
		1	2	1	2
azimuth closer at azimuth check point	$1.7\sqrt{N}$	$2.0\sqrt{N}$	$2.5\sqrt{N}$	$1.0\sqrt{N}$	$1.2\sqrt{N}$
Position closer after azimuth adjustment	$0.4\sqrt{K}$ OR 1:100000	$0.4\sqrt{K}$ OR 1:50000	$0.2\sqrt{K}$ OR 1:20000	$0.4\sqrt{K}$ OR 1:10000	$0.8\sqrt{K}$ OR 1:5000

In which:

N is number of segment.

K is root distance in km.

4.3.4 FGCS for evaluating the local survey

Accuracies of a traverse on a local scale continue to be evaluated on the basis of ratio of misclosure (ROM) or relative positional accuracy, which is the ratio of the resultant error misclosure for the traverse to the total length of the traverse.

For example, if a traverse has a resultant closure error of 0.36m for a traverse having a total length of 1762 m. The ROM for this traverse is $0.36/1762$ or 1 part in 4894.

Allowable azimuth and position closures for 1st, 2nd and 3rd order traverses, should be checked by (FGCS), in table (4.4).

4.4 Map accuracy standards

Map accuracy is determined by comparing the mapped location of selected well-defined points to their “true” location as determined by a conventional field survey. A map accuracy standard classifies a map as statistically meeting a certain level of accuracy. Horizontal (or planimetric) map accuracy standards are usually expressed in terms of two-dimensional radial positional error measures the Root Mean Square (RMS) statistic.

Vertical map accuracy standards are in Terms of one-dimensional RMSE elevation errors. Map accuracy classifications are dependent on the specified (i.e., designed) target scale and vertical relief, or contour interval. There are six generally recognized

industry standards which can be used for specializing spatial mapping products and resultant accuracy compliance criteria.

- Office of Management and Budget (OMB), United States National Map Accuracy Standards.
- American Society of Photogrammetry (ASP) specifications for aerial surveys and mapping by photogrammetric methods for highways.
- U.S. Department Of Transportation (DOT) surveying and mapping manual map standards.
- American Society of Photogrammetry and Remote Sensing (ASPRS) accuracy standards for large scale maps.

Each of these standards has applications to different types of functional products, ranging from wide-area small-scale mapping (OMB national map accuracy standards) to large-scale engineering design (ASPRS accuracy standards for large scale maps). Their resultant accuracy criteria (i.e., spatial errors in X, Y, and Z), including quality control compliance procedures, do not differ significantly from one another. In general, use of any of these standards will result in a quality map.

4.4.1 Federal Geographic Data Committee (FGDC)

The National Standard for Spatial Data Accuracy (NSSDA) implements a testing and statistical methodology for positional accuracy of fully georeferenced maps and digital geospatial data. The NSSDA uses root-mean-square error (RMSE) to estimate positional accuracy. RMSE is the square root of the average of the set of squared differences between dataset coordinate values and coordinate values from an independent source of higher accuracy for identical points.

$$RMSE_x = \sqrt{\sum \left(X_{data_i} - X_{check_i} \right)^2 / n} \dots\dots\dots(4.2)$$

$$RMSE_y = \sqrt{\sum \left(y_{data_i} - y_{check_i} \right)^2 / n} \dots\dots\dots(4.3)$$

In which

X data i, Y data i, are the coordinates of the ith check point in the dataset.

X checks j, Y check j, are the coordinates of the jth check point in the independent more source of higher accuracy.

N is the number of the check points tested.

i is an integer ranging from 1 to n.

Horizontal error at point i is defined as:

$$\sqrt{(X_{data_i} - X_{check_j})^2 + (Y_{data_i} - Y_{check_j})^2} \dots\dots\dots(4.4)$$

Horizontal RMSE is:

$$\sqrt{\frac{(X_{data_i} - X_{check_j})^2 + (Y_{data_i} - Y_{check_j})^2}{n}} = \sqrt{RMSE_X^2 + RMSE_Y^2} \dots\dots(4.5)$$

Accuracy is reported in ground distances at the 95% confidence level. This means that 95% of the positions in the dataset will have an error with respect to true ground position that is equal to or smaller than the reported accuracy value. The reported accuracy value reflects all uncertainties, including those introduced by geodetic control coordinates, compilation, and final computation of ground coordinate values in the product.

FGDC, “Engineering, Construction, And Facilities Management “ provides accuracy standards for engineering surveys and maps used to support planning, design,

construction, operation, maintenance, and management of facilities, installations, structures, transportation systems, and related projects. It uses the NSSDA for accuracy testing and verification of fully georeferenced maps for Facility Management applications such as preliminary site planning and reconnaissance mapping. It will also provide guidance in developing positional accuracy specifications for geospatial data products, such as architectural and engineering drawings, construction site plans, regional master planning maps, and related Geographical Information Systems (GIS), [ref.12].

4.4.2 National Map Accuracy Standards (NMAS)

1. Horizontal accuracy, for maps on publication scales larger than 1:20,000, not more than 10 percent of the points tested shall be in error by more than 1/30 inch, measured on the publication scale; for maps on publication scales of 1:20,000 or smaller, 1/50 inch. These limits of accuracy shall apply in all cases to positions of well-defined points only. Well-defined points are those that are easily visible or recoverable on the ground, such as the following: monuments or markers, such as bench marks, property boundary monuments; intersections of roads, railroads, etc.; corners of large buildings or structures (or center points of small buildings); etc. In general what is well defined will be determined by what is plotted on the scale of the map within 1/100 inch. Thus while the intersection of two roads or property lines meeting at right angles would come within a sensible interpretation, identification of the intersection of such lines meeting at an acute angle would obviously not be practicable within 1/100 inch. Similarly, features not identifiable upon the ground within close limits are not to be considered as test points within the limits quoted, even though their positions may be scaled closely upon the map. In this class would come timber lines, soil boundaries, etc.

2. Vertical accuracy, as applied to contour maps on all publication scales, shall be such that not more than 10 percent of the elevations tested shall be in error more than

one-half the contour interval. In checking elevations taken from the map, the apparent vertical error may be decreased by assuming a horizontal displacement within the permissible horizontal error for a map of that scale, [ref.10].

4.4.3 United State Geological Survey (USGS) standards

The horizontal accuracy standards requires that the positions of 90% of all points tested must be accurate within 1/30 of an inch (0.05 cm) on the map measured at publication scale (scale >1:20,000). The “United States National Map Accuracy Standards” are perhaps the most widely used standards and recommended for USGS small-scale mapping.

The vertical accuracy standards require that the elevation of 90% of all points tested must be correct within half of the contour interval. On a map with a contour of 10 feet, the map must be correctly showing 90% of all points tested within 5 feet (1.5 m) of the actual elevation.

4.4.4 American Society for Photogrammetry and Remote Sensing

It provide accuracy tolerances for maps at 1:20,000-scale or large-scale maps (ASPRS Specifications larger prepared for special purposes or engineering applications.) RMSE is the statistic used by the ASPRS standards. Three map accuracy classes are defined in table (4.5). Class 1 maps are the most accurate. Class 2 maps have twice the root mean square error (RMSE) of a class 1 map; class 3 maps have thrice the RMSE of a class 1 map. Lower classifications will be more economical, but less accurate.

Table (4.5): ASPRS Planimetric Feature Coordinate Accuracy Requirement (Ground X or Y) for Well-Defined Points, [ref.8].

Target map scale (ratio)	ASPRS limiting RMSE in X or Y (m)		
	Class 1	Class 2	Class 3
1:500	0.125	0.25	0.375
1:1000	0.25	0.5	0.75
1:2000	0.5	1.0	1.5
1:2500	0.63	1.25	1.9
1:3000	0.75	1.5	2.25
1:4000	1.0	2.0	3.0
1:5000	1.25	2.5	3.75
1:8000	2.0	4.0	6.0
1:9000	2.25	4.5	6.75
1:10000	2.5	5.0	7.5
1:16000	4.0	8.0	12.0
1:20000	5.0	10.0	15.0

The project engineer/manager coupled with the ASPRS Accuracy Standards mapping specialist must determine the specific map accuracy requirement and class for a given project based on the functional requirements. The RMSE defined in terms of feet or meters at ground scale rather than in inches or millimeters at the target map scale. This results in a linear relationship between RMSE and target map scale; as map scale decreases, the RMSE increases linearly.

Vertical map accuracy defined by the ASPRS Accuracy Standards as the RMSE in terms of the project’s elevation datum for well-define points only. For Class I maps according to the ASPRS Accuracy Standards, the limiting RMSE is set at one third

the contour interval, table (4.6). Spot elevations should be shown on the map with a limiting RMSE of one-sixth the contour interval or less.

Table (4.6): ASPRS Topographic Elevation Accuracy Requirement for Well-Defined Points, [ref.8].

Target contour interval (m)	ASPRS limiting RMSE (m)					
	Topographic feature points			Spot or DEM points		
	Class 1	Class 2	Class 3	Class 1	Class 2	Class 3
0.5	0.17	0.33	0.5	0.05	0.16	0.25
1	0.33	0.66	1.0	0.17	0.33	0.5
2	0.67	1.33	2.0	0.33	0.67	1.0
4	1.33	2.67	4.0	0.67	1.33	2.0
5	1.67	3.33	5.0	0.83	1.67	2.5

This standard, like most other mapping standards, defines map accuracy by comparing the mapped location of selected well-defined points to their “true” location, as determined by a more accurate, independent field survey. When no independent check is feasible or practicable, a map’s accuracy may be estimated based on the accuracy of the technique used to locate mapped features (e.g., GPS, total station, plane table, etc.) For small-scale general location mapping work (i.e., scales smaller than 1:20,000).

4.4.5 U.S. Department of Transportation (DOT) surveying and mapping manual map standards.

These standards can be summarized in the following table.

Table (4.7): Standard accuracies for photogrammetric mapping, [ref.17].

Scale	Contour interval	Cultural Feature	Contour*	Spot Elevation	Maximum Sheet Size
1: 2000	2m accentuate 10m contour	90% shall be within 1.5m of the actual position, 10% shall not exceed 3 of the actual position,	90% shall be within 1m of the actual elevation, 10% shall not exceed 2 of the actual elevation,	90% shall be within 0.5m of the actual elevation, 10% shall not exceed 1 of the actual	1.5m Long. 0.75 wide
1: 1000	1m accentuate 5m contour	90% shall be within 0.75m of the actual position, 10% shall not exceed 1.5 of the actual position,	90% shall be within 0.5m of the actual elevation, 10% shall not exceed 1 of the actual	90% shall be within 0.25m of the actual elevation, 10% shall not exceed 0.5 of the actual	1.5m Long. 0.75 wide
1:500 & 1:300	0.5m (1:500), 0.25(1:300) accentuate Every	90% shall be within 0.3m of the actual position, 10% shall not exceed 0.6 of the actual position,	90% shall be within 0.25m of the actual elevation, 10% shall not exceed 0.5 of the actual	90% shall be within 0.12m of the actual elevation, 10% shall not exceed 0.25 of the actual	1.5m Long. 1 wide
As Determined	As Determined	90% shall be within, 10% shall not exceed of the map scale actual position	90% shall not exceed 0.5 of the contour interval of the actual elevation, 10% shall not exceed one of the contour interval	90% shall not exceed 0.25 of the contour interval of the actual elevation, 10% shall not exceed 0.5 of the contour interval	As Determined
* contours may be shifted 0.64mm to achieve the vertical requirements					

4.5 Map testing

Maps can test for accuracy by using several techniques and each agency uses its own methods.

4.5.1 American Society for Photogrammetry and Remote Sensing (ASPRS)

At least 20 checkpoints measured from the map. The points selected in an agreement between the map producer and the client. A survey party then locates the same points on the ground. Third-Order survey methods are sufficient in most cases, depending again on the map scale and the area of the project. The survey methods used for map testing must be superior to the methods used to construct the map in order to establish a truth basis.

To test horizontal features, planimetric coordinates of well-defined points scaled from the finished map in ground scale units and subtracted from the same actual coordinates obtained during the field check survey. The test checks the x and y directions separately. 'The planimetric coordinate differences inspected for any discrepancies exceeding three times the limiting RMSE according to class in table (4.7). If more than 20 points were selected for the check survey, the discrepancies in excess of three times the RMS may be thrown out; but the entire point must be discarded (x, y, z). Outlier values existing in a minimum data set of 20 must be resolved in the field. Outlier values are consider blunders and shall be resolved before an ASPRS accuracy statement printed on the finished map. The discrepancies are square the same survey datum's must use for both the mapping and check surveys. Care should take to ensure that datum's are consistent and that any datum conversion calculated properly. Any check point whose discrepancy exceeds three times the limiting RMSE should correct before the map is consider to meet the

standard. The squares summed and divided by the number of points used for the sample. This same procedure is then performing for the Y and Z coordinates.

4.5.2 Federal Geographic Data Committee (FGDC)

Horizontal accuracy shall tested by comparing the planimetric coordinates of well-defined points in the dataset with the same points from an independent source of higher accuracy. Vertical accuracy shall tested by comparing the elevations in the dataset with elevations of the same points as determined from an independent source of higher accuracy. A minimum of 20 checkpoints shall test, distributed to reflect the geographic area of interest and the distribution of error in the dataset. When 20 points are tested, the 95% confidence level allows one point to fail the threshold given in product specifications.

4.5.3 United State Geological Survey (USGS) Standards

The USGS experts select 20 or more well defined points; using sophisticated surveying techniques to determine positions. Field survey methods are the only tests accepted for official accuracy testing.

Positions must obtained by surveys of a higher accuracy. Vertical tests run separately to determine precise elevations. The mapped positions are check against the field determined positions results.

4.5.4 National Map Accuracy Standards (NMAS)

The accuracy of any map may tested by comparing the positions of points whose locations or elevations are shown upon it with corresponding positions as determined by surveys of a higher accuracy. Tests shall made by the producing agency, which shall also determine which of its maps are to be tested, and the extent of the testing.

4.6 Photogrammetry accuracy standards

4.6.1 Nevada Department of Transportation (NDOT) standards

The primary map testing technique used at NDOT for maps is the NSSDA (National Standard for Spatial Data Accuracy) method. Previously used map accuracy standards such as NMAS (National Map Accuracy Standards) and ASPRS (American Society of Photogrammetry and Remote Sensing) fail because they apply only to paper maps compiled at a specific scale. In the digital age data may be collected at one scale and used or misused at various scales. The NSSDA was developed to report accuracy of digital geospatial data that is not constrained by scale and was developed to replace those older standards.

NDOT standards generally follow:

1. Use a methodology that compares sample-mapped points with independent measurements of their location to derive a statistical assessment that is valid for 95% of the points
2. Decide whether to test for horizontal or vertical accuracy or both.
3. Select a minimum of 20 representatives, well-defined, non-random and identifiable points from the mapped set.
4. Select corresponding points from an independent more accurate dataset.
5. Record the measurement values.
6. Calculate the sum of all error radius measurements, then calculate the average, and then take the square root to yield the root mean square (RMS) error. Multiply the RMS error by 1.7308 for horizontal error and 1.96 for vertical error.
7. Prepare an accuracy statement assuring the data or map user to expect locational errors, regardless of the scale at which the map is displayed.

Note that this well defined statistic and testing methodology tests only the positional accuracy of spatial data. There are other components of data quality such as attribute accuracy, logical consistency, completeness and lineage, which may be of importance that is more critical. The NSSDA testing standard does not define a “pass-fail” accuracy value but has allowed this agency to define its own minimum standards; our standards developed using traditional technical needs and correlating them to NSSDA. It is also important to note that different features may require different minimum accuracies as needed.

NDOT testing performs as follow:

- 1- Analysis of one model in five or at least one model per strip will viewed to determine the quality of the project. Analysis of mapping terrain model data takes place upon the completion. It is necessary to have the mathematical surface completed before any analysis of a photogrammetric. The essence of this analysis is the relationship between the final DEM surface and the surface generated from a field surveyed check point file compiled by qualified personnel.
- 2- Following NDOT written procedures, the editor prepares a check point file. A statistical comparison of elevation values taken from the compiled surface and check point file (20 minimum) made.

Table (4.8): Accuracy standard for NDOT intermediate scale digital photogrammetry
 "1:1000 final mapping", [ref.16].

Maximum flying height (m)	1100
Camera focal length (mm)	153
Minimum contour interval (m)	0.56
Minimum photo scale	1:7200
Aerotriangulation (max RMSE) (m)	Horizontal (0.26) , vertical (0.26)
Control elevations (95%) (m)	Spot/DEM=0.18
Features (95%) (m)	Horizontal=0.62
The minimum image point residual for any point shall not exceed (micron)	25

Table (4.9): Accuracy standard for NDOT intermediate scale digital photogrammetry
 "1:1700 final mapping", [ref.16].

Maximum flying height (m)	1830
Camera focal length (mm)	153
Minimum contour interval (m)	0.92
Minimum photo scale	1:12000
Aerotriangulation (max RMSE) (m)	Horizontal (0.55) , vertical (0.60)
Control elevations (95%) (m)	Spot/DEM=0.35
Features (95%) (m)	Horizontal=1.25
The minimum image point residual for any point shall not exceed (micron)	25

Table (4.10): Accuracy standard for NDOT intermediate scale digital photogrammetry 1:500 final mapping", [ref.16].

Maximum flying height (m)	550
Camera focal length (mm)	153
Minimum contour interval (m)	0.27
Minimum photo scale	1:3600
Aerotriangulation (max RMSE) (m)	Horizontal (0.13) , vertical (0.13)
Control elevations (95%) (m)	Spot/DEM=0.09
Features (95%) (m)	Horizontal=0.31
The minimum image point residual for any point shall not exceed (micron)	25

4.7 Relation ship between NSSDA and other accuracies

The National Standard for Spatial Data Accuracy was developed by the FGDC (Established by Office of Management and Budget Circular A-16), ad hoc working group on spatial data accuracy, with the intent to update the United States National Map Accuracy Standards (NMAS), [ref.12].

Computing Accuracy According to the NSSDA

We have two cases:

Case 1:

when $RMSE_x = RMSE_y$

$$\begin{aligned}
 RMSE_r &= \sqrt{2 * RMSE_x^2} = \sqrt{2 * RMSE_y^2} \\
 &= 1.4142 * RMSE_x = 1.4142 * RMSE_y \\
 RMSE_x &= RMSE_y = RMSE_r / 1.4142 \qquad \dots\dots\dots(4.6)
 \end{aligned}$$

It is assumed that systematic errors have been eliminated as best as possible. If error is normally distributed and independent in each the x- and y-component and error, the factor 2.4477 is used to compute horizontal accuracy at the 95% confidence level. When the preceding conditions apply, Accuracyr, the accuracy value according to NSSDA, shall be computed by the formula:

$$\begin{aligned}
 \text{Accuracyr} &= 2.4477 * \text{RMSE}_x = 2.4477 * \text{RMSE}_y \\
 &= 2.4477 * \text{RMSE}_r / 1.4142 \\
 \text{Accuracyr} &= 1.7308 * \text{RMSE}_r \\
 \text{RMSE}_x = \text{RMSE}_y &= \text{Accuracyr} / 2.4477 \quad \dots\dots\dots(4.7)
 \end{aligned}$$

Case 2:

1. Horizontal Accuracy

Approximating circular standard error when $\text{RMSE}_x \neq \text{RMSE}_y$

If $\text{RMSE}_{\text{min}}/\text{RMSE}_{\text{max}}$ is between 0.6 and 1.0 (where RMSE_{min} is the smaller value between RMSE_x and RMSE_y and RMSE_{max} is the larger value), circular standard error may be approximated as $0.5 * (\text{RMSE}_x + \text{RMSE}_y)$. If error is normally distributed and independent in each the x- and y-component and error, the accuracy value according to NSSDA may be approximated according to the following formula:

$$\text{Accuracyr} \sim 2.4477 * 0.5 * (\text{RMSE}_x + \text{RMSE}_y) \quad \dots\dots\dots(4.8)$$

You can use case1 by substitute

$$(\text{RMSE}_x = \text{RMSE}_y) \text{ average} = \frac{(\text{RMSE}_x + \text{RMSE}_y)}{2}$$

2. Vertical Accuracy

$$RMSE_z = \sqrt{(\sum (z_{data\ i} - z_{check\ i})^2) / n} \dots\dots\dots(4.9)$$

It is assumed that systematic errors have been eliminated as best as possible. If vertical error is normally distributed, the factor 1.9600 is applied to compute linear error at the 95% confidence level. Therefore, vertical accuracy, Accuracy_z, reported according to the NSSDA shall be computed by the following formula:

$$Accuracy_z = 1.9600 * RMSE_z. \dots\dots\dots(4.10)$$

4.8 Relationship between NSSDA and NMAS

4.8.1 Relationship between NSSDA and NMAS (horizontal)

NMAS (U.S. Bureau of the Budget, 1947) specifies that 90% of the well-defined points that are tested must fall within a specified tolerance:

If error is normally distributed in each the x- and y-component and error for the x-component is equal to and independent of error for the y-component, the factor 2.146 is applied to compute circular error at the 90% confidence level accuracy standard, (CMAS) Circular Map Accuracy Standard based on NMAS is: [ref.12]

$$\begin{aligned} CMAS &= 2.1460 * RMSE_x = 2.1460 * RMSE_y \\ &= 2.1460 * RMSE_r / 1.4142 \\ &= 1.5175 * RMSE_r \dots\dots\dots(4.11) \end{aligned}$$

1.5175 * [S * (1/30")*0.0254] m, or 0.00128* S, for map scales larger than 1:20,000
 1.5175*[S*(1/50")*0.0254] m, or 0.00077*S, for map scales of 1:20,000 or smaller.

The CMAS can be converted to accuracy reported according to NSSDA, Accuracyr, using the equation:

$$\text{Accuracyr} = 2.4477/2.1460 * \text{CMAS} = 1.1406 * \text{CMAS}. \quad \dots\dots\dots(4.12)$$

Therefore, NMAS horizontal accuracy reported according to the NSSDA is:
 1.1406* [S * (1/30")*0.0254] m, or 0.00097 * S, for map scales larger than 1:20,000
 1.1406*[S*(1/50")*0.0254] m, or 0.00058*S, for map scales of 1:20,000 or smaller
 where S is the map scale denominator.

4.8.2 Relationship between NSSDA and NMAS (vertical)

NMAS (U.S. Bureau of the Budget, 1947) specifies the maximum allowable vertical tolerance to be one half the contour interval, at all contour intervals. If vertical error is normally distributed, the factor 1.6449 is applied to compute vertical accuracy at the 90% confidence level. Therefore, the Vertical Map Accuracy Standard (VMAS) based on NMAS is estimated by the following formula:

$$\text{VMAS} = 1.6449 * \text{RMSEz} \quad \dots\dots\dots(4.13)$$

The VMAS can be converted to Accuracyz, accuracy reported according to the NSSDA using equations:

$$\text{Accuracyz} = 1.9600/1.6449 * \text{VMAS} = 1.1916 * \text{VMAS}. \quad \dots\dots\dots(4.14)$$

Therefore, vertical accuracy reported according to the NSSDA is $\frac{1.1916}{2} * \text{CI}$
 = 0.5958 * CI, where CI is the contour interval. [ref.12]

4.9 ASPRS classes

4.9.1 Horizontal accuracy

Comparable horizontal accuracy allowances stated by ASPRS standards for ASPRS Class 1 mapping can be determined by using Equation

$$e_{h1} = \frac{0.3048 * s_m}{1200} \dots\dots\dots(4.15)$$

Where:

s_m = map scale denominator (meter)

e_{h1} = maximum allowable ASPRS Class 1 RMSE

Once the ASPRS Class 1 inaccuracy is calculated, the error tolerance for ASPRS Class 2 can be determined with Equation

$$e_{h2} = 2 * e_{h1} \dots\dots\dots(4.16)$$

ASPRS Class 3 error can be determined with Equation

$$e_{h3} = 3 * e_{h1} \dots\dots\dots(4.17)$$

4.9.2 Spot Elevation accuracy

Maximum allowable errors of spot elevations for ASPRS Class 1 can be determined by applying Equation:

$$e_{c1} = C_i / 3 \dots\dots\dots(4.18)$$

Where:

C_i = contour interval

e_{c1} = maximum allowable ASPRS Class 1 error

Once the ASPRS Class 1 allowable error is computed, the ASPRS Class 2 error can be determined by using Equation

$$e_{c2} = 2 * e_{c1} \quad \dots\dots\dots(4.19)$$

The ASPRS Class 3 error can be determined with Equation

$$e_{c3} = 3 * e_{c1} \quad \dots\dots\dots(4.20)$$

Maximum allowable errors of spot elevations for ASPRS Class 1 can be determined by applying Equation: [ref.8]

$$e_{s1} = C_i / 6 \quad \dots\dots\dots(4.21)$$

$$e_{s2} = 2 * e_{s1} \quad \dots\dots\dots(4.22)$$

$$e_{s3} = 3 * e_{s1}$$

CHAPTER

5

MEASUREMENTS AND CALCULATIONS

The following contents are going to be covered in this chapter:

5.1 Overview

5.2 Calculate the observed angle and its propagate error coordinates

5.3 Least Squares Solution for the traverse

5.4 Degrees of traverse

CHAPTER FIVE

Measurements and Calculations

5.1 Overview

This chapter covers all field measurements. It includes measurement of vertical and horizontal angles and slope distance using Total Station instrument, and the determination of control points and check points coordinates using GPS instrument.

Then most probable value of the unknown control points in the traverse that measured using triangulation method of Least Square will be calculated.

5.2 Calculate the observed angle and it's propagate error coordinates

The measured distance and angle with the total station will contain an error that depend an

$$\sigma_D = \pm \sqrt{\sigma_i^2 + \sigma_t^2 + a^2 + \left(D * b_{\text{ppm}} \right)^2} \dots\dots\dots(5.1)$$

Where :

σ_D : Is the Error in the Measured Distance (D)

σ_i : Instrument Centering Error = 0.002m

σ_t : Target Centering Error = 0.002m

a and b : Are the Instrument's Specifred Accuracy Parameters = (5mm + 5ppm)

D : Distance between point A and B

Fig. (5.1) shows a sketch of two fixed point B and C and one unknown point A at the study area. Table (5.1), shows the observed and average angle for points A, B, and C.

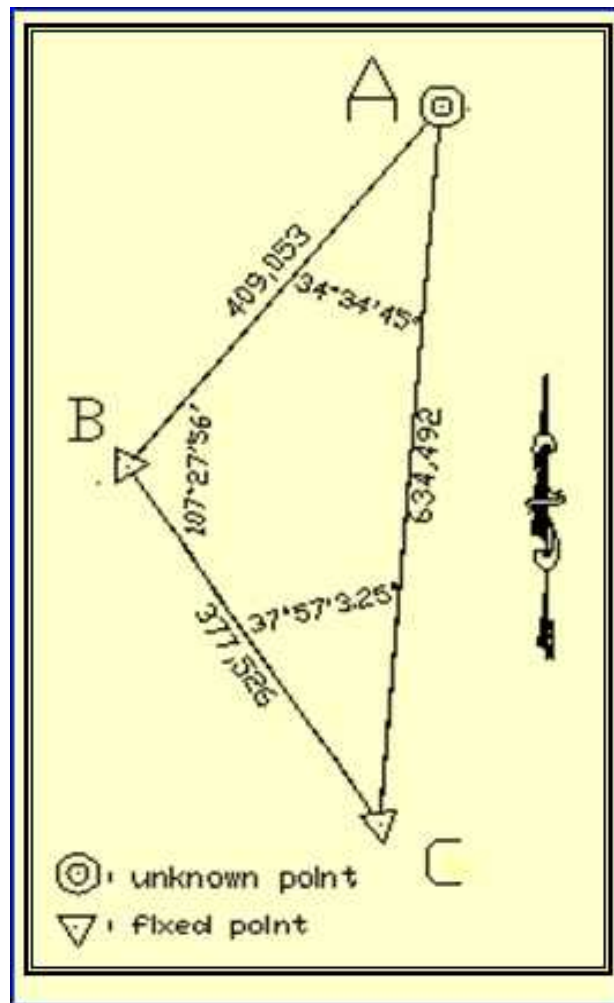


Fig. (5.1): Study area, traverse sketch

Table (5.1): Study area, reading angles from instrument (Total Station)

Angle observation		
A	B	C
34.3445	107.2755	37.5705
69.0930	214.5550	75.5405
103.4420	322.2350	113.5110
138.1900	69.5145	151.4810
Average angle		
34.3445	107.2756	37.5703

Calculation of distances, and error in angles of traverse.

For angle A:

$$BA = 409.053 \text{ m}$$

$$AC = 634.492 \text{ m}$$

$$MA = 377.526 \text{ m}$$

$$\sigma_D = \pm \sqrt{\sigma_i^2 + \sigma_t^2 + a^2 + \left(D * b_{\text{ppm}} \right)^2}$$

Where :

σ_D : Is the Error in the Measured Distance (D)

$$D_3 = \sqrt{D_1^2 + D_2^2 - 2 * D_1 * D_2 * \cos(\gamma)}$$

$$D_3 = \sqrt{409.053^2 + 634.492^2 - 2 * 409.053 * 634.492 * \cos(34.3445)} = 377.521m$$

$$\sigma_{ri} = \frac{D_3 * \sigma_i * 206264.80}{D_1 * D_2 * \sqrt{2}} = 0.42''$$

$$\sigma_{rt} := \frac{\sqrt{D_1^2 + D_2^2}}{D_1 * D_2} * 0.002 * 206264.80$$

$$\sigma_{rt} := \frac{\sqrt{409.053^2 + 634.492^2}}{409.053 * 634.492} * 0.002 * 206264.80 = 1.2''$$

$$ERROR = \sqrt{1.2^2 + 0.42^2} = 1.27''$$

$$\sigma_{D_{AC}} = \pm \sqrt{(0.002)^2 + (0.002)^2 + (0.005)^2 + \left(\frac{0.005}{1 * 10^6} * 634.492\right)^2} = \pm 0.0057 m$$

$$D_3 = \sqrt{D_1^2 + D_2^2 - 2 * D_1 * D_2 * \cos(\gamma)}$$

$$D_3 = \sqrt{409.053^2 + 377.526^2 - 2 * 409.053 * 377.526 * \cos(107.2756)} = 634.467m$$

$$\sigma_{ri} = \frac{D_3 * \sigma_i * 206264.80}{D_1 * D_2 * \sqrt{2}} = 1.2''$$

$$\sigma_{rt} := \frac{\sqrt{D_1^2 + D_2^2}}{D_1 * D_2} * 0.002 * 206264.80$$

$$\sigma_{rt} := \frac{\sqrt{409.053^2 + 377.526^2}}{409.053 * 377.526} * 0.002 * 206264.80 = 1.49''$$

$$ERROR = \sqrt{1.2^2 + 1.49^2} = 1.91''$$

$$\sigma_{D_{AB}} = \pm \sqrt{(0.002)^2 + (0.002)^2 + (0.005)^2 + \left(\frac{0.005}{1 * 10^6} * 409.053\right)^2} = \pm 0.0059 m$$

$$D_3 = \sqrt{D_1^2 + D_2^2 - 2 * D_1 * D_2 * \cos(\alpha)}$$

$$D_3 = \sqrt{634.492^2 + 377.526^2 - 2 * 634.492 * 377.526 * \cos(37.57325)} = 409.069m$$

$$\sigma_{ri} = \frac{D_3 * \sigma_i * 206264.80}{D_1 * D_2 * \sqrt{2}} = 0.50''$$

$$\sigma_{rt} := \frac{\sqrt{D_1^2 + D_2^2}}{D_1 * D_2} * 0.002 * 206264.80$$

$$\sigma_{rt} := \frac{\sqrt{634.492^2 + 377.526^2}}{634.492 * 377.526} * 0.002 * 206264.80 = 1.27''$$

$$ERROR = \sqrt{1.27^2 + 0.50^2} = 1.37''$$

Actual misclosure error= 180- \sum angles = 15.75"

According to Palestine accuracy, table (4.1), the permissible error = $60''\sqrt{3} = 104''$

Where $104'' > 15.75''$, so traverse can be adjusted.

* In the figure (5.1) the point B and C are control points.

* The coordinate of control points are stated in table (5.2).

Table (5.2): Fixed control points

NO.	East	North	Elevation	Remark
B	158568.374	101505.006	899.70	B: Building ppu B
C	158775.68	101189.49	921.57	C: Ghaleb Zahdeh house

5.3 Least Squares Solution for the traverse

- Calculate initial approximate for the unknown station coordinates:

$$\begin{aligned}
 E &= E_0 + D\sin(Az) \\
 N &= N_0 + D\cos(Az)
 \end{aligned}
 \dots\dots\dots (5.2)$$

$$Az_{(A-B)} = \tan^{-1} \left(\frac{E_B - E_A}{N_B - N_A} \right) \dots\dots\dots(5.3)$$

- Instrument on control point (C)

$$Az_{(B-C)} = \tan^{-1} \frac{E_C - E_B}{N_C - N_B} = \tan^{-1} \frac{158775.68 - 158568.374}{101189.49 - 101505.006} = -146^{\circ}41' 36.8''$$

$$Az_{(B-A)} = 146^{\circ}41' 36.8'' - 107^{\circ}27' 56'' = 39^{\circ}13' 40.8''$$

$$E_A = 158568.374 + 409.053 * \sin 39^{\circ} 13' 40.8'' = 158827.0624$$

$$N_A = 101505.006 + 409.053 * \cos 39^{\circ} 13' 40.8'' = 101821.873$$

Formulate (X) and (K) matrices:

The elements of the (X) matrix consist of the ∂x and ∂y (called correction). The value of (K) matrix is derived by subtracting computed distance, based on the initial coordinate so the initial value denoted by (quantity)₀.

$$K = \begin{bmatrix} BA - BA_{o} \\ CA - CA_{o} \\ r_C - r_{C_{o}} \\ r_A - r_{A_{o}} \\ r_A - r_{B_{o}} \end{bmatrix} \quad X = \begin{bmatrix} \partial x_A \\ \partial y_A \end{bmatrix}$$

- Calculate the Jacobin matrix. The J matrix is found using proto type equation for distance and angle.

Distance observation equation from Fig. (5.2):

$$\frac{(X_i - X_j)_o}{(IJ)_o} \partial x_i + \frac{(Y_i - Y_j)_o}{(IJ)_o} \partial y_i + \frac{(X_j - X_i)_o}{(IJ)_o} \partial x_j + \frac{(Y_j - Y_i)_o}{(IJ)_o} \partial y_j = K_{ij} + V_{ij} \dots\dots\dots(5.4)$$

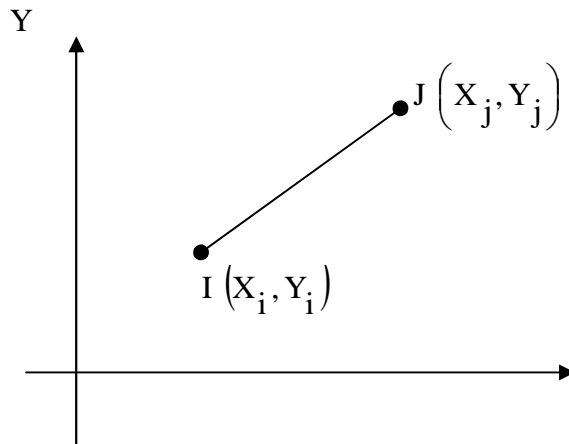


Fig. (5.2): Distance observation equation

$$\frac{(Y_I - Y_B)_o}{(BI)_o^2} \partial X_B + \frac{(X_B - X_I)_o}{(IB)_o^2} \partial Y_B + \frac{(Y_F - Y_I)_o}{(FI)_o^2} \partial X_F + \frac{(X_I - X_F)_o}{(IF)_o^2} \partial Y_F +$$

$$\left(\frac{(Y_B - Y_I)_o}{(IB)_o^2} - \frac{(Y_F - Y_I)_o}{(IF)_o^2} \right) \partial x_I + \left(\frac{(X_I - X_B)_o}{(IB)_o^2} - \frac{(X_I - X_F)_o}{(IF)_o^2} \right) \partial Y_I \quad \dots\dots\dots (5.5)$$

$$= K_{r_{BIF}} + V_{r_{BIF}}$$

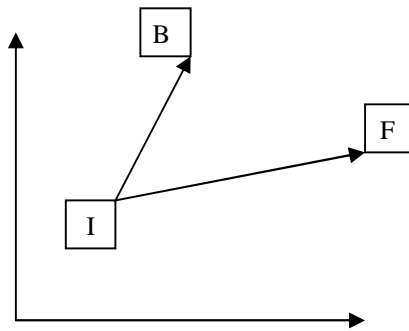


Fig. (5.3): Angle observation equation

$$CA = \sqrt{(X_A - X_C)^2 + (Y_A - Y_C)^2}$$

$$AB = \sqrt{(X_B - X_A)^2 + (Y_B - Y_A)^2} \quad \dots\dots\dots (5.6)$$

* Formulate the weight (W) matrix:

$$W = \begin{bmatrix} 1/(S_{CA})^2 & 0 & 0 & 0 & 0 \\ 0 & 1/(S_{AB})^2 & 0 & 0 & 0 \\ 0 & 0 & 1/(S_{r_{CA}})^2 & 0 & 0 \\ 0 & 0 & 0 & 1/(S_{r_{A}})^2 & 0 \\ 0 & 0 & 0 & 0 & 1/(S_{r_{B}})^2 \end{bmatrix}$$

- Solve the matrix system. The problem is iterative and need more than one iteration to reach minimum corrections according to sheet Excel.

$$J * X = K + V \quad \dots\dots\dots (5.7)$$

$$J * X = K$$

$$X = \left(J^T * W * J \right)^{-1} * \left(J^T * W * K \right) \quad \dots\dots\dots (5.8)$$

$$X = N^{-1} * \left(J^T * W * K \right)$$

$$S_o = \sqrt{\frac{V^T * V}{m - n}} \quad \dots\dots\dots (5.9)$$

Where:

S_o = Reference standard deviation (sample).

V = Observation residual.

m = Number of equation of observation.

n = Number of unknowns.

[ref.2]

$$S_o = \sqrt{\frac{104.0289}{5 - 2}} = +5.8887$$

$$\dagger_{xA} = \dagger_o \sqrt{q_{xx}} = +5.8887 * \sqrt{9.969 * 10^{-6}} = 0.0186m \quad \dots\dots\dots (5.10)$$

$$\dagger_{yA} = \dagger_o \sqrt{q_{yy}} = +5.8887 * \sqrt{8.426 * 10^{-6}} = 0.0171m$$

Table (5.3): Study area, summery of the traverse

Summery of Traverse ABC from Total Station measurements						
Point	Northing	Easting	\dagger_N	\dagger_E	Actual Error	Palestine Error
A	101821.8974	158827.0616	0.0171	0.0186	15.75"	104"
B	101505.006	158568.374	0	0		
C	101189.46	158775.68	0	0		

5.3.1 First iteration of least square solution

	C		B		A
	158775.68 101189.49	158568.374	101505.006	158827.0629 101821.874	
	BA 409.053			<C 37.95090278	
	GA 634.492			<A 34.57916667	
				<B 107.4655556	
	BA.. 409.0541241			C. 37.95166594	
	CA.. 634.4680653			A. 34.582737	
				B. 107.4655971	
J	0.080985794 0.996715256 0.63240751 0.774635877 324.030933 -26.32838438 66.57781445 -292.5619649 -390.6087474 318.8903493				
K	0.023934713 -0.001124056 -2.747374794 -12.8532046 -0.149240604				
W	30778.70114 0 0 0 0 0 28727.37719 0 0 0 0 0 0.532793436 0 0 0 0 0 0.62000124 0 0 0 0 0 0.274115293				
AT	0.080985794 0.63240751 324.030933 66.57781445 -390.6087474 0.996715256 0.774635877 -26.32838438 -292.5619649 318.8903493				
at*w	2492.637548 18167.40907 172.6415541 41.27832751 -107.0718312 30677.60098 22253.25701 -14.02759038 -181.388781 87.41272149				
at*w*a	112203.6927 -34208.43872 -34208.43872 129126.8594				
Qxx	9.69545E-06 2.56853E-06 2.56853E-06 8.42478E-06				

At*w	2492.637548	18167.40907	172.6415541	41.27832751	-107.0718312
	30677.60098	22253.25701	-14.02759038	-181.388781	87.41272149

At*w*K	-949.6509977
	3066.16632

For second iteration

		x	y
X	-0.001331754 dx	158827.0616	101821.8974
	0.02339257 dy		

5.3.2 Second iteration of least square solution

	C	B	A
	158775.68	158568.374	158827.0616
	101189.49	101505.006	101821.8974

BA	409.053	<C	37.95090278
CA	634.492	<A	34.57916667
		<B	107.4655556
BA..	409.0714287	C.	37.9513778
CA..	634.4912831	A.	34.58081139
		B.	107.4678108

J	0.080980782	0.996715663
	0.63237758	0.774660311
	324.0192081	-26.32579148
	66.58533584	-292.5359764
	-390.604544	318.8617679

K	0.00071685
	-0.018428711
	-1.710088344
	-5.921002644
	-8.118729012

W	30778.70114	0	0	0	0
	0	28727.37719	0	0	0
	0	0	0.532793436	0	0
	0	0	0	0.62000124	0
	0	0	0	0	0.274115293

AT	0.080980782	0.63237758	324.0192081	66.58533584	-390.604544
	0.996715663	0.774660311	-26.32579148	-292.5359764	318.8617679

at*w	2492.483274	18166.54926	172.6353072	41.28299079	-107.070679
	30677.61351	22253.95894	-14.0262089	-181.3726681	87.40488689

at*w*a	112198.2528	-34205.0653
	-34205.0653	129113.475

Qxx	9.69588E-06	2.56866E-06
	2.56866E-06	8.42562E-06

At*w	2492.483274	18166.54926	172.6353072	41.28299079	-107.070679
	30677.61351	22253.95894	-14.0262089	-181.3726681	87.40488689

At*w*K	-3.379847152
	0.156981211

Iteration enough

		x	y
X	-3.23674E-05 dx	158827.0616	101821.8974
	-7.35901E-06 dy		

5.4 Degrees of traverse

To calculate the degree of the traverse, using values of the second iteration as initial values

Degree of traverse can be determined using the relative error. In which:

Relative ellipse					
C		B		A	
158775.68	101189.49	158568.374	101505.006	158827.062	101821.897
BA	409.053	<C	37.9509028		
CA	634.492	<A	34.5791667		
CB	377.5263221	<B	107.465556		
BA..	409.0714287	C.	37.9513778		
CA..	634.4912831	A.	34.5808114		
		B.	107.467811		

J	0.080980782	0.99671566	0	0	-0.08098069	-0.99671566
	0.63237758	0.77466031	-0.63237758	-0.7746603	0	0
	324.0192081	-26.3257915	-0.00221374	-0.0014545	-324.016994	26.327246
	66.58533584	-292.535976	-0.00189387	0.00154602	0.00157089	-0.00012763
	-390.604544	318.861768	390.606758	-318.86031	-0.00221374	-0.00145451
	0	0	1	0	0	0
	0	0	0	1	0	0
	0	0	0	0	1	0
0	0	0	0	0	1	

Jt								
0.080980782	0.63237758	324.019208	66.5853358	-390.60454	0	0	0	0
0.996715663	0.774660311	-26.3257915	-292.535976	318.861768	0	0	0	0
0	-0.63237758	-0.00221374	-0.00189387	390.606758	1	0	0	0
0	-0.77466031	-0.00145451	0.00154602	-318.86031	0	1	0	0
-0.08098069	0	-324.016994	0.00157089	-0.0022137	0	0	1	0
-0.996715663	0	26.327246	-0.00012763	-0.0014545	0	0	0	1

W								
16.9975377	0	0	0	0	0	0	0	0
0	15.86469405	0	0	0	0	0	0	0
0	0	0.00029424	0	0	0	0	0	0
0	0	0	0.0003424	0	0	0	0	0
0	0	0	0	0.00015138	0	0	0	0
0	0	0	0	0	22.09	0	0	0
0	0	0	0	0	0	22.09	0	0
0	0	0	0	0	0	0	22.09	0
0	0	0	0	0	0	0	0	22.09

Jt*W								
1.376473888	10.03247683	0.09533785	0.02279853	-0.0591298	0	0	0	0
16.94171206	12.28974882	-0.00774597	-0.10016306	0.04826935	0	0	0	0
0	-10.0324768	-6.5136E-07	-6.4845E-07	0.05913012	22.09	0	0	0
0	-12.2897488	-4.2797E-07	5.2935E-07	-0.0482691	0	22.09	0	0
-1.376472333	0	-0.0953372	5.3786E-07	-3.351E-07	0	0	22.09	0
-16.94171206	0	0.0077464	-4.37E-08	-2.202E-07	0	0	0	22.09

Jt*W*J								
61.96148509	-18.8897473	-29.4410603	11.0822759	-31.0023842	1.138113			
-18.8897473	71.3029166	11.0827791	-24.911704	1.13761144	-17.0900574			
-29.4410603	11.0827791	51.5309369	-11.082486	8.0152E-05	-0.00010315			
11.0822759	-24.9117039	-11.0824862	47.0014901	0.00024553	5.8941E-05			
-31.0023842	1.13761144	8.0152E-05	0.00024553	53.0923397	-1.13801431			

1.138112999 -17.0900574 -0.00010315 5.8941E-05 -1.13801431 39.1800112

K

0.00071685
 -0.01842871
 -1.71008834
 -5.92100264
 -8.11872901
 0
 0
 0
 0

Jt*K

-0.00186652
 8.66929E-05
 -0.29517083
 0.618365802
 0.162047841
 -0.02538965

(Jt*W*J)inv

0.040316938 0.00747737 0.02131474 -0.0005173 0.02344156 0.00277138
 0.007477372 0.02135392 0.00182702 0.0099857 0.00410624 0.00921649
 0.02131474 0.00182702 0.03193752 0.00347313 0.01241872 0.00053857
 -0.00051732 0.0099857 0.00347313 0.02750944 -0.00042276 0.00435841
 0.023441558 0.00410624 0.01241872 -0.0004228 0.03247943 0.0020536
 0.002771376 0.00921649 0.00053857 0.00435841 0.0020536 0.02952253

(Jt*W*J)inv *Jt*K =X

-0.0029577
 0.00605483
 -0.00532023
 0.015808396
 0.001240621
 0.002114964

J*X

0.003586943
 -0.00606169
 -1.46406191
 -1.96815877
 -4.03284975
 -0.00532023
 0.015808396
 0.001240621
 0.002114964

V	0.002870093
	0.012367023
	0.246026436
	3.952843877
	4.085879266
	-0.00532023
	0.015808396
	0.001240621
	0.002114964

Vt

0.002870093	0.012367023	0.24602644	3.95284388	4.08587927	-0.00532023	0.0158084	0.0012406	0.002115
-------------	-------------	------------	------------	------------	-------------	-----------	-----------	----------

Vt*W

0.048784518	0.196199044	7.239E-05	0.00135344	0.00061852	-0.11752392	0.34920746	0.0274053	0.0467194
-------------	-------------	-----------	------------	------------	-------------	------------	-----------	-----------

Vt*W*V

0.016739824

o

0.074699006

Qxx=Ninv=
(Jt*W*J) inv

0.040316938	0.00747737	0.02131474	-0.0005173	0.02344156	0.00277138
0.007477372	0.02135392	0.00182702	0.0099857	0.00410624	0.00921649
0.02131474	0.00182702	0.03193752	0.00347313	0.01241872	0.00053857
-0.00051732	0.0099857	0.00347313	0.02750944	-0.00042276	0.00435841
0.023441558	0.00410624	0.01241872	-0.0004228	0.03247943	0.0020536
0.002771376	0.00921649	0.00053857	0.00435841	0.0020536	0.02952253

o²*Qxx=Cxx

0.000224966	4.1723E-05	0.00011893	-2.887E-06	0.0001308	1.5464E-05
4.17233E-05	0.00011915	1.0195E-05	5.572E-05	2.2913E-05	5.1427E-05
0.000118935	1.0195E-05	0.00017821	1.938E-05	6.9296E-05	3.0052E-06
-2.8866E-06	5.572E-05	1.938E-05	0.0001535	-2.359E-06	2.432E-05
0.000130803	2.2913E-05	6.9296E-05	-2.359E-06	0.00018123	1.1459E-05
1.54641E-05	5.1427E-05	3.0052E-06	2.432E-05	1.1459E-05	0.00016473

line AB

Delta X -258.6876

Delta Y -316.8914

Cxx for line (AB)	0.000224966	4.1723E-05	0.00011893	-2.887E-06
	4.17233E-05	0.00011915	1.0195E-05	5.572E-05
	0.000118935	1.0195E-05	0.00017821	1.938E-05
	-2.8866E-06	5.572E-05	1.938E-05	0.0001535

A	-1	0	1	0
	0	-1	0	1

At	-1	0
	0	-1
	1	0
	0	1

A*Cxx	-0.00010603	-3.1529E-05	5.9274E-05	2.2266E-05
	-4.461E-05	-6.3434E-05	9.1852E-06	9.7781E-05

A*Cxx*At	0.000165306	5.3795E-05
	5.37951E-05	0.00016122

semimajor axes 0.014734128

semiminor axes 0.010460714

a=d/s 27762.28046

line AC

Delta X -51.3816

Delta Y -632.4074

Cxx for line (AC)	0.000224966	4.1723E-05	0.0001308	1.5464E-05
	4.17233E-05	0.00011915	2.2913E-05	5.1427E-05
	0.000130803	2.2913E-05	0.00018123	1.1459E-05
	1.54641E-05	5.1427E-05	1.1459E-05	0.00016473

A	-1	0	1	0
	0	-1	0	1

At	<table style="margin: auto; border-collapse: collapse;"> <tr><td style="padding: 2px 10px;">-1</td><td style="padding: 2px 10px;">0</td></tr> <tr><td style="padding: 2px 10px;">0</td><td style="padding: 2px 10px;">-1</td></tr> <tr><td style="padding: 2px 10px;">1</td><td style="padding: 2px 10px;">0</td></tr> <tr><td style="padding: 2px 10px;">0</td><td style="padding: 2px 10px;">1</td></tr> </table>	-1	0	0	-1	1	0	0	1
-1	0								
0	-1								
1	0								
0	1								
A*Cxx	<table style="margin: auto; border-collapse: collapse;"> <tr><td style="padding: 2px 10px;">-9.4164E-05</td><td style="padding: 2px 10px;">-1.8811E-05</td><td style="padding: 2px 10px;">5.0431E-05</td><td style="padding: 2px 10px;">-4.005E-06</td></tr> <tr><td style="padding: 2px 10px;">-2.6259E-05</td><td style="padding: 2px 10px;">-6.7726E-05</td><td style="padding: 2px 10px;">-1.1454E-05</td><td style="padding: 2px 10px;">0.00011331</td></tr> </table>	-9.4164E-05	-1.8811E-05	5.0431E-05	-4.005E-06	-2.6259E-05	-6.7726E-05	-1.1454E-05	0.00011331
-9.4164E-05	-1.8811E-05	5.0431E-05	-4.005E-06						
-2.6259E-05	-6.7726E-05	-1.1454E-05	0.00011331						
A*Cxx*At	<table style="margin: auto; border-collapse: collapse;"> <tr><td style="padding: 2px 10px;">0.000144594</td><td style="padding: 2px 10px;">1.4806E-05</td></tr> <tr><td style="padding: 2px 10px;">1.48056E-05</td><td style="padding: 2px 10px;">0.00018103</td></tr> </table>	0.000144594	1.4806E-05	1.48056E-05	0.00018103				
0.000144594	1.4806E-05								
1.48056E-05	0.00018103								
Semimajor axes	0.013648807								
Semiminor axes	0.011804116								
a=d/s	46486.99284								

With respect to the table (4.2), the traverse is classified as second order class2.

Table (5.4) Summarized the instrument reading in the study area and while table (5.5) tabulated the calculated X,Y and Z coordinates of 31 control points and check points that are distributed all over the study area.

Table (5.4): Study area, reading from Instrument (Total Station)

NO.	Horizontal Angle	Slope Distance	Vertical Angle	Height Prime	Instnt. Height
From station (A)					
1	347.0435	109.966	101.3620	0.10	1.58
2	347.5325	96.847	103.1330	0.10	1.58
3	245.0200	82.528	101.3235	0.10	1.58
4	287.4625	196.875	100.1210	0.10	1.58
5	262.0035	270.992	96.4250	0.10	1.58
6	255.4300	414.387	95.2940	0.10	1.58
7	642.0325	249.971	96.1330	0.10	1.58
8	237.1435	754.217	93.5320	0.10	1.58

9	223.2710	782.076	93.2510	0.10	1.58
10	222.3550	599.453	95.5655	0.10	1.58
11	211.2200	823.037	92.0900	0.10	1.58
12	181.4750	454.459	90.0215	0.10	1.58
13	140.2740	350.777	88.1110	0.10	1.58
14	120.3310	369.037	88.4800	0.10	1.58
15	95.1425	262.469	91.2905	0.10	1.58
16	359.2925	398.053	90.1315	0.10	1.58
52	17.5925	232.313	96.4535	2.65	1.58
From station (C)					
17	246.4710	109.499	94.5410	0.87	1.61
18	233.5045	459.905	97.0805	1.27	1.61
19	289.3755	568.015	93.1230	0.87	1.61
20	297.4235	668.420	91.2055	0.87	1.61
21	292.3005	803.142	90.3425	0.62	1.61
22	301.1045	734.222	90.0310	0.87	1.61
23	316.2250	880.717	89.4005	0.62	1.61
24	343.4745	817.729	89.1035	0.62	1.61
25	354.5750	706.451	90.5050	0.87	1.61
26	27.3910	478.935	93.2800	1.62	1.61
27	52.3055	708.003	95.3130	0.87	1.61
28	47.3455	1012.153	94.4115	0.87	1.61
29	43.2410	1146.145	93.1025	0.87	1.61
30	2.2445	396.251	90.1310	1.62	1.61
31	357.1420	396.251	90.0300	1.62	1.61
32	249.0755	96.047	101.3835	1.62	1.61
33	233.3040	242.821	97.2915	1.62	1.61
34	270.3300	462.248	95.1625	1.62	1.61
35	288.0455	535.007	94.0820	1.62	1.61
36	293.1745	776.824	90.5720	1.62	1.61
37	314.5105	887.325	90.0510	1.62	1.61
38	344.1110	803.259	89.2520	1.62	1.61
39	18.1325	495.203	92.3820	1.62	1.61
40	39.1910	521.832	94.3120	1.62	1.61
41	48.3120	739.754	95.0210	1.75	1.61
42	38.4040	1067.024	93.4340	1.65	1.61
43	27.2825	422.074	92.0935	1.62	1.61

Table (5.5): Coordinates collected by Total Station.

NO	X	Y	Z
1	158779.3313	101725.3316	896.9200
2	158784.0900	101737.9815	896.8800
3	158905.4293	101801.9813	902.5300
4	158932.5936	101659.3962	884.1700
5	159057.1825	101682.3364	887.3600
6	159201.0675	101647.9529	876.8100
7	159460.7100	101695.4900	848.5600
8	159574.7512	101737.1212	867.8900
9	159601.3800	101921.3900	872.3900
10	159417.2251	101906.6997	855.4400
11	159602.7861	102095.1885	888.1600
12	159125.3510	102164.7623	917.2700
13	158825.1455	102172.4934	928.6700
14	158690.2015	102193.4426	927.3300
15	158639.8093	102005.6916	910.7700
16	158590.9013	101501.4724	917.5100
17	158463.5082	101535.0993	907.9000
18	158112.6857	101529.4586	859.7400
19	158275.0767	101990.3998	885.4700
20	158306.5813	102119.8250	901.5300
21	158187.9680	102212.2992	909.4700
22	158322.1376	102196.7062	916.5800
23	158500.9041	102383.1200	922.6100
24	158888.1367	102257.5313	929.2600
25	158965.3093	102089.3058	906.8100
26	159008.0323	101692.7309	887.5500
27	159048.5431	101490.4107	870.7900
28	159304.5096	101546.0631	856.8100
29	159624.9563	101641.6971	858.1100
30	158848.8086	101820.4426	914.8100
31	158803.8764	101823.6803	916.0800
32	158479.0906	101534.6334	897.1300
33	158327.8981	101516.5016	884.8700
34	158214.6135	101799.4946	874.0200
35	158280.1558	101954.0847	877.9000
36	158209.9861	102194.0966	903.5600

37	158476.8116	102387.5932	915.1800
38	158887.5231	102242.0971	924.6100
39	158985.3460	101771.1648	893.7100
40	159078.2198	101608.3165	875.3700
41	159273.0991	101532.7196	854.2100
42	159555.9594	101716.6623	850.6200
43	159620.2940	101958.0481	873.2400
52	158633.1095	101696.9806	889.1500

CHAPTER

6

DATA ANALYSIS

The following contents are going to be covered in this chapter:

6.1 Overview

6.2 Photo quality

6.3 Photogrammetry models

6.4 Correlation of the resultant RMSE of the three generated photogrammetry models

6.5 DEM and interpolations techniques

6.6 Testing of photogrammetry resultant grid

6.7 Correlation of time needed by EDM and photogrammetry technique

CHAPTER SIX

Data Analysis

6.1 Overview

The National Standard for Spatial Data Accuracy (NSSDA) implements a statistical and testing methodology for estimating the positional accuracy of points on maps and in digital geospatial data, with respect to georeferenced ground positions of high accuracy.

In this chapter we will discuss the obtained data from photogrammetry models with respect to NSSDA and NMAS standards according to allowable error.

As discussed in chapter five, NSSDA and NMAS are the most popular and used standards for map testing and Photogrammetry application at large scale maps.

6.2 Photo quality

The photo was exposed by RMK30/29 camera with focal length (305.004) mm, unfortunately camera calibration sheet haven't photo exposures, and were calculated using the space resection program presented in appendix C. This software was programmed by the project staff to be used for solving space resection problems.

Table (6.1): Photo exposure parameter

	Photo 29	photo 30
XL	158965.83	158968.74
YL	102261.00	101615.23
ZL	3073.52	3067.40
W	0.44	0.12
Phi	1.95	1.41
k	-93.74	-93.37

6.2.1 Photo quality parameters

1. Photo scale

From camera calibration sheet, the elevation of the plane is 3073m above see level, and the average study area elevation is 890m above see level.

According the scale of photos could be calculated using following equation

$$s = \frac{f}{H - h_{avg}} \quad , \quad s = \frac{0.305004}{3073 - 890} \approx 1 : 7000$$

Where f is the camera focal length

The scale is very important to determine quality of the photo and to guess the final allowable scale of the cultural feature according to magnification factor.

2. Resolution

Resolution is define as how much detail appears on the photo. This is related directly to the pixel size of the image, as pixel size decrease the resolution increase. It was

found that a 10 micron resolution is sufficient and gives a high accuracy and photo quality.

3. Magnification factor

Magnification factor can be calculated using the following relation:

Magnification factor = $105/\text{resolution}$.

Model built on 10 micron and hence, the resolution, then:

Magnification factor = $105/10 = 10.5$

4. Radiometric resolution

The scanned photo is of 256 levels (8 bit). This radiometric resolution is sufficient for current study.

6.3 Photogrammetry models

In the Photogrammetric lab. Three models were prepared in order to verify that whether the collected coordinates meet the allowable error or not.

6.3.1 Model built using three control points

X, Y and Z Photogrammetric coordinates of 31 points are collected from the model, table (6.2).

Table (6.2): Coordinates from three control points model

NO.	X	Y	Z	X	Y	Z	X ²	Y ²	E.P	Z ²
1	.	.	.	-0.545	0.466	-2.893	0.30	0.22	0.72	8.37
2	.	.	.	-0.359	0.318	-1.547	0.13	0.10	0.48	2.39
3	.	.	.	0.272	-0.101	-1.636	0.07	0.01	0.29	2.68
4	.	.	.	-0.146	0.026	0.610	0.02	0.00	0.15	0.37

5	.	.	.	0.030	0.399	-1.500	0.00	0.16	0.40	2.25
6	.	.	.	0.875	0.211	-1.892	0.76	0.04	0.90	3.58
7	.	.	.	0.907	-0.131	-0.657	0.82	0.02	0.92	0.43
8	.	.	.	1.116	0.181	-2.358	1.24	0.03	1.13	5.56
9	.	.	.	0.921	-0.526	-0.590	0.85	0.28	1.06	0.35
10	.	.	.	0.902	0.135	0.334	0.81	0.02	0.91	0.11
11	.	.	.	0.696	0.524	1.571	0.48	0.27	0.87	2.47
12	.	.	.	0.368	0.622	-0.441	0.14	0.39	0.72	0.19
13	.	.	.	0.294	-0.637	-0.269	0.09	0.41	0.70	0.07
14	.	.	.	-0.213	0.032	0.747	0.05	0.00	0.22	0.56
15	.	.	.	-0.743	0.655	-1.524	0.55	0.43	0.99	2.32
16	.	.	.	-0.311	0.443	-1.317	0.10	0.20	0.54	1.73
17	.	.	.	-0.082	0.474	-1.845	0.01	0.22	0.48	3.40
18	.	.	.	0.621	0.517	-1.938	0.39	0.27	0.81	3.75
19	.	.	.	-0.521	0.364	-1.490	0.27	0.13	0.64	2.22
20	.	.	.	-0.304	0.577	-0.119	0.09	0.33	0.65	0.01
21	.	.	.	-0.243	0.301	0.160	0.06	0.09	0.39	0.03
22	.	.	.	-0.129	0.282	0.117	0.02	0.08	0.31	0.01
23	.	.	.	-0.015	0.225	-0.637	0.00	0.05	0.23	0.41
24	.	.	.	0.266	0.219	1.497	0.07	0.05	0.34	2.24
25	.	.	.	0.172	-0.269	-2.065	0.03	0.07	0.32	4.26
26	.	.	.	0.090	-0.279	-0.461	0.01	0.08	0.29	0.21
27	.	.	.	0.114	-0.178	-1.009	0.01	0.03	0.21	1.02
28	.	.	.	0.593	0.359	-0.035	0.35	0.13	0.69	0.00
29	.	.	.	0.780	-0.511	-2.178	0.61	0.26	0.93	4.75
30	.	.	.	0.027	0.588	1.383	0.00	0.35	0.59	1.91
31	.	.	.	-0.206	0.511	0.014	0.04	0.26	0.55	0.00
							8.37	4.98		57.68
							RMSx	RMSy		average
							0.52	0.40		RMSEz
							RMSEr			1.36
							0.66			

6.3.1.1 NSSDA standard

The resultant RMSE_x, RMSE_y, RMSE_z and RMSE_r will be discussing according to NSSDA and NMAS standards.

- **Horizontal accuracy**

Since $RMSE_x \neq RMSE_y$ and $(RMSE_{min}/RMSE_{max}=0.8)$ is between 0.6 and 1.0, the formula $Accuracy \sim 2.4477 * 0.5 * (RMSE_x + RMSE_y)$.

May be used to estimate the accuracy.

The resultant horizontal accuracy value according to the NSSDA, at 95% confidence.

Accuracy ~ 1.13 meter.

So allowable error in position is ≤ 1.13 m.

Since 31 points were collected at 95% confidence level, this mean:

$31 * 95\% = 29.45$ (≈ 29) points must have an error less than 1.13

But 30 points succeed and point # 8 is critical but you can consider it succeed.

As a result, one can said that the model which has been built on three controls is passing in cultural feature.

- **Vertical Accuracy**

$$RMSE_z = \sqrt{\frac{\sum (Z_{data\ i} - Z_{check\ i})^2}{n}}$$

$$Accuracy_z = 1.9600 * RMSE_z.$$

Accuracy $= 1.96 * 1.36 = 2.67$ m

But 30 point succeeds and point #1 is failed.

According to this result the model that has been built on three controls is passing in elevation.

6.3.1.2 Analyze and correlated the result with NMAS standard

- **Horizontal accuracy**

Therefore, NMAS horizontal accuracy reported according to the NSSDA is:

$$\text{CMAS} = \text{Accuracy} / 1.1406$$

$$\text{Accuracy} = 1.13\text{m}$$

$$\text{CMAS} = 1.13 / 1.1406 = 0.99\text{m at } 90\% \text{ confidence.}$$

$$\text{CMAS} = (1/30'') / 12' * 0.3048 * S$$

$$S = 0.99 / 0.00085 = 1165$$

• • Then max. final map scale is 1:1200

Since, 29 points succeed and point # 8, #9 failed.

According to this result the model that has been built on three controls is passing in cultural feature.

- **Vertical accuracy**

The Vertical Map Accuracy Standard (VMAS) based on NMAS is estimated by the following formula:

$$\text{VMAS} = 1.6449 * \text{RMSE}_z = 1.6449 * 1.36 = 2.24\text{m}$$

The VMAS can be converted to Accuracy_z, accuracy reported according to the NSSDA using equations:

$$\text{Accuracy}_z = 1.9600 / 1.6449 * \text{VMAS} = 1.1916 * \text{VMAS.}$$

Therefore, vertical accuracy reported according to the NSSDA is:

$$(1.1916) / 2 * \text{CI} = 0.5958 * \text{CI, where CI is the contour interval.}$$

$$\text{VMAS} = 1.6449 * \text{RMSE}_z$$

$$VMAS=0.5CI$$

$$0.5CI=1.6449*RMSEz$$

$$CI=2*1.6449*RMSEz$$

$$CI=1.6449*1.36*2=4.47m\approx 4.5m$$

Where we have contour interval 4.5m we have accuracyz is:

$$Accuracyz = 0.5958*4.5 = 2.68m.$$

But 30 points succeed and point # 1 is failed.

According to this result the model that has been built on three controls is passing in vertical feature.

Table (6.3) and (6.4) summarized the results of accuracy calculation, for the horizontal and vertical components respectively.

Table (6.3): Horizontal accuracy of three control points model

Standard	Scale	Accuracy(m)	# of pass points	# of fail points
NSSDA 95% confidence	1:1164	1.13	30	1
NMAS CMAS 90%		0.99	29	2

Table (6.4): Vertical accuracy of three control points model

Standard	contour interval(m)	Accuracy(m)	# of pass points	# of fail points
NSSDA 95% confidence	4.5	2.68	30	1
NMAS VMAS 90%		2.24	29	2

6.3.2 Model built using six control points

X, Y and Z are Photogrammetric coordinates of 31 points are collected from the model, table (6.5).

Table (6.5): Coordinates from six control points model

NO.	X	Y	Z	X	Y	Z	X ²	Y ²	E.P	Z ²
1	.	.	.	0.323	0.553	-2.458	0.10	0.31	0.64	6.04
2	.	.	.	0.222	0.294	0.405	0.05	0.09	0.37	0.16
3	.	.	.	0.200	0.053	-0.083	0.04	0.00	0.21	0.01
4	.	.	.	0.807	-0.022	0.081	0.65	0.00	0.81	0.01
5	.	.	.	-0.080	0.158	-0.958	0.01	0.03	0.18	0.92
6	159201.63	101648.09	.	0.566	0.138	-1.310	0.32	0.02	0.58	1.72
7	.	.	.	0.253	-0.747	-1.176	0.06	0.56	0.79	1.38
8	.	.	.	0.655	-0.244	-1.442	0.43	0.06	0.70	2.08
9	.	.	.	0.312	-0.080	-0.357	0.10	0.01	0.32	0.13
10	.	.	.	0.198	-0.018	-0.290	0.04	0.00	0.20	0.08
11	.	.	.	-0.094	0.033	0.038	0.01	0.00	0.10	0.00
12	.	.	.	0.317	0.388	-0.446	0.10	0.15	0.50	0.20
13	.	.	.	-0.004	-0.277	-0.163	0.00	0.08	0.28	0.03
14	.	.	.	0.118	-0.128	0.852	0.01	0.02	0.17	0.73
15	.	.	.	-0.076	0.213	-1.440	0.01	0.05	0.23	2.07
16	.	.	.	0.223	-0.117	0.755	0.05	0.01	0.25	0.57
17	.	.	.	0.300	0.050	0.464	0.09	0.00	0.30	0.22
18	.	.	.	1.547	0.653	0.512	2.39	0.43	1.68	0.26
19	.	.	.	0.807	-0.010	-2.691	0.65	0.00	0.81	7.24
20	.	.	.	0.807	-0.212	-1.241	0.65	0.04	0.83	1.54
21	.	.	.	0.883	-0.657	-0.223	0.78	0.43	1.10	0.05
22	.	.	.	0.055	0.018	-0.163	0.00	0.00	0.06	0.03
23	.	.	.	0.045	-0.508	0.123	0.00	0.26	0.51	0.02
24	.	.	.	-0.108	-0.065	0.650	0.01	0.00	0.13	0.42
25	.	.	.	-0.201	0.066	-1.435	0.04	0.00	0.21	2.06
26	.	.	.	0.055	-0.074	-0.227	0.00	0.01	0.09	0.05
27	.	.	.	0.072	0.576	-0.048	0.01	0.33	0.58	0.00
28	.	.	.	0.122	0.150	-0.830	0.02	0.02	0.19	0.69
29	159625.60	101641.69	857.80	0.640	-0.003	-0.311	0.41	0.00	0.64	0.10
30	.	.	.	0.535	-0.546	0.980	0.29	0.30	0.76	0.96
31	.	.	.	-0.137	0.136	0.933	0.02	0.02	0.19	0.87
							7.34	3.22		30.62

RMSE _x	RMSE _y	RMSE _z
0.49	0.32	0.99
RMSE _r		
0.58		

6.3.2.1 NSSDA standard

The resultant RMSE_x, RMSE_y, RMSE_z and RMSE_r will be discussing according to NSSDA and NMAS standards.

- **Horizontal accuracy**

Since $RMSE_x \neq RMSE_y$ and $(RMSE_{min}/RMSE_{max}=0.7)$ is between 0.6 and 1.0, the formula $Accuracy \sim 2.4477 * 0.5 * (RMSE_x + RMSE_y)$.

May be used to estimate the accuracy.

The resultant horizontal accuracy value according to the NSSDA, at 95% confidence.

Accuracy_r ~0.99meter.

So allowable error in position is $\leq 0.99m$.

Since 31 points were collected at 95% confidence level, this mean:

$31 * 95\% = 29.45$ (≈ 29) point must have an error less than 0.99m

But 29 points succeed and point # 18, #21 failed.

According to this result the model that has been built on six controls is passing in cultural feature.

- **Vertical Accuracy**

$$RMSE_z = \sqrt{(z_{data\ i} - z_{check\ i})^2 / n}$$

$$Accuracy_z = 1.9600 * RMSE_z.$$

Accuracy_z = $1.96 * 0.99 = 1.94m$

But 29 point succeeds and point # 1, #19 failed.

According to this result the model that has been built on three controls is passing in elevation.

6.3.2.2 Analyze and correlated the result with NMAS standard

- **Horizontal accuracy**

Therefore, NMAS horizontal accuracy reported according to the NSSDA is:

$$\text{CMAS} = \text{Accuracy} / 1.1406$$

$$\text{Accuracy} = 0.99\text{m}$$

$$\text{CMAS} = 0.99 / 1.1406 = 0.87\text{m at } 90\% \text{ confidence.}$$

$$\text{CMAS} = (1/30") / 12' * 0.3048 * S$$

$$S = 0.87 / 0.00085 = 1023$$

• • Then max. final map scale is 1:1100

Since 29 points succeed and point # 18, #21 failed.

According to this result the model that has been built on six controls is passing in cultural feature.

- **Vertical accuracy**

The Vertical Map Accuracy Standard (VMAS) based on NMAS is estimated by the following formula:

$$\text{VMAS} = 1.6449 * \text{RMSE}_z = 1.6449 * 0.99 = 1.63\text{m}$$

The VMAS can be converted to Accuracy_z, accuracy reported according to the NSSDA using equations:

$Accuracy_z = 1.9600/1.6449 * VMAS = 1.1916 * VMAS.$

Therefore, vertical accuracy reported according to the NSSDA is $(1.1916)/2 * CI = 0.5958 * CI$, where CI is the contour interval.

$$CI = 1.6449 * RMSE_z * 2 = 3.25m \approx 3m$$

Where we have contour interval 3m we have accuracy_z is:

$$Accuracy_z = 0.5958 * 3 = 1.79m.$$

But 29 points succeed and point # 1, #19 failed.

According to this result the model that has been built on six controls is passing in vertical feature.

Table (6.6) and (6.7) summarized the results of accuracy calculation, for the horizontal and vertical components respectively.

Table (6.6): Horizontal accuracy of six control points model

Standard	Scale	Accuracy(m)	# of pass points	# of fail points
NSSDA 95% confidence	1:1023	0.99	29	2
NMAS CMAS 90%		0.87	29	2

Table (6.7): Vertical accuracy of six control points model

Standard	contour interval(m)	Accuracy(m)	# of pass points	# of fail points
NSSDA 95% confidence	3	1.79	29	2
NMAS VMAS 90%		1.63	29	2

6.3.3 Model built using nine control points

X, Y and Z Photogrammetric coordinates of 31 points are collected from the model, table (6.8).

Table (6.8): Coordinates from nine control points model

NO.	X	Y	Z	X	Y	Z	X ²	Y ²	E.P	Z ²
1
2
3
4
5
6
7
8
9
10
11
12
13
14
15
16
17
18
19
20
21
22
23
24
25
26
27
28
29
30
31
							RMSx	RMSy		average RMSEz
							.	.		.
							.	.		.

6.3.3.1 NSSDA standard

The resultant RMSE_x, RMSE_y, RMSE_z and RMSE_r will be discussing according to NSSDA and NMAS standards.

- **Horizontal accuracy**

Since $RMSE_x \neq RMSE_y$ and $(RMSE_{min}/RMSE_{max}=0.98)$ is between 0.6 and 1.0, the formula $Accuracy \sim 2.4477 * 0.5 * (RMSE_x + RMSE_y)$ may be used to estimate accuracy

The resultant horizontal accuracy value according to the NSSDA, at 95% confidence.

Accuracy ~ 0.97 meter.

So allowable error in position ≤ 0.97 m,

Since 31 points were collected at 95% confidence level, this mean:

$31 * 95\% = 29.45$ (≈ 29) point must have an error less than 0.92m

But 30 points succeed and point #22 is failed.

According to this result the model that has been built on nine controls is passing in cultural feature.

- **Vertical Accuracy**

$$RMSE_z = \sqrt{(z_{data} - z_{check})^2 / n}$$

$$Accuracy_z = 1.9600 * RMSE_z.$$

Accuracy_z = $1.96 * 0.63 = 1.235$ m

Since 30 points succeeds and point #22 is failed.

According to this result the model that has been built on nine controls is passing in elevation.

6.3.3.2 Analyze and correlated the result with NMAS standard

- **Horizontal accuracy**

Therefore, NMAS horizontal accuracy reported according to the NSSDA is:

$$CMAS = \text{Accuracy} / 1.1406$$

$$\text{Accuracy} = 0.97\text{m}$$

$$CMAS = 0.97 / 1.1406 = 0.85\text{m at } 90\% \text{ confidence.}$$

$$CMAS = (1/30") / 12' * 0.3048 * S$$

$$S = 0.85 / 0.00085 = 1000$$

• • Then max. final map scale is 1:1000

Since 30 points succeed and point # 22 is failed.

According to this result the model that has been built on nine controls is passing in cultural feature.

- **Vertical accuracy**

The Vertical Map Accuracy Standard (VMAS) based on NMAS is estimated by the following formula:

$$VMAS = 1.6449 * RMSE_z = 1.6449 * 0.63 = 1.04\text{m}$$

The VMAS can be converted to Accuracy_z, accuracy reported according to the NSSDA using equations:

$$\text{Accuracy}_z = 1.9600 / 1.6449 * VMAS = 1.1916 * VMAS.$$

Therefore, vertical accuracy reported according to the NSSDA is $(1.1916) / 2 * CI = 0.5958 * CI$, where CI is the contour interval.

$$CI = 1.6449 * RMSE_z * 2 = 2.07 \text{ m} \approx 2 \text{ m}$$

Where we have contour interval 2m we have accuracy is:

$$Accuracy = 0.5958 * 2 = 1.19 \text{ m}$$

Since 30 points succeed and point # 31 is failed.

According to this result the model that has been built on nine controls is passing in vertical feature.

Table (6.9) and (6.10) summarized the results of accuracy calculation, for the horizontal and vertical components respectively.

Table (6.9): Horizontal accuracy of nine control points model

Standard	Scale	Accuracy(m)	# of pass points	# of fail points
NSSDA 95% confidence	1:1000	0.97	30	1
NMAS CMAS 90%		0.85	30	1

Table (6.10): Vertical accuracy of nine control points model

Standard	contour interval(m)	Accuracy(m)	# of pass points	# of fail points
NSSDA 95% confidence	2	1.19	30	1
NMAS VMAS 90%		1.04	30	1

6.4 Correlation of the resultant RMSE of the three generated photogrammetry models

1. Horizontal accuracy

It was found that the RMSE_x is decrease, and the accuracy increase, as the number of control points used in the model increase, fig. (6.1). The RMSE is accepted to follow the following equation:

$$Y = -0.021X + 0.6739$$

Where:

Y: the expected RMSE

X: the number of control points use in the model

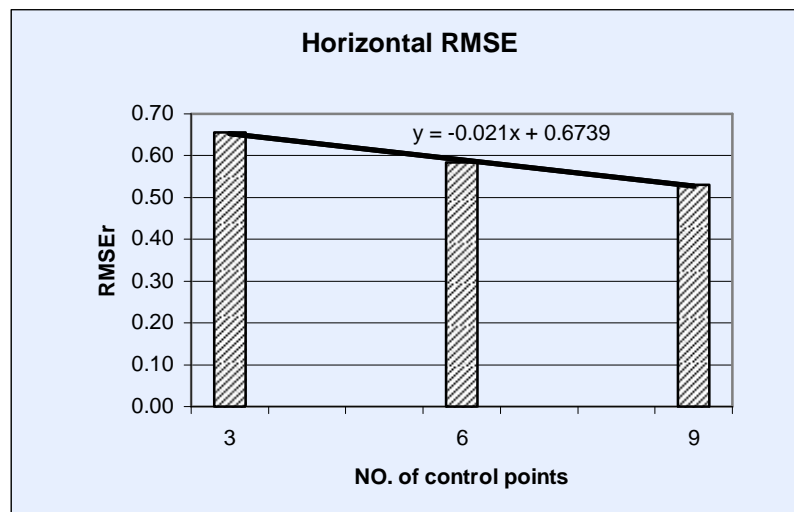


Fig. (6.1): Correlation of horizontal RMSE of the three models

2. vertical accuracy

It was found that the RMSEz is decrease, and the accuracy increase, as the number of control points used in the model increase, fig. (6.2). The RMSE is accepted to follow the following equation:

$$Y = -0.1222X + 1.4851$$

Where

Y: the expected RMSE

X: the number of control points use in the model

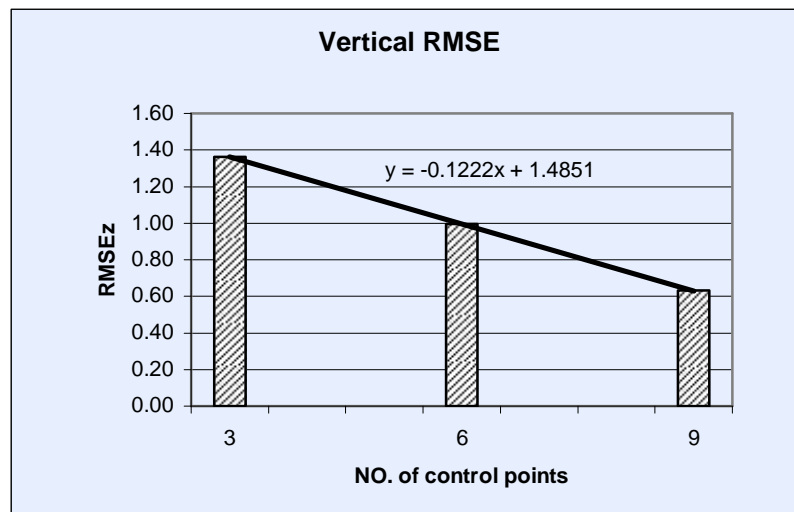


Fig.(6.2): Correlation of vertical RMSE of the three models

6.5 DEM and Interpolations techniques

The spatial interpolation is procedure of estimate the value of appropriators at unsampled site within the area covered by existing observations, [ref.17].

Spatial interpolation may be used in geographic information system (GIS):

- To provide contour for displaying data graphically
- To calculate some properties of the surface at a given points

- To have continuous surface to express different properties

For Interpolation method there are two methods to create a surface from measured points and lines which are:

6.5.1 Global techniques

Those methods calculate prediction using all the entire data set which includes trend surface and Fourier series, the function used to fit the sample point could be of linear or higher polynomial (as kriging).

6.5.1.1 Kriging method

The Kriging is an interpolation technique depend the surrounding measured values are weighted to derive a prediction for an unmeasured location. The Weights are based on the distance between the measured points, and the overall spatial arrangement among the measured points. The Kriging method is based on regionalized variable theory, which assumes that the spatial variation in the data being modeled is statistically homogeneous throughout the surface.

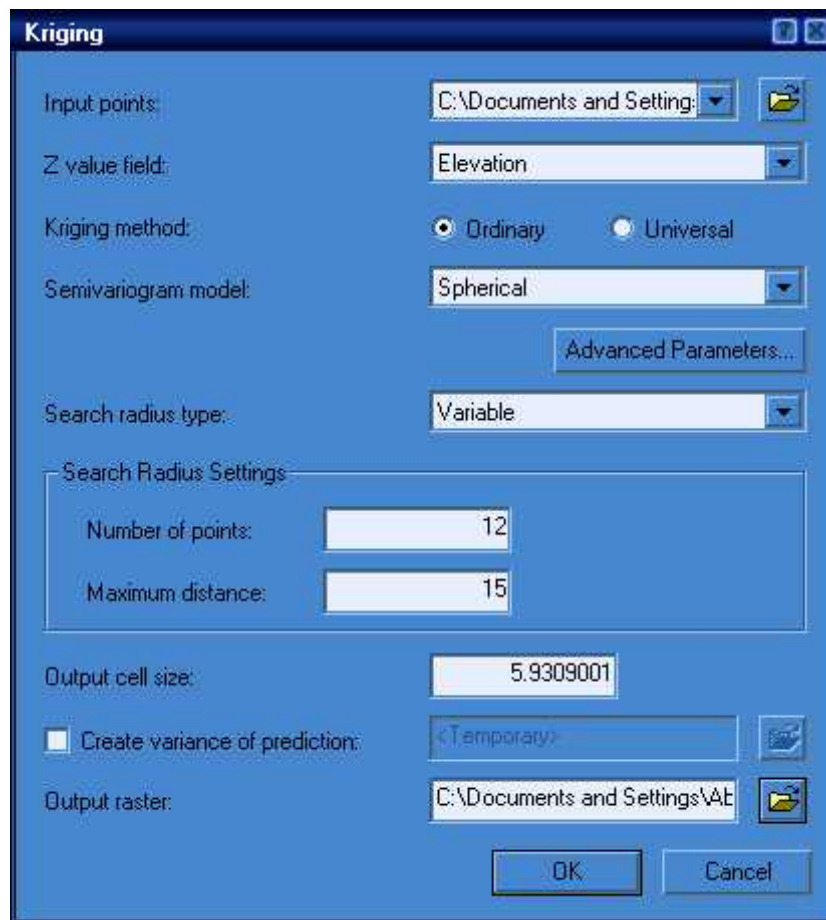


Fig. (6.3): Kriging interpolation by GIS

6.5.2 Local techniques

Those techniques predict the attribute value from the measured points within the neighborhood, inverse distance weighted (IDW), and spline method.

6.5.2.1 The Spline method

The Spline method is an interpolation method that estimates values using a mathematical function that minimizes overall surface curvature, resulting in a smooth surface that passes exactly through the input points.

Conceptually, the sample points are extruded to the height of their magnitude; spline bends a sheet of rubber that passes through the input points while minimizing the total curvature of the surface. It fits a mathematical function to a specified number of nearest input points while passing through the sample points. This method is best for generating gently varying surfaces such as elevation, water table heights, or pollution concentrations.

There are two Spline methods: Regularized and Tension.

The Regularized method creates a smooth, gradually changing surface with values that may lie outside the sample data range.

The Tension method controls the stiffness of the surface according to the character of the modeled phenomenon. It creates a less smooth surface with values more closely constrained by the sample data range.

Additional parameters

- **Regularized Spline method**

The weight parameter defines the weight of the third derivatives of the surface in the curvature minimization expression. For higher weights, the smoother the output surface will be generated. The typical values that may be used are 0, 0.001, 0.01, 0.1, and 0.5.

- **Tension Spline method**

The weight parameter defines the weight of tension. The higher the weight, the coarser the output surface will be generated. The typical values are 0, 1, 5, and 10.

- **Number of points**

Number of points identifies the number of points used in the calculation of each interpolated cell. The more input points you specify, the more each cell is influenced by distant points and the smoother the output surface. The larger the number of points, the longer it will take to process the output raster.

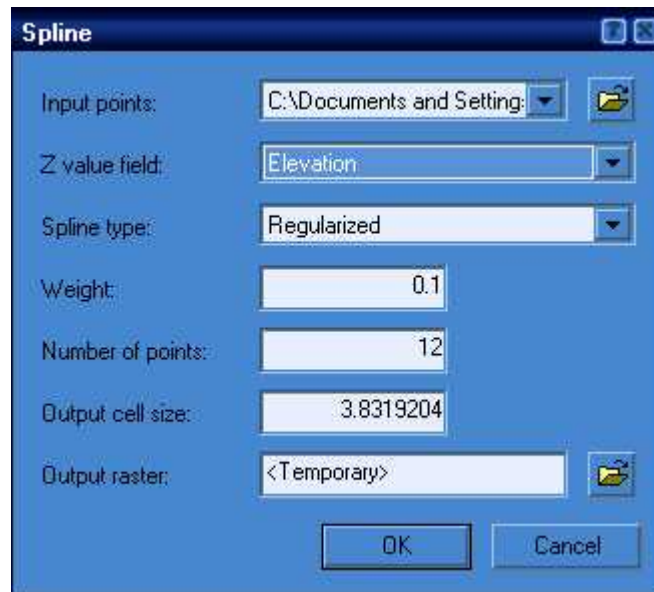


Fig. (6.4): Spline interpolation by GIS

6.5.2.2 Inverse Distance Weighted Interpolation (IDW)

IDW is a method of interpolation that estimates cell values by averaging the values of sample data points in the neighborhood of each processing cell. The closer a point is to the center of the cell being estimated, the more influence, or weight; it has in the averaging process.

This method assumes that the variable being mapped decreases in influence with distance from its sampled location. For example, when interpolating a surface of consumer purchasing power for a retail site analysis, the purchasing power of a more distant location will have less influence because people are more likely to shop closer to home.

- **Power**

By defining a higher power, more emphasis is placed on the nearest points, and the resulting surface will have more detail (be less smooth). Specifying a lower power will give more influence to the points that are farther away, resulting in a smoother surface. A power of 2 is most commonly used with IDW and is the default.

- **Search radius**

The characteristics of the interpolated surface can also be controlled by applying a search radius (fixed or variable), which limits the number of input points that can be used for calculating each interpolated cell.

- **Fixed search radius**

A fixed search radius requires a neighborhood distance and a minimum number of points. The distance dictates the radius of the circle of the neighborhood (in map units). The distance of the radius is constant, so for each interpolated cell, the radius of the circle used to find input points is the same. The minimum number of points indicates the minimum number of measured points to use within the neighborhood. All the measured points that fall within the radius will be used in the calculation of each interpolated cell. When there are fewer measured points in the neighborhood than the specified minimum, the search radius will increase until it can encompass the minimum number of points.

- **Variable search radius**

With a variable search radius, the number of points used in calculating the value of the interpolated cell is specified, which makes the radius distance vary for each interpolated cell, depending on how far it has to search around each interpolated cell to reach the specified number of input points. Thus, some neighborhoods can be small and others can be large, depending on the density of the measured points near the interpolated cell. You can also specify a maximum distance (in map units) that

the search radius cannot exceed. If the radius for a particular neighborhood reaches the maximum distance before obtaining the specified number of points, the prediction for that location will be performed on the number of measured points within the maximum distance. Generally you will use smaller neighborhoods or a minimum number of points when the phenomenon has a great amount of variation.

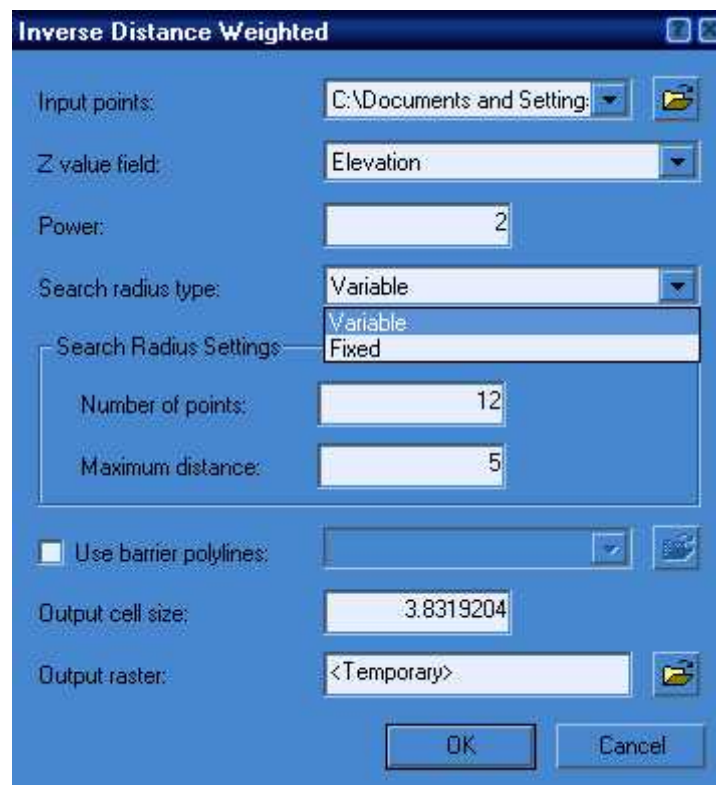


Fig. (6.5): Inverse Distance Weighted (IDW)

6.6 Testing of Photogrammetry resultant grid

A digital elevation model (DEM) can be constructed in GIS environment from the grid coordinates, that are created as a result of the Photogrammetry model of 9 control points.

In order to check the accuracy of the generated DEM, an accuracy assessment is performed between the Z of the check points and the corresponding coordinates from DEM.

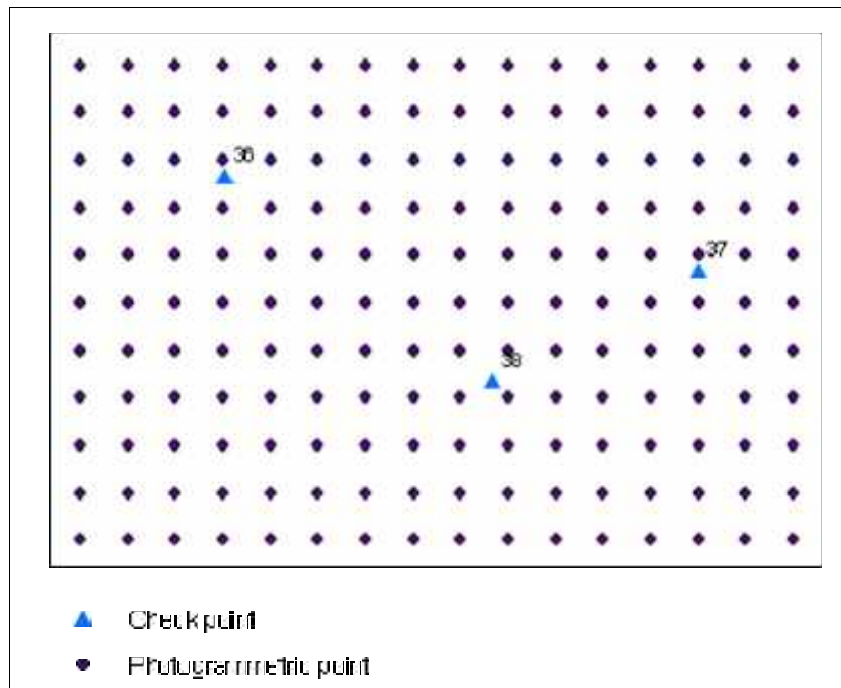


Fig. (6.6): Photogrammetric and check elevation points

The interpolation has been done using kriging method as recommended by graduation project in Palestine polytechnic university which is comparing the output of different interpolators within the (GIS).

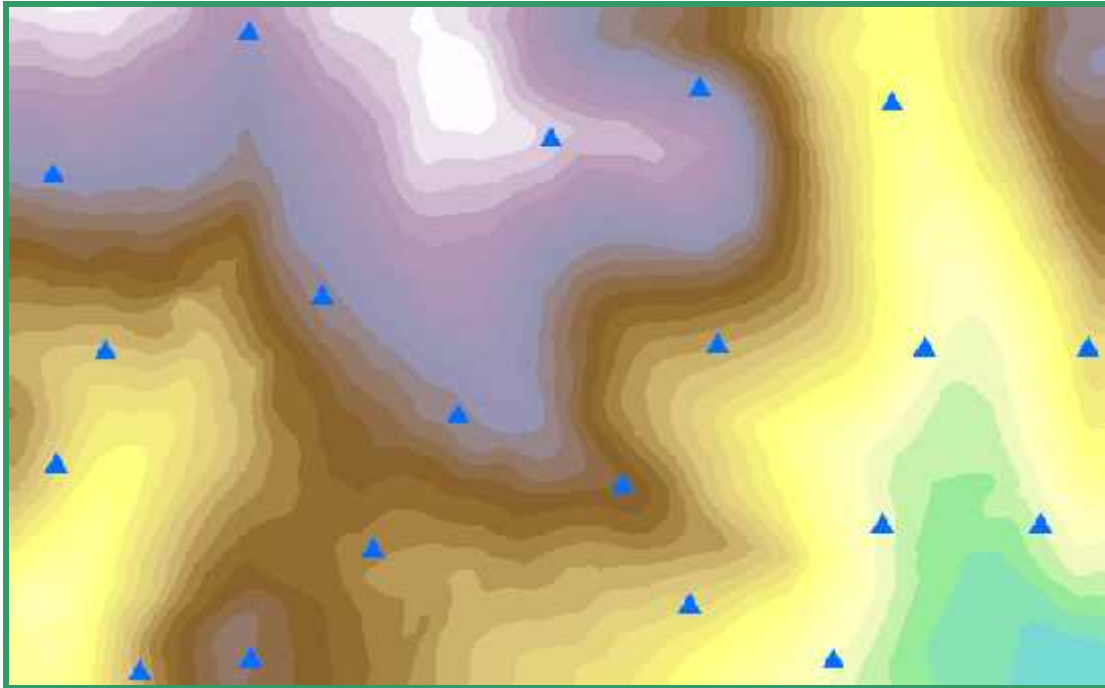


Fig. (6.7): DEM interpolated by kriging method

Table (6.11) summarizes the DEM grid size effects on RMSEz, and hence, on the accuracy. It is obvious that the accuracy increases with

1. increasing in number of control points used to construct the photogrammetric model, and
2. with decreasing the grid size, fig. (6.8).

Table (6.11): DEM grid effects on the RMSEz

		grid		
		15*15	10*10	5*5
		RMSE	RMSE	RMSE
Model	3-control	1.24	1.07	1.05
	6-control	0.92	0.80	0.65
	9-control	0.74	0.67	0.61
File volume		374 K	847 K	3340 K
Time needed		2.1min	2.75min	3.5min

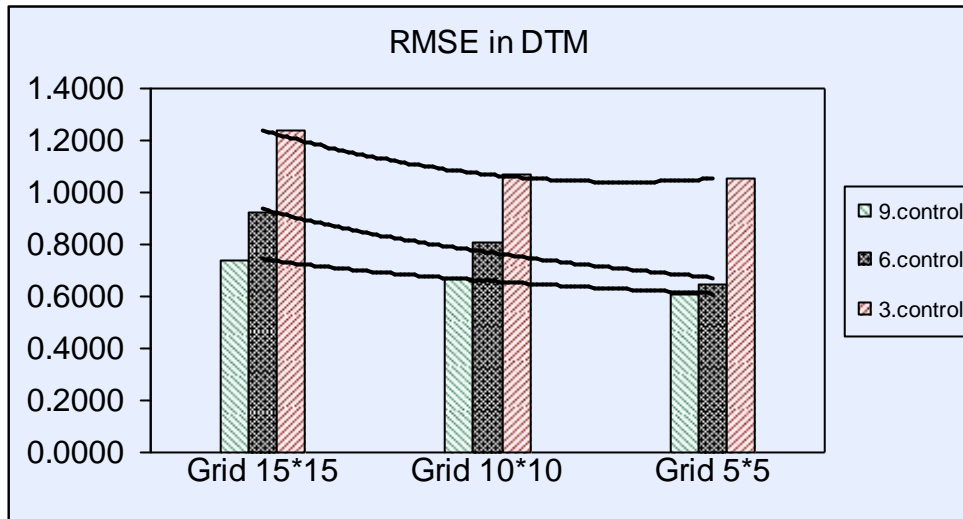


Fig. (6.8) RMSE in DEM

6.7 Correlation of time needed by land survey and Photogrammetry technique

The following table summarizes the time consumed to accomplish the total station and Photogrammetry survey of 31 check points.

Table (6.12): Correlation of time needed and survey technique

Control points	Survey technique	Positional RMSE m	Vertical RMSE	Standard accuracy NSSDA	Time
3	Total station	0.0057	0.007	Accepted	16-hours
	Photogrammetry	1.13	2.68	Accepted	2+3-hours*
6	Total station	0.0057	0.007	Accepted	16-hours
	Photogrammetry	0.99	1.79	Accepted	3+3-hours
9	Total station	0.0057	0.007	Accepted	16-hours
	Photogrammetry	0.97	1.19	Accepted	4+3-hours

* 2-hours to collect three controls by total station, 3-hours to build the model

CHAPTER

7

CONCLUSIONS & RECOMMENDATIONS

The following contents are going to be covered in this chapter:

7.1 Conclusions

7.2 Recommendations

CHAPTER SEVEN

Conclusions & Recommendations

7.1 Conclusions

1. It is noted from this project when the number of control points increase to accomplish the model, the RMSE decreases, and the accuracy increase.
2. If the generated model has small RMSE, the obtained information can be printed at large scale.
3. When the map will be printed at small scale, it must take in consideration the contour interval will be large.
4. According to specification, if specific small feature could be noted at captured photo, which mean specific flying height of aircraft could be determined according to photogram metric planning.
5. It is noted that when grid of DEM is decreases, accuracy of DEM will be increases. And as the number of control points increase to build the model the accuracy of DEM increase.
6. With allowable error and specific scale photogrammetry give suitable result with small efforts and time consuming on the other hand EDM gives accurate result with large efforts and time consuming.
7. 1:1000 is the larger scale that the produced map of the photos can printed.

7.2 Recommendations

1. The quality of used image is accepted, angle of the sun not vertical so the suitable time for capturing photos in the mid of the day (11am-1pm).

2. The photos have four fiducial points, which are not clearly and also it is preferred eight points to have the best transformation (interior orientation).
3. It is noted that the specific areas in the model have large parallax during the work.
4. The flying height of aircraft is too high, it is preferred to have another low flying height of aircraft to compare between two results.
5. In order to make the orientation, the marking control points were missed so it's preferred that the photo pre-marked before exposing, in order to have more accurate orientation.
6. Updating of the workstation is highly recommended.
7. It was planned to use GPS techniques to comparing the results with EDM and aerial photogrammetry, but unfortunately GPS instrument broken - down.

TABLE OF CONTENTS

Subject	Page No.
Title	I
Certification	II
Dedication	III
Acknowledgment	IV
Abstract (English)	V
Abstract (Arabic)	VII
Table of content	VIII
List of figures	XII
List of tables	XIV
Abbreviations	XV
Chapter One	Introduction
1.1 Overview	2
1.2 Project importance	3
1.3 Studying area.....	3
1.4 Project methodology	3
1.4.1 Control and check points collection using land survey method	6
1.4.2 Photogrammetry method	6
1.5 Project outline	7
1.6 Project time table "Schedule"	8
Chapter Two	land survey Techniq
2.1 Overview	11
2.2 Electronic distance measurement	12
2.3 Basic principles of electromagnetic waves in EDM instruments ...	12
2.4 Errors in Total Station	15
2.4.1 Errors in distance measurement in Total Station	15
2.4.2 Scale error	16
2.5 Applications of the Total Station	17
Chapter Three	Aerial Photogrammetry
3.1 Overview	19
3.2 Type of photographs	19

3.3	Taking vertical aerial photographs	21
3.4	Acquisitions of aerial photos	21
3.4.1	Scanners	21
3.4.2	Digital cameras	
3.4.2.1	Flying spot scanners	
3.4.2.2	Linear array sensor	24
3.4.2.3	Digital frame camera	25
3.5	Stereoviewing	25
3.6	Parallactic angle	26
3.7	X- Parallax	27
3.8	Two images - not one!	29
3.9	Specifications for ground control	31
3.10	Types of control points	31
3.11	Space resection	32
3.12	Stereoplotters	33
3.13	Types of Stereoplotters	34
3.13.1	Analytical stereoplotters	34
3.13.2	Digital stereoplotters	36
3.14	Stereoplotter operations	38
3.14.1	Interior orientation	38
3.14.2	Relative orientation	38
3.14.3	Absolute orientation	40
3.15	Image matching	41
3.16	Aerotriangulation	42
3.17	Digital elevation model (DEM)	44

Chapter Four	Accuracy Standards
---------------------	---------------------------

4.1	Overview	47
4.2	Error sources	47
4.2.1	Instrumental errors	47
4.2.2	Natural errors	48
4.2.3	Personal errors	48
4.3	Survey accuracy standards	50
4.3.1	Palestine traverse standards	50
4.3.2	FGDC Relative Accuracy Standards for Horizontal and Vertical Control	51
4.3.3	Horizontal control accuracy standards for traverses (FGCS, 1994)	52
4.3.4	FGCS for evaluating the local survey	53
4.4	Map accuracy standards	53
4.4.1	Federal Geographic Data Committee (FGDC)	54

4.4.2	National Map Accuracy Standards (NMAS)	56
4.4.3	United State Geological Survey (USGS) standards	57
4.4.4	American Society for Photogrammetry and Remote Sensing	57
4.4.5	U.S. Department of Transportation (DOT) surveying and mapping manual map standards	59
4.5	Map testing	61
4.5.1	American Society for Photogrammetry and Remote Sensing (ASPRS)	61
4.5.2	Federal Geographic Data Committee (FGDC)	62
4.5.3	United State Geological Survey (USGS) Standards	62
4.5.4	National Map Accuracy Standards (NMAS)	62
4.6	Photogrammetry accuracy standards	63
4.6.1	Nevada Department of Transportation (NDOT) standards .	63
4.7	Relation ship between NSSDA and other accuracies	66
4.8	Relationship between NSSDA and NMAS	68
4.8.1	Relationship between NSSDA and NMAS (horizontal)	68
4.8.2	Relationship between NSSDA and NMAS (vertical)	69
4.9	ASPRS classes	70
4.9.1	Horizontal accuracies	70
4.9.2	Spot Elevation accuracies	0

Chapter Five	Measurements and Calculations
---------------------	--------------------------------------

5.1	Overview	7
5.2	Calculate the observed angle and its propagate error coordinates ..	7
5.3	Least Squares Solution for the traverse	7
5.3.1	First iteration of least square solution	82
5.3.2	Second iteration of least square solution	83
5.4	Degrees of traverse	84

Chapter Six	Data Analysis
--------------------	----------------------

6.1	Overview	94
6.2	Photo quality	94
6.2.1	Photo quality parameters	95
6.3	Photogrammetry models	96
6.3.1	Model built using three control points	96
6.3.1.1	NNSDA standard	97
6.3.1.2	Analyze and correlated the result with NMAS standard	99
6.3.2	Model built using six control points	101

6.3.2.1	NSSDA standard	102
6.3.2.2	Analyze and correlated the result with NMAS standard	103
6.3.3	Model built using nine control points	104
6.3.3.1	NSSDA standards	106
6.3.3.2	Analyze and correlated the result with NMAS standard	107
6.4	Correlation of the resultant RMSE of the three generated photogrammetry models.....	109
6.5	EDM and Interpolations techniques	110
6.5.1	Global techniques.....	111
6.5.1.1	Kriging method.....	111
6.5.2	Local techniques.....	112
6.5.2.1	The Spline method	112
6.5.2.2	Inverse Distance Weighted Interpolation (IDW).....	114
6.6	Testing of Photogrammetry resultant grid	116
6.7	Correlation of time needed by land survey and Photogrammetry technique	119

Chapter Seven	Conclusions & Recommendations
----------------------	------------------------------------------

7.1	Conclusions	121
7.2	Recommendations	121

References-----	123
------------------------	------------

Appendices-----	124
------------------------	------------

List of Figures

Figure	Page No.
Figure 1.1: Location of Study area within Hebron city	4
Figure 1.2: Overlap photos of the study area	5
Figure 2.1: Phase comparison	14
Figure 3.1: Camera orientation	20
Figure 3.2: End lap and side lap	21
Figure 3.3: Geometry of flying spot scanner	23
Figure 3.4: Geometry of a linear array sensor	24
Figure 3.5: Geometry of a digital frame camera	25
Figure 3.6: Stereoviewing	26
Figure 3.7: Parallaxic angle	27
Figure 3.8: Geometry of an overlapping pair of vertical photographs	28
Figure 3.9: 2D versus 3D viewing methods	30
Figure 3.10: \check{S}, w, k and X, Y, Z in space resection	32
Figure 3.11: Typical analytical stereoplotter	35
Figure 3.12: Schematic diagram of components and operation of analytical plotter	36
Figure 3.13: Typical softcopy workstation	37
Figure 3.14: Analytical relative orientation of a stereopair	39
Figure 3.15: Block of photos in overlapped position	43
Figure 5.1: Study area, traverse sketch	74
Figure 5.2: Distance observation equation	79
Figure 5.3: Angle observation equation	80
Figure 6.1: Correlation of horizontal RMSE of the three models	109
Figure 6.2: Correlation of vertical RMSE of the three models	110
Figure 6.3: Kriging interpolation by GIS.....	112
Figure 6.4: Spline interpolation by GIS	114
Figure 6.5: Inverse Distance Weighted (IDW)	116
Figure 6.6: Photogrammetric and check elevation points	117
Figure 6.7: DEM interpolated by kriging method	118
Figure 6.8: RMSE in DEM	119
Figure A.1: XYZ and xyz right-handed three-dimensional coordinate systems	A-1
Figure A.2: The three sequential angular rotations	A-2
Figure A.3: Omega rotation about the x' axis	A-3
Figure A.4: Phi rotation about the y1 axis	A-4

Figure A.5: Kappa rotation about the z_2 axis	A-5
Figure B.1: The collinearity condition	B-1
Figure B.2: Image coordinate system rotated such that it is parallel to the object	B-2
Figure B.3: Measurement x - y - z and rotated x' - y' - z' image coordinate systems	B-4

List of Tables

Table	Page No.
Table 1.1: Project Schedule for first course in year 2006 - 2007	8
Table 1.2: Project Schedule for second course in year 2006 – 2007	9
Table 3.1: Types of ground control points	31
Table 4.1: Allowable error in closed traverse in Palestinian standards	50
Table 4.2: FGDC horizontal distance accuracy standards	51
Table 4.3: FGDC vertical distance accuracy standards	52
Table 4. : Horizontal control accuracy standards for traverses (FGCS) ..	52
Table 4.5: ASPRS Planimetric Feature Coordinate Accuracy Requirement	58
Table 4.6: ASPRS Topographic Elevation Accuracy Requirement for Well-Defined points.....	59
Table 4.7: Standard accuracies for photogrammetric mapping	60
Table 4.8: Accuracy standard for NDOT intermediate scale digital photogrammetry	65
Table 4.9: Accuracy standard for NDOT intermediate scale digital photogrammetry	65
Table 4.10: Accuracy standard for NDOT intermediate scale digital photogrammetry	66
Table 5.1: Study area, reading angles from instrument (Total Station)....	75
Table 5.2: Fixed control points	77
Table 5.3: Study area, summery of the traverse	81
Table 5.4: Study area, reading from Instrument (Total Station).....	89
Table 5.5: Coordinates collected by Total Station	91
Table 6.1: Photo exposure parameter	95
Table 6.2: Coordinates from three control points model	96
Table 6.3: Horizontal accuracy of three control points model	100
Table 6.4: Vertical accuracy of three control points model	100
Table 6.5: Coordinates from six control points model	101
Table 6.6: Horizontal accuracy of six control points model	104
Table 6.7: Vertical accuracy of six control points model	104
Table 6.8: Coordinates from nine control points model	105
Table 6.9: Horizontal accuracy of nine control points model	108
Table 6.10: Vertical accuracy of nine control points model	108
Table 6.11: DEM grid effects on the RMSEz	118
Table 6.12: Correlation of time needed and survey technique.....	119

ABBREVIATIONS

- GPS: Global Position System.
- EDM: Electronic Distance Measurement.
- GIS: Geographic Information System.
- RMSE: Root Mean Square Error.
- Hz: Hertz.
- ppm: Part Per Million.
- mb: Millie Bar.
- MSL: Mean Sea Level.
- WGS84: World Geodetic System 84.
- CCD: Charged Cabled Device.
- DEM: Digital Elevation Model.
- NGS: National Geodetic Standards.
- ROM: Ratio Of Misclosure.
- OMB: Office of Management and Budget.
- ASP: American Society of Photogrammetry.
- DOT: Department Of Transportation.
- ASPRS: American Society of Photogrammetry and Remote Sensing.
- ASCE: American Society of Civil Engineers.
- FGDC: Federal Geographic Data Committee.
- NSSDA: National Standard for Spatial Data Accuracy.
- NMAS: National Map Accuracy Standards.
- USGS: United State Geological Survey.
- NDOT: Nevada Department of Transportation.

REFERENCES

1. ACKERMANN, F. 1984: Digital image correlation: performance and potential application in photogrammetry. *Photogrammetric record*, 11(64): 429-439 (October 1984).
2. American Society Of Photogrammetry, Digital Photogrammetry Bethesda USA 1998
3. James M.Anderson & Edowarad M.Mikhail, Surveying Theory and Practice, seventh Edition, 1998.
4. Maher Owaiwi, Notes, PPU, Palestine, 2006.
5. Paul R. Wolf, Adjustment Computations Statistics and Least Squares in Surveying and GIS, John Wiley & Sons, Inc., Canada, 1997.
6. Paul R. Wolf and Bon A Dewiytt, Elements of Photogrammetry with application in GIS, Mc-graw Hill Inc., USA, 2000.
7. Peter A.Burrough and Rachael A.Mcdnnell, principles of geographical information system, published in united states by Oxford University Press Inc., New York 2000.
8. <http://www.ASPRS.org>
9. <http://www.canada center for remote sensing>
10. <http://www.erg.usgs.gov/isb/pubs/pubslists/>
11. http://www.fes_uwaterloo_ca-crs-geog165-images-apg_overlap_gif_files\apg.htm.
12. <http://www.FGDC.gov>
13. http://www.foto.hut.fi/opetus/301/luennot/6/6_pr2004.html
14. http://www.gmat.unsw.edu.au/snap/gps/gps_survey/principles_gps.htm
15. <http://www.luzarns.elc.hu/mc/ik/ohp17.htm>
16. <http://www.mnplan.state.mn.us/press/accurate.html>
17. [http://www.NJDOT - Minimum Guidelines For Aerial Photogrammetric Mapping \(Metric\).htm](http://www.NJDOT - Minimum Guidelines For Aerial Photogrammetric Mapping (Metric).htm)

GLOSSARY

- GPS: Global Position System.
- EDM: Electronic Distance Measurement.
- GIS: Geographic Information System.
- RMSE: Root Mean Square Error.
- Hz: Hertz.
- ppm: Part Per Million.
- mb: Millie Bar.
- MSL: Mean Sea Level.
- WGS84: World Geodetic System.
- CCD: Charged Cabled Device.
- DEM: Digital Elevation Model.
- NGS: National Geodetic Standards.
- ROM: Ratio Of Misclosure.
- OMB: Office of Management and Budget.
- ASP: American Society of Photogrammetry.
- DOT: Department Of Transportation.
- ASPRS: American Society of Photogrammetry and Remote Sensing.
- ASCE: American Society of Civil Engineers.
- FGDC: Federal Geographic Data Committee.
- NSSDA: National Standard for Spatial Data Accuracy.
- NMAS: National Map Accuracy Standards.
- USGS: United State Geological Survey.
- NDOT: Nevada Department of Transportation.

APPENDICES

APPENDIX-A

THREE-DIMENSIONAL CONFORMAL COORDINATE TRANSFORMATIONS

APPENDIX-B

COLINEARITY CONDITION EQUATIONS

APPENDIX-C

SPACE RESECTION PROGRAMME

APPENDIX-A

A - THREE-DIMENSIONAL CONFORMAL COORDINATE TRANSFORMATIONS

It is a transformation including convert coordinate from one 3D system to another, such as:

1. Convert coordinate of tilted photo to another system parallel to the ground coordinate system.
2. To form continuous 3D "strip model" from independent stereo model

In fig. (A-1), the rotation are generated on the positive axis and contour clockwise, omega (\mathcal{S}), phi (W), and kappa ($|$) rotation about x' , y' and z' coordinate system

The point in xyz system will be transform to XYZ ground system, so seven parameter are developed which is three rotation angles, omega (\mathcal{S}), phi (W), and kappa ($|$); a scale factor (s); and three translation factors, T_x , T_y , and T_z . and three translation factors, T_x , T_y , and T_z .

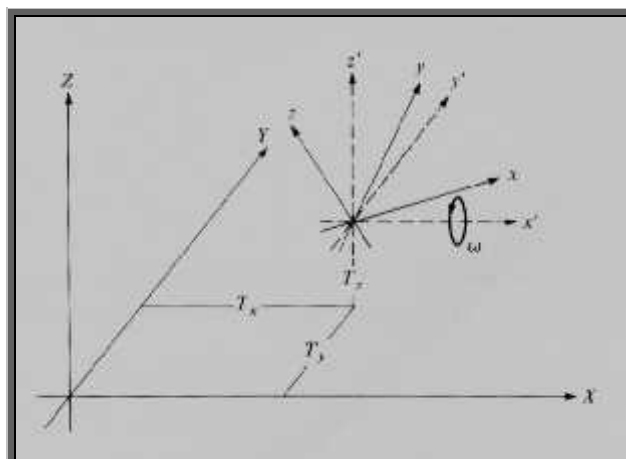


Fig. (A-1): XYZ and xyz right-handed three-dimensional coordinate systems

The transformation includes three steps which are:

1. Rotation

$x'y'z'$ coordinate system parallel to XYZ ground system, so to convert $x'y'z'$ coordinate system to XYZ ground system the rotation about axis must take place, that will be developed in sequence of two dimensional as in fig. (A-2).

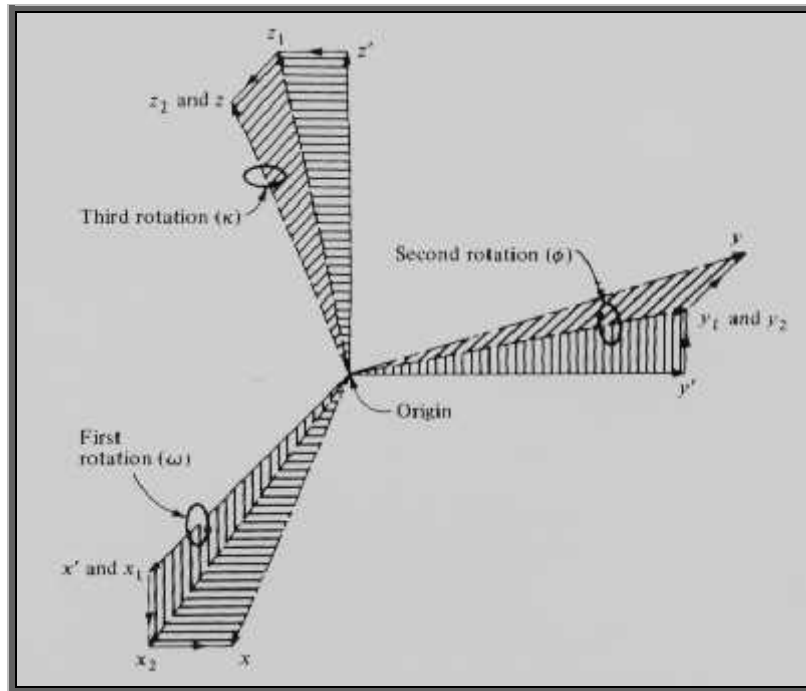


Fig. (A-2): The three sequential angular rotations

Rotation about x' axis (S), convert the point coordinate from $x'y'z'$ coordinate system to $x_1y_1z_1$ system, then second rotation is W rotation about the once rotated y_1 axis which converts coordinates from the $x_1y_1z_1$ system into an $x_2 y_2 z_2$, and third is $|$ rotation about the twice rotated z_2 axis which converts coordinates from the $x_2y_2z_2$ system into the xyz system of fig.(A-1), then the actual rotation and transformation is converting xyz to XYZ .

$|$ Rotation: rotation about $z_2, x_2y_2z_2 \longrightarrow x y z$

The development of the rotation formulas is as follows:

a) **First**, fig. (A-3), rotation through the angle ω about the x' axis,

ω Rotation: rotation about x' , $x'y'z' \longrightarrow x_2 y_2 z_2$

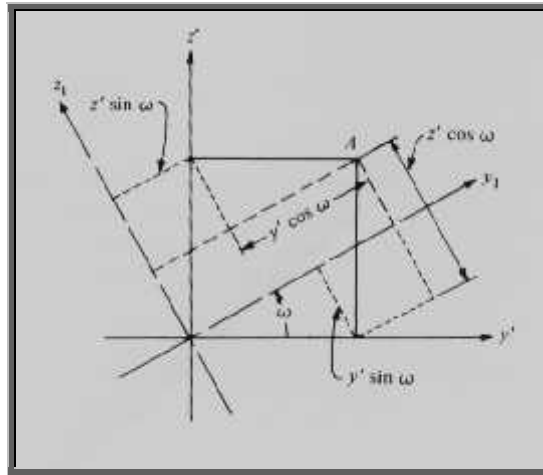


Fig. (A-3): Omega rotation about the x' axis

$$\begin{aligned}
 x_1 &= x' \\
 y_1 &= y' \cos \omega + z' \sin \omega \\
 z_1 &= -y' \sin \omega + z' \cos \omega
 \end{aligned}
 \tag{1}$$

Since this rotation was about x' , the x' and x_1 axes are coincident and therefore the x coordinate of A is unchanged.

b) **Second**, fig.(A-4), rotation through ω about the y_1 axis,

ω Rotation: rotation about y_1 , $x_1 y_1 z_1 \longrightarrow x_2 y_2 z_2$

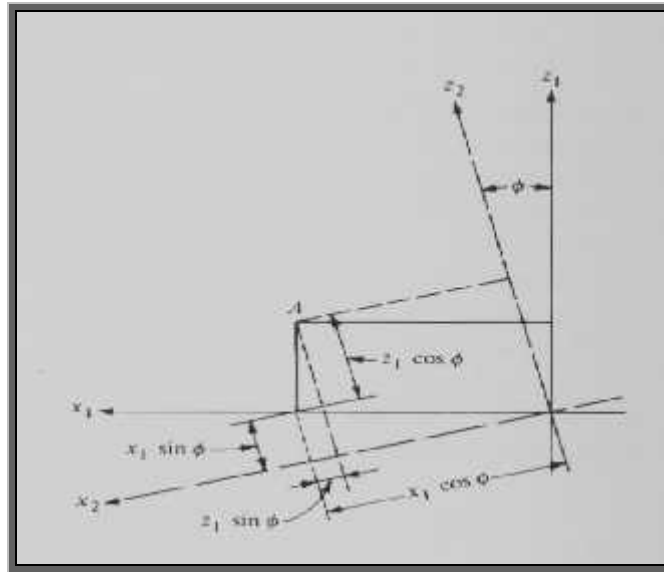


Fig. (A-4): Phi rotation about the y1 axis

$$\begin{aligned}
 x_2 &= -z_1 \sin \phi + x_1 \cos \phi \\
 y_2 &= y_1 \quad \dots\dots\dots (2) \\
 z_2 &= z_1 \cos \phi + x_1 \sin \phi
 \end{aligned}$$

In this rotation about y_1 , the y_1 and y_2 axes are coincident and therefore the y coordinate of A is unchanged. Substituting Eqs. (1) into (2):

$$\begin{aligned}
 x_2 &= -(-y' \sin \tilde{\theta} + z' \cos \tilde{\theta}) \sin \phi + x' \cos \phi \\
 y_2 &= y' \cos \tilde{\theta} + z' \sin \tilde{\theta} \quad \dots\dots\dots (3) \\
 z_2 &= (-y' \sin \tilde{\theta} + z' \cos \tilde{\theta}) \cos \phi + x' \sin \phi
 \end{aligned}$$

c) **Third**, fig. (A-5), rotation through κ about the z_2 axis,

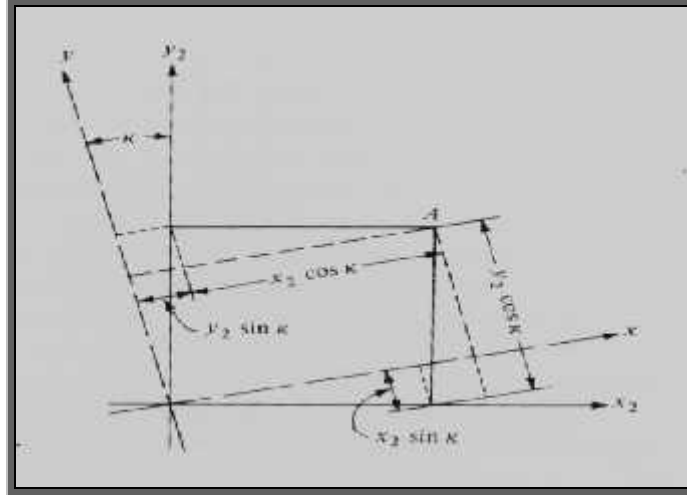


Fig. (A-5): Kappa rotation about the z_2 axis

After three times of rotation, the coordinate of point system, become in the xyz system as shown graphically in fig. (A-5), are:

$$\begin{aligned} x &= x_2 \cos \kappa + y_2 \sin \kappa \\ y &= -x_2 \sin \kappa + y_2 \cos \kappa \\ z &= z_2 \end{aligned} \dots\dots\dots (4)$$

In this rotation about z_2 , the z_2 and z axes are coincident and therefore the z coordinate of A is unchanged. Substituting Eqs. (3) into (4):

$$\begin{aligned} x &= [(y' \sin \tilde{S} - z' \cos \tilde{S}) \sin w + x' \cos w] \cos \kappa + (y' \cos \tilde{S} + z' \sin \tilde{S}) \sin \kappa \\ y &= [(-y' \sin \tilde{S} + z' \cos \tilde{S}) \sin w - x' \cos w] \sin \kappa + (y' \cos \tilde{S} + z' \sin \tilde{S}) \cos \kappa \\ z &= (-y' \sin \tilde{S} + z' \cos \tilde{S}) \cos w + x' \sin w \end{aligned} \dots\dots\dots (5)$$

Factoring Eqs. (5),

$$\begin{aligned} x &= x' (\cos w \cos \kappa) + y' (\sin \tilde{S} \sin w \cos \kappa + \cos \tilde{S} \sin \kappa) + z' (-\cos \tilde{S} \sin w \cos \kappa + \sin \tilde{S} \cos \kappa) \\ y &= x' (-\cos w \sin \kappa) + y' (-\sin \tilde{S} \sin w \sin \kappa + \cos \tilde{S} \cos \kappa) + z' (\cos \tilde{S} \sin w \sin \kappa + \sin \tilde{S} \cos \kappa) \\ z &= x' (\sin w) + y' (-\sin \tilde{S} \cos w) + z' (\cos \tilde{S} \cos w) \end{aligned} \dots (6)$$

Substituting m's for the coefficients of x', y', and z' in Eqs. (6), these equations are:

$$\begin{aligned}
 x &= m_{11}x' + m_{12}y' + m_{13}z' \\
 y &= m_{21}x' + m_{22}y' + m_{23}z' \\
 z &= m_{31}x' + m_{32}y' + m_{33}z'
 \end{aligned}
 \tag{7}$$

Equations (7) may be expressed in matrix form as

$$\begin{aligned}
 m_{11} &= \cos W \cos \checkmark \\
 m_{12} &= \sin \checkmark \sin W \cos \checkmark + \cos \checkmark \sin \checkmark \\
 m_{13} &= -\cos \checkmark \sin W \cos \checkmark + \sin \checkmark \sin \checkmark \\
 m_{21} &= -\cos W \sin \checkmark \\
 m_{22} &= -\sin \checkmark \sin W \sin \checkmark + \cos \checkmark \cos \checkmark \\
 m_{23} &= \cos \checkmark \sin W \sin \checkmark + \sin \checkmark \cos \checkmark \\
 m_{31} &= \sin W \\
 m_{32} &= -\sin \checkmark \cos W \\
 m_{33} &= \cos \checkmark \cos W
 \end{aligned}
 \tag{8}$$

$$\begin{aligned}
 X &= MX' \\
 X = \begin{bmatrix} x \\ y \\ z \end{bmatrix} M = \begin{bmatrix} m_{11} & m_{12} & m_{13} \\ m_{21} & m_{22} & m_{23} \\ m_{31} & m_{32} & m_{33} \end{bmatrix} \text{ and } X' = \begin{bmatrix} x' \\ y' \\ z' \end{bmatrix}
 \end{aligned}
 \tag{9}$$

The matrix M is commonly called the **rotation matrix**. Express m-matrix in terms of direction cosine which relates the two axes.

$$M = \begin{bmatrix} \cos xx' & \cos xy' & \cos xz' \\ \cos yx' & \cos yy' & \cos yz' \\ \cos zx' & \cos zy' & \cos zz' \end{bmatrix}
 \tag{10}$$

cos xx' is the direction cosine relating the x and x' axes, cos xy' relates the x and y' axes, etc. these angle taken between 0 and 180.

The rotation matrix can be called *orthogonal* matrix since the some square of the direction is line unity, so the sum of square of any column or row elements equal one, this yield

$$M^{-1} = M^T \dots\dots\dots (11)$$

To get X' from Eq. (9) use the property of Eq(11) as follows:

$$M^{-1} X = M^{-1} X' \dots\dots\dots (12)$$

$$M^T X = X'$$

In expanded form, this equation is:

$$\begin{aligned} x' &= m_{11}x + m_{21}y + m_{31}z \\ y' &= m_{12}x + m_{22}y + m_{32}z \\ z' &= m_{13}x + m_{23}y + m_{33}z \end{aligned} \dots\dots\dots (13)$$

2. Scaling and Translation

As in fig(A-1), the x'y'z' system will convert to XYZ ground system but the measurement is not absolutely so a factor of scale will be applied in addition of shifting Tx, Ty, and Tz.

Equations (13) will be transforming to XYZ ground system by multiply each of equation by a scale factor s

$$\begin{aligned} X &= sx' + T_x = s(m_{11}x + m_{21}y + m_{31}z) + T_x \\ Y &= sy' + T_y = s(m_{12}x + m_{22}y + m_{32}z) + T_y \\ Z &= sz' + T_z = s(m_{13}x + m_{23}y + m_{33}z) + T_z \end{aligned} \dots\dots\dots (14)$$

In matrix form, Eqs. (14) are

$$\overline{X} = sM^T X + T \dots\dots\dots (15)$$

In Eqs. (15) matrixes M and X are as previously defined, s is the scale factor.

$$\bar{X} = \begin{bmatrix} X \\ Y \\ Z \end{bmatrix} \text{ and } T = \begin{bmatrix} T_x \\ T_y \\ T_z \end{bmatrix}$$

In Eqs. (14), the system have seven parameter, which are three rotation angles S , w and $|$, three translation and the scale, o to have unique solution if x & y can find two horizontal point and z of three vertical point are known in both coordinate system Equation (14) not linear so it must be linearized:

$$\begin{aligned} X_p &= (X_p)_o + \left(\frac{\partial X_p}{\partial s} \right)_o ds + \left(\frac{\partial X_p}{\partial \check{S}} \right)_o d\check{S} + \left(\frac{\partial X_p}{\partial w} \right)_o dw + \left(\frac{\partial X_p}{\partial k} \right)_o dk \\ &+ \left(\frac{\partial X_p}{\partial T_x} \right)_o dT_x + \left(\frac{\partial X_p}{\partial T_y} \right)_o dT_y + \left(\frac{\partial X_p}{\partial T_z} \right)_o dT_z \\ Y_p &= (Y_p)_o + \left(\frac{\partial Y_p}{\partial s} \right)_o ds + \left(\frac{\partial Y_p}{\partial \check{S}} \right)_o d\check{S} + \left(\frac{\partial Y_p}{\partial w} \right)_o dw + \left(\frac{\partial Y_p}{\partial k} \right)_o dk \\ &+ \left(\frac{\partial Y_p}{\partial T_x} \right)_o dT_x + \left(\frac{\partial Y_p}{\partial T_y} \right)_o dT_y + \left(\frac{\partial Y_p}{\partial T_z} \right)_o dT_z \\ Z_p &= (Z_p)_o + \left(\frac{\partial Z_p}{\partial s} \right)_o ds + \left(\frac{\partial Z_p}{\partial \check{S}} \right)_o d\check{S} + \left(\frac{\partial Z_p}{\partial w} \right)_o dw + \left(\frac{\partial Z_p}{\partial k} \right)_o dk \\ &+ \left(\frac{\partial Z_p}{\partial T_x} \right)_o dT_x + \left(\frac{\partial Z_p}{\partial T_y} \right)_o dT_y + \left(\frac{\partial Z_p}{\partial T_z} \right)_o dT_z \end{aligned} \tag{16}$$

where, $(Fq)_o$, $(Gq)_o$, $(Hq)_o$, etc., are the right-hand sides of the respective Eqs. (14) evaluated at the initial approximations; $\left(\frac{\partial F_q}{\partial s} \right)_o$, $\left(\frac{\partial F_q}{\partial \check{S}} \right)_o$, $\left(\frac{\partial F_q}{\partial w} \right)_o$, etc., are partial derivatives with respect to the indicated unknowns.

And ds , dS , d^w , $d|$ in radian, dTx , dTy , dTz are correction to the initial value partial derivative can be expressed by letters as follow:

$$\begin{aligned}
a_{11}ds + a_{12}d\check{S} + a_{13}dW + a_{14}dk + a_{15}T_X + a_{16}dT_Y + a_{17}dT_Z &= [X_p - (X_p)_o] + v_{Xp} \\
a_{21}ds + a_{22}d\check{S} + a_{23}dW + a_{24}dk + a_{25}T_X + a_{26}dT_Y + a_{27}dT_Z &= [Y_p - (Y_p)_o] + v_{Yp} \\
a_{31}ds + a_{32}d\check{S} + a_{33}dW + a_{34}dk + a_{35}T_X + a_{36}dT_Y + a_{37}dT_Z &= [Z_p - (Z_p)_o] + v_{Zp}
\end{aligned}
\tag{17}$$

Where:

$$a_{11} = m_{11}x_p + m_{21}y_p + m_{31}z_p$$

$$a_{12} = 0$$

$$a_{13} = [(-\sin w \cos k)x_p + \sin w \sin k(y_p) + \cos w(z_p)]s$$

$$a_{14} = (m_{21}x_p - m_{11}y_p)s$$

$$a_{15} = a_{26} = a_{37} = 1$$

$$a_{16} = a_{17} = a_{25} = a_{27} = a_{36} = 0$$

$$a_{21} = m_{12}x_p + m_{22}y_p + m_{32}z_p$$

$$a_{22} = (-m_{13}x_p - m_{23}y_p + m_{33}z_p)s$$

$$a_{23} = [(\sin \check{S} \cos w \cos k)x_p + (-\sin \check{S} \cos w \sin k)y_p + (\sin \check{S} \sin w)z_p]s$$

$$a_{24} = (m_{22}x_p - m_{12}y_p)s$$

$$a_{31} = m_{13}x_p + m_{23}y_p + m_{33}z_p$$

$$a_{32} = (m_{12}x_p + m_{22}y_p + m_{32}z_p)s$$

$$a_{23} = [(-\cos \check{S} \cos w \cos k)x_p + (\cos \check{S} \cos w \sin k)y_p + (-\cos \check{S} \sin w)z_p]s$$

$$a_{34} = (m_{23}x_p - m_{13}y_p)s$$

Equation(17) can be solved according to least square solution ,so it is easy to express as matrices form

$${}_{3n}A^7 {}_7X^1 = {}_{3n}L^1 + {}_{3n}v^1$$

$${}_{3n}A^7 = \begin{bmatrix} a_{111} & a_{112} & a_{113} & a_{114} & 1 & 0 & 0 \\ a_{121} & a_{122} & a_{123} & a_{124} & 0 & 1 & 0 \\ a_{131} & a_{132} & a_{133} & a_{134} & 0 & 1 & 1 \\ \cdot & \cdot & \cdot & \cdot & 1 & 0 & 0 \\ \cdot & \cdot & \cdot & \cdot & 0 & 1 & 0 \\ \cdot & \cdot & \cdot & \cdot & 0 & 0 & 1 \\ a_{n11} & a_{n12} & a_{n13} & a_{n14} & 1 & 0 & 0 \\ a_{n21} & a_{n22} & a_{n23} & a_{n24} & 0 & 1 & 0 \\ a_{n31} & a_{n32} & a_{n33} & a_{n34} & 0 & 0 & 1 \end{bmatrix} \quad {}_7X^1 = \begin{bmatrix} ds \\ d\check{S} \\ dW \\ dk \\ dT_X \\ dT_Y \\ dT_Z \end{bmatrix}$$

$${}_{3n}L^1 = \begin{bmatrix} X_{p_1} - (X_{p_1})_o \\ Y_{p_1} - (Y_{p_1})_o \\ Z_{p_1} - (Z_{p_1})_o \\ \cdot \\ X_{p_n} - (X_{p_n}) \\ X_{p_n} - (X_{p_n}) \\ X_{p_n} - (X_{p_n}) \end{bmatrix} \quad {}_{3n}v^1 = \begin{bmatrix} v_{X_1} \\ v_{Y_1} \\ v_{Z_1} \\ \cdot \\ v_{X_n} \\ v_{Y_n} \\ v_{Z_n} \end{bmatrix}$$

APPENDIX-B

Collinearity Condition Equations

B-1 Collinearity Equations

Collinearity is a condition that has an exposure, ground object and its image, at which all lie on a straight line as illustrated in fig. (B-1).

The condition is interrupted as mathematical equation in order to obtain the features from the photos.

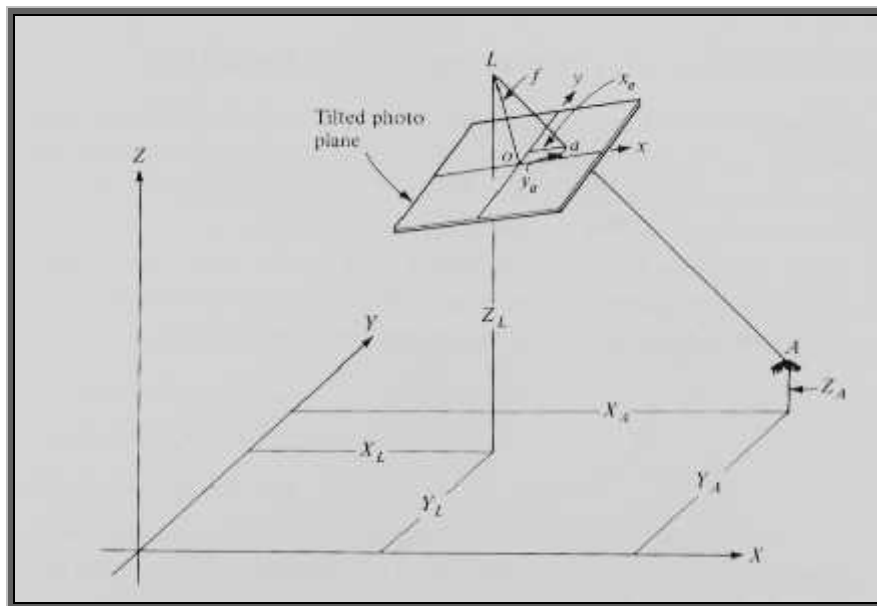


Fig. (B-1): The collinearity condition

In the fig. (B-2) the photo exposure consist of $(X_L, Y_L, \text{ and } Z_L)$ which is exposure station at ground coordinate system, so a point on the rotated photo has image space coordinate $x'_a, y'_a, \text{ and } -z'_a$ where the rotated image space coordinate system $x'y'z'$ is parallel to object space coordinate system XYZ .

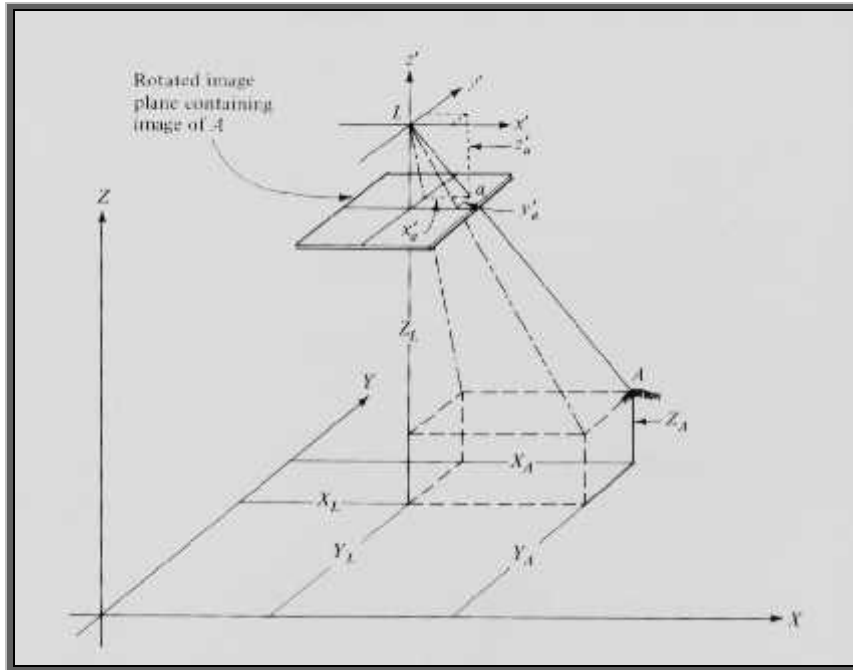


Fig. (B-2): Image coordinate system rotated such that it is parallel to the object space coordinates system

B-2 ROTATION IN TERMS OF OMEGA, PHI, AND KAPPA

According to three-dimensional rotation formulas developed in Appendix A, any point has an image coordinates x_a, y_a and $-z_a$ in a tilted photo described in fig. (B-1), so the point must transform or corrected to the $x'y'z'$ parallel coordinate system (parallel to XYZ) as shown in fig. (B-3).

The rotated image coordinates x'_a, y'_a and $-z'_a$ \longrightarrow photo coordinates x_a and y_a, f

As description in previous appendix the rotation formulas are eqs(7) which are:

$$\begin{aligned}
 x_a &= m_{11}x'_a + m_{12}y'_a + m_{13}z'_a \\
 y_a &= m_{21}x'_a + m_{22}y'_a + m_{23}z'_a \\
 z_a &= m_{31}x'_a + m_{32}y'_a + m_{33}z'_a
 \end{aligned}
 \dots\dots\dots (1)$$

In Eqs. (1) the m 's are functions of the rotation angles ω , ϕ , and κ . These functions are given as Eqs. (8) in Appendix A. Also note on Fig.(B-3) that the value for z_a is equal to $(-f)$.

B-3 DEVELOPMENT OF THE COLLINEARITY CONDITION EQUATIONS

The collinearity condition equations are developed from similar triangles of fig. (B-2) as follows:

$$\frac{x'_a}{X_A - X_L} = \frac{y'_a}{Y_A - Y_L} = \frac{z'_a}{Z_A - Z_L}$$

Reducing,

$$x'_a = \left(\frac{X_A - X_L}{Z_A - Z_L} \right) z'_a \tag{a}$$

$$y'_a = \left(\frac{Y_A - Y_L}{Z_A - Z_L} \right) z'_a \tag{b}$$

Also, by identity,

$$z'_a = \left(\frac{Z_A - Z_L}{Z_A - Z_L} \right) z'_a \tag{c}$$

Substituting (a), (b), and (c) into Eqs. (1),

$$x_a = m_{11} \left(\frac{X_A - X_L}{Z_A - Z_L} \right) z'_a + m_{12} \left(\frac{Y_A - Y_L}{Z_A - Z_L} \right) z'_a + m_{13} \left(\frac{Z_A - Z_L}{Z_A - Z_L} \right) z'_a \dots \tag{2}$$

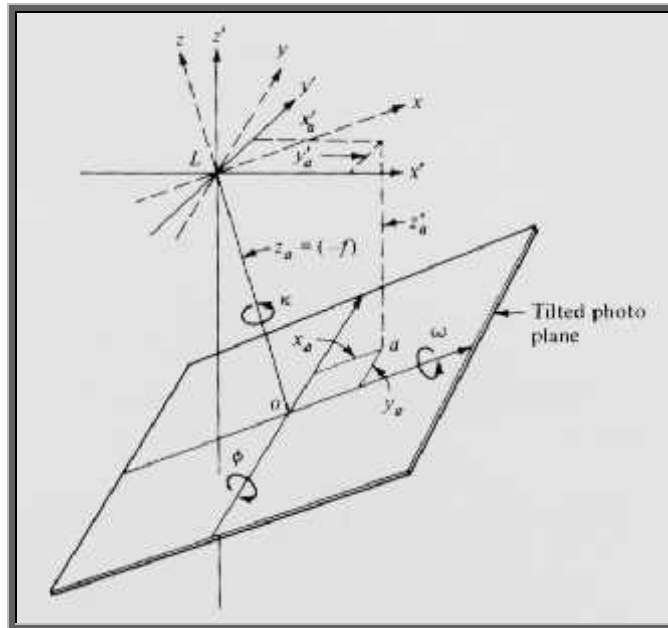


Fig. (B-3): Measurement x-y-z and rotated x'-y'-z' image coordinate systems

$$y_a = m_{21} \left(\frac{X_A - X_L}{Z_A - Z_L} \right) z'_a + m_{22} \left(\frac{Y_A - Y_L}{Z_A - Z_L} \right) z'_a + m_{23} \left(\frac{Z_A - Z_L}{Z_A - Z_L} \right) z'_a \dots\dots\dots (3)$$

$$z_a = m_{31} \left(\frac{X_A - X_L}{Z_A - Z_L} \right) z'_a + m_{32} \left(\frac{Y_A - Y_L}{Z_A - Z_L} \right) z'_a + m_{33} \left(\frac{Z_A - Z_L}{Z_A - Z_L} \right) z'_a \dots\dots\dots (4)$$

Factoring the term (z'a/ZA-ZL) from Eqs. (2) through (4), dividing (2) and (3) by (4), and substituting (-f) for z_a, the following collinearity equations result:

$$x_a = -f \left[\frac{m_{11}(X_A - X_L) + m_{12}(Y_A - Y_L) + m_{13}(Z_A - Z_L)}{m_{31}(X_A - X_L) + m_{32}(Y_A - Y_L) + m_{33}(Z_A - Z_L)} \right] \dots\dots\dots (5)$$

$$y_a = -f \left[\frac{m_{21}(X_A - X_L) + m_{22}(Y_A - Y_L) + m_{23}(Z_A - Z_L)}{m_{31}(X_A - X_L) + m_{32}(Y_A - Y_L) + m_{33}(Z_A - Z_L)} \right] \dots\dots\dots (6)$$

B-4 LINEARIZATION OF THE COLLINARITY EQUATIONS

Equations (5) and (6) are nonlinear and involve nine unknowns: the three rotation angles omega, phi, and kappa which are inherent in the m's; the three exposure station coordinates X_L, Y_L and Z_L ; and the three object point coordinates X_A, Y_A and Z_A .

The nonlinear equations are linearized using Taylor's theorem. In linearizing the collinearity equations, the Eqs. (5) & (6) are rewritten as Follows:

$$F = 0 = qx_a + r f \dots\dots\dots(7)$$

$$G = 0 = qy_a + s f \dots\dots\dots (8)$$

Where:

$$r = m_{11}(X_A - X_L) + m_{12}(Y_A - Y_L) + m_{13}(Z_A - Z_L)$$

$$s = m_{21}(X_A - X_L) + m_{22}(Y_A - Y_L) + m_{23}(Z_A - Z_L)$$

$$q = m_{31}(X_A - X_L) + m_{32}(Y_A - Y_L) + m_{33}(Z_A - Z_L)$$

According to Taylor's theorem, Eqs. (7) and (8) may be expressed in linearized form as:

$$0 = (F)_0 + \left(\frac{\partial F}{\partial x_a}\right)_0 dx_a + \left(\frac{\partial F}{\partial \tilde{S}}\right)_0 d\tilde{S} + \left(\frac{\partial F}{\partial w}\right)_0 dw + \left(\frac{\partial F}{\partial k}\right)_0 dk + \left(\frac{\partial F}{\partial X_L}\right)_0 dX_L + \left(\frac{\partial F}{\partial Y_L}\right)_0 dY_L \dots(9)$$

$$+ \left(\frac{\partial F}{\partial Z_L}\right)_0 dZ_L + \left(\frac{\partial F}{\partial X_A}\right)_0 dX_A + \left(\frac{\partial F}{\partial Y_A}\right)_0 dY_A + \left(\frac{\partial F}{\partial Z_A}\right)_0 dZ_A$$

$$0 = (G)_0 + \left(\frac{\partial G}{\partial x_a}\right)_0 dx_a + \left(\frac{\partial G}{\partial \tilde{S}}\right)_0 d\tilde{S} + \left(\frac{\partial G}{\partial w}\right)_0 dw + \left(\frac{\partial G}{\partial k}\right)_0 dk + \left(\frac{\partial G}{\partial X_L}\right)_0 dX_L + \left(\frac{\partial G}{\partial Y_L}\right)_0 dY_L \dots(10)$$

$$+ \left(\frac{\partial G}{\partial Z_L}\right)_0 dZ_L + \left(\frac{\partial G}{\partial X_A}\right)_0 dX_A + \left(\frac{\partial G}{\partial Y_A}\right)_0 dY_A + \left(\frac{\partial G}{\partial Z_A}\right)_0 dZ_A$$

In Eqs. (9) and (10), F_0 and G_0 are the functions F and G of Eqs. (7) and (8) evaluated at the initial approximations for the nine unknowns; the terms, $\left(\frac{\partial F}{\partial \check{S}}\right)_0$, $\left(\frac{\partial F}{\partial W}\right)_0$, $\left(\frac{\partial F}{\partial k}\right)_0$ etc., are partial derivatives of the functions F and G with

respect to the indicated unknowns $X_L, Y_L, Z_L, \check{S}, W, k, (X, Y, Z)_{point}$ approximations; and the correction of angles in radian

Substitute the derivatives by letters (b) in order to simplify the equations with the residual (v's) to meat least square solution

The following simplified forms of the linearized collinearity equations are obtained:

$$v_{x_a} = b_{11}d\check{S} + b_{12}dW + b_{13}dk - b_{14}dX_L - b_{15}dY_L - b_{16}dZ_L + b_{14}dX_A + b_{15}dY_A + b_{16}dZ_A + J \dots\dots\dots (11)$$

$$v_{y_a} = b_{21}d\check{S} + b_{22}dW + b_{23}dk - b_{24}dX_L - b_{25}dY_L - b_{26}dZ_L + b_{24}dX_A + b_{25}dY_A + b_{26}dZ_A + K \dots\dots\dots (12)$$

In Eqs. (11) And (12), J and K are equal to $\frac{F_0}{q_0}$ and $\frac{G_0}{q_0}$ respectively. The b's are coefficients equal to the partial derivatives. For convenience these coefficients are given below. In these coefficients ΔX , ΔY , and ΔZ are equal to $(X_A - X_L)$, $(Y_A - Y_L)$, and $(Z_A - Z_L)$ respectively. Numerical values for these coefficient terms are obtained by using initial approximations for the unknowns.

$$b_{11} = \frac{x}{q}(-m_{33}\Delta Y + m_{32}\Delta Z) + \frac{f}{q}(-m_{13}\Delta Y + m_{12}\Delta Z)$$

$$b_{12} = \frac{x}{q}[\Delta X \cos w + \Delta Y (\sin \check{S} \sin w) + \Delta Z (-\sin w \cos \check{S})]$$

$$+ \frac{f}{q}[\Delta X (-\sin w \cos k) + \Delta Y (\sin \check{S} \cos w \cos k) + \Delta Z (-\cos \check{S} \cos w \cos k)]$$

$$b_{13} = \frac{f}{q}(m_{21}\Delta X + m_{22}\Delta Y + m_{23}\Delta Z)$$

$$b_{14} = \frac{x}{q}m_{31} + \frac{f}{q}m_{11}$$

$$b_{15} = \frac{x}{q}m_{32} + \frac{f}{q}m_{12}$$

$$b_{16} = \frac{x}{q}m_{33} + \frac{f}{q}m_{13}$$

$$J = \frac{(qx + rf)}{q}$$

$$b_{21} = \frac{y}{q}(-m_{33}\Delta Y + m_{32}\Delta Z) + \frac{f}{q}(-m_{23}\Delta Y + m_{22}\Delta Z)$$

$$b_{22} = \frac{y}{q}[\Delta X \cos w + \Delta Y (\sin \tilde{S} \sin w) + \Delta Z (-\sin w \cos \tilde{S})] \\ + \frac{f}{q}[\Delta X (\sin w \cos k) + \Delta Y (-\sin \tilde{S} \cos w \sin k) + \Delta Z (\cos \tilde{S} \cos w \sin k)]$$

$$b_{23} = \frac{f}{q}(-m_{11}\Delta X - m_{12}\Delta Y - m_{13}\Delta Z)$$

$$b_{24} = \frac{y}{q}m_{31} + \frac{f}{q}m_{21}$$

$$b_{25} = \frac{y}{q}m_{32} + \frac{f}{q}m_{22}$$

$$b_{26} = \frac{y}{q}m_{33} + \frac{f}{q}m_{23}$$

$$K = \frac{(qy + sf)}{q}$$


```

#include <stdio.h>
#include <conio.h>
#include <math.h >
#define pi 0.017453292
int main (void)
{ clrscr();

double

x[20],y[20],X[20],Y[20],Z[20],Xa[20],Ya[20],A[20][20],L[20][1],
un[20][1],AT[20][20],F[20][20],N[20][20],ZL,g,f,a,b,c,XL,YL,k,
m[20][20],q,r,s,B[20][20],phi,w,LL[20][1],Dx,Dy,Dz,BT[20][20];

int i,n,j,K,I,it;

printf("\t\t*****\n");
printf("\t\t* Space----Resection----Solution *\n");
printf("\t\t* *\n");
printf("\t\t*****");
textcolor(210);
cprintf(" Majdi");
printf("*");
textcolor(155);
cprintf(" SADEQ ");
printf("*");
textcolor(210);
cprintf(" Hani");
printf("*****\n\n");

printf("please how many point would you are use = ....");
scanf("%d",&n);
if((n<3))
printf("please you have not solution since point must >=3");

printf("please enter camera focal length (f) ....");
scanf("%lf",&f) ;
printf("please how many iteration would you like = ....");
scanf("%d",&it);

printf("please enter measured photo coordinate (x,y) ....");

for(i=1;i<=n;++i)
{
printf("x-photo[%d]= ",i);

```

```

        scanf("%lf",&x[i]) ;
printf("y-photo[%d]= ",i);
        scanf("%lf",&y[i]) ;

}

printf("please enter corosponding control points (X,Y,Z) ....");

        for(i=1;i<=n;++i)
{
printf("X-control[%d]= ",i);
        scanf("%lf",&X[i]) ;
printf("Y-control[%d]= ",i);
        scanf("%lf",&Y[i]) ;
printf("Z-control[%d]= ",i);
        scanf("%lf",&Z[i]) ;
}

g=sqrt( (X[2]-X[1])*(X[2]-X[1])+(Y[2]-Y[1])*(Y[2]-Y[1]) );

a= x[2]*x[2]-2*x[1]*x[2]+x[1]*x[1]+y[2]*y[2]-2*y[1]*y[2]+y[1]*y[1];

b=-2*Z[2]*x[2]*x[2]+2*Z[1]*x[1]*x[2]+2*Z[2]*x[1]*x[2]-2*Z[1]*x[1]*
*x[1]-2*Z[2]*y[2]*y[2]+2*Z[1]*y[1]*y[2]+2*Z[2]*y[1]*y[2]-2*Z[1]*y[1]*y[1];

c=-1*g*g*f*f+ Z[1]*Z[1]*x[1]*x[1]- 2*x[1]*x[2]*Z[1]*Z[2]+ x[2]*x[2]*
*Z[2]*Z[2]+ Z[1]*Z[1]*y[1]*y[1]-2*y[1]*y[2]*Z[1]*Z[2] +y[2]*y[2]*Z[2]*Z[2];

ZL=( -b+sqrt(b*b-4*a*c) ) / (2*a);

        for(i=1;i<=n;++i)
{
Xa[i]=x[i]*(ZL-Z[i])/f;
Ya[i]=y[i]*(ZL-Z[i])/f;
}

        for(i=1;i<=2*n;++i)
        for(j=1;j<=4;++j)
{

if((i%2)!=0)

        {
if(j==1) A[i][j]=Xa[(i+1)/2];
if(j==2) A[i][j]=-Ya[(i+1)/2];

```

```

if(j==3) A[i][j]=1;
if(j==4) A[i][j]=0;

    }

if((i%2)==0)

    {
if(j==1) A[i][j]=Ya[(i/2)];
if(j==2) A[i][j]=Xa[(i/2)];
if(j==3) A[i][j]=0;
if(j==4) A[i][j]=1;

    }

}

    for(i=1;i<=2*n;++i)
    for(j=1;j<=1;++j)

{
if((i%2)!=0)
L[i][j]= X[(i+1)/2];

if((i%2)==0)
L[i][j]=Y[(i/2)];
}

    for(i=1;i<=4;++i)
    for(j=1;j<=2*n;++j)

        AT[i][j]=A[j][i];

for(i=1; i<=4;i++)
for(K=1; K<=4;K++){
N[i][K]=0;
for(j=1;j<=2*n;++j)
N[i][K]=N[i][K]+AT[i][j]*A[j][K] ;
}

for(i=1; i<=4;i++)

```



```

for(I=1; I<=it;I++)
{

m[1][1]=cos(phi*pi)*cos(k*pi);
m[1][2]=sin(w*pi)*sin(phi*pi)*cos(k*pi)+cos(w*pi)*sin(k*pi);
m[1][3]=-cos(w*pi)*sin(phi*pi)*cos(k*pi)+sin(w*pi)*sin(k*pi);
m[2][1]=-cos(phi*pi)*sin(k*pi);
m[2][2]=-sin(w*pi)*sin(phi*pi)*sin(k*pi)+cos(w*pi)*cos(k*pi);
m[2][3]=cos(w*pi)*sin(phi*pi)*sin(k*pi)+sin(w*pi)*cos(k*pi);
m[3][1]=sin(phi*pi);
m[3][2]=-sin(w*pi)*cos(phi*pi);
m[3][3]=cos(w*pi)*cos(phi*pi);

for(i=1; i<=2*n;i++)
for(j=1; j<=6;j++)
    {

        if((i%2)!=0)
        {

Dx=X[(i+1)/2]-XL;
Dy=Y[(i+1)/2]-YL;
Dz=Z[(i+1)/2]-ZL;

q=m[3][1]*Dx+m[3][2]*Dy+m[3][3]*Dz;

r=m[1][1]*Dx+m[1][2]*Dy+m[1][3]*Dz;

s=m[2][1]*Dx+m[2][2]*Dy+m[2][3]*Dz;

if(j==1)
    B[i][j]=f/(q*q)*( r*(-m[3][3]*Dy+m[3][2]*Dz) -q*(-
m[1][3]*Dy+m[1][2]*Dz ) );

if(j==2)
    B[i][j]=f/(q*q)*( r*(cos(phi*pi)*Dx+sin(w*pi)*sin(phi*pi)*Dy-cos(w*pi)
*sin(phi*pi)*Dz)-q*(-sin(phi*pi)*cos(k*pi)*Dx+sin(w*pi)*cos(phi*pi)*cos(k*pi)
*Dy-cos(w*pi)*cos(phi*pi)*cos(k*pi)*Dz));

if(j==3)
    B[i][j]=-f/q*(m[2][1]*Dx+m[2][2]*Dy+m[2][3]*Dz);
if(j==4)
    B[i][j]=-f/(q*q)*(r*m[3][1]-q*m[1][1]) ;
if(j==5)

```

```

        B[i][j]=-f/(q*q)*(r*m[3][2]-q*m[1][2]) ;
if(j==6)
        B[i][j]=-f/(q*q)*(r*m[3][3]-q*m[1][3]) ;
if(j==1)
        LL[i][1]=x[(i+1)/2]+f*r/q;

}

        if((i%2)==0)
{

Dx=X[i/2]-XL;
Dy=Y[i/2]-YL;
Dz=Z[i/2]-ZL;

q=m[3][1]*Dx+m[3][2]*Dy+m[3][3]*Dz;

r=m[1][1]*Dx+m[1][2]*Dy+m[1][3]*Dz;
s=m[2][1]*Dx+m[2][2]*Dy+m[2][3]*Dz;

if(j==1)
        B[i][j]=f/(q*q)*( s*(-m[3][3]*Dy+m[3][2]*Dz)-q*(-
m[2][3]*Dy+m[2][2]*Dz));
if(j==2)
        B[i][j]= f/(q*q)*( s*(cos(phi*pi)*Dx+sin(w*pi)*sin(phi*pi)*Dy-cos(w*pi)
*sin(phi*pi)*Dz)-q*(sin(phi*pi)*cos(k*pi)*Dx-sin(w*pi)*cos(phi*pi)*cos(k*pi)*Dy
+cos(w*pi)*cos(phi*pi)*sin(k*pi)*Dz));

if(j==3)
        B[i][j]=f/q*(m[1][1]*Dx+m[1][2]*Dy+m[1][3]*Dz);
if(j==4)
        B[i][j]=-f/(q*q)*(s*m[3][1]-q*m[2][1]) ;
if(j==5)
        B[i][j]=-f/(q*q)*(s*m[3][2]-q*m[2][2]) ;
if(j==6)
        B[i][j]=-f/(q*q)*(s*m[3][3]-q*m[2][3]) ;
if(j==1)
        LL[i][1]=y[i/2]+f*s/q;

}

}

for(i=1;i<=6;++i)

```

```

    for(j=1;j<=2*n;++j)

        BT[i][j]=B[j][i];

for(i=1; i<=6;i++)
for(K=1; K<=6;K++){
N[i][K]=0;
for(j=1;j<=2*n;++j)
N[i][K]=N[i][K]+BT[i][j]*B[j][K] ;
}

for(i=1; i<=6;i++)
for(K=1; K<=1;K++){
F[i][K]=0;
for(j=1;j<=2*n;++j)
F[i][K]=F[i][K]+BT[i][j]*LL[j][K] ;
}

for(K=1; K<=6;K++)
{
for(j=1; j<=6;j++)
if(j!=K)N[K][j]=N[K][j]/N[K][K];
N[K][K]=1.0/N[K][K];
for(i=1;i<=6;i++)
if(i!=K){
for(j=1;j<=6;++j)
if(j!=K)N[i][j]=N[i][j]-N[i][K]*N[K][j];
N[i][K]=-N[i][K]*N[K][K];
}
}

for(i=1; i<=6;i++)
for(K=1; K<=1;K++){
un[i][K]=0;
for(j=1;j<=6;++j)
un[i][K]=un[i][K]+N[i][j]*F[j][K] ;
}

w+=un[1][1]/pi;
phi+=un[2][1]/pi;
k+=un[3][1]/pi;
XL+=un[4][1];
YL+=un[5][1];
ZL+=un[6][1];
}
printf("\ncorrection after iterations are\n");

```

```
printf("dw=%lf\n",un[1][1]);
printf("dphi=%lf\n",un[2][1]);
printf("dkappa=%lf\n",un[3][1]);
printf("dXL=%lf\n",un[4][1]);
printf("dYL=%lf\n",un[5][1]);
printf("dZL=%lf\n\n",un[6][1]);
```

```
printf("Exposure station is:\n\n");
```

```
printf("\t\tXL=%lf\n\n",XL);
printf("\t\tYL=%lf\n\n",YL);
printf("\t\tZL=%lf\n\n",ZL);
printf("\t\tw=%lf\n\n",w);
printf("\t\tphi=%lf\n\n",phi);
printf("\t\tkappa=%lf\n\n",k);
```

```
getch();
return 0;
}
```